

On Resource Efficient and Obstacle Aware Link Selection in D2D Communications

by

Rathindra Nath Dutta

A thesis submitted in partial fulfillment of
the requirements for the degree of
Doctor of Philosophy
in
Computer Science

under supervision of
Prof. Sasthi C. Ghosh



Advanced Computing and Microelectronics Unit
Indian Statistical Institute
Kolkata, India
December 2023

To all my teachers...*

*Parents being the first!

Acknowledgements

This thesis would not have been possible without my supervisor, Prof. Sasthi C. Ghosh. He was there to guide, encourage, and motivate me throughout my PhD journey. He is like a father figure to me, who loves and cares for his students like his own children. There was a time when I started having self-doubts regarding my choice to opt for a PhD (among other things), that is, sticking to academics and not pursuing (provably high-paid) IT jobs, and thus I used to often get distracted from my research work. As per my limited experience, most students, if not all, have struggled through this phase, and I only wish that all research students could have such a caring supervisor. I really doubt whether I would have been able to continue my research and materialize this thesis if it had not been for his constant support. He is a perfect example of a teacher: a friend (we had many friendly discussions, even on mundane personal matters), a philosopher (he taught me how to do critical thinking and pursue research), and a guide (he showed me the right tracks). I cannot thank him enough for bearing with me for the past six years.

I thank the Indian Statistical Institute (ISI) for giving me the opportunity to pursue a career in research. I am grateful to all the members of the Advanced Computing and Microelectronics Unit (ACMU) at ISI, Kolkata, for providing a homely research atmosphere. Over the past few years at ISI, I had almost regular interactions with Prof. Sandip Das, Prof. Nabanita Das (currently retired), and Prof. Krishnendu Mukhopadhyaya, who used to tell us many stories and interesting facts both related to academics and, of course, outside of it. I also thank other faculty members of ACMU, namely Prof. Susmita Sur-Kolay, Prof. Subhas C. Nandy, Prof. Ansuman Banerjee, Prof. Arijit Bishnu, Prof. Sasanka Roy, Dr. Arijit Ghosh, and Dr. Sourav Chakraborty. Prof. Mandar Mitra (of the CVPR Unit) gave me the opportunity to serve as a teaching assistant in the data and file structures lab of MTech CS, where I learned a lot. I am grateful to Mandar sir for his support and motivating words. I am also thankful to our proficient ACMU office staff: Sachi da, Suchitra di, Biswajit da, Rakesh da, and Rajendra da, all of whom are very active and efficient in their duties. I am also thankful to all research scholars, students, and project personnel at

ACMU for providing a friendly environment.

It would be a sin not to mention Satya da, Sanjana di, and Avirup da for their constant motivation and love; Shankar da, Durgesh da, Subhankar da, Souvik, Lakshmikanta, and Priyadarshi da for their guidance and input for my research; and my batch mates Abhinav, Anjan, Arun, Bibhuti, Debendranath, Drimit, Joginder, Kaustabha, Prasun da, Sankar, Subhojit, and Surochita for their love and support. Over the last few years, I probably had the most tea breaks in my entire life; our discussions over tea (not to be confused with its translation in Hindi) probably were the most enjoyable ones during my PhD. Our tea party group was mostly comprised of me, Bibhuti, Abhinav, Sankar, Subhojit, Sucheta, Sukriti, and Kaustav da. I also thank the workforce of our Dean's office, namely Manas da, Surajit da, Monami di and others, who always had the time to listen to our problems and requests and resolve them amidst their ever-busy schedules. Also, I thank Sahadeb da for serving us food and tea, which have been my primary fuel for the past few years.

I am fortunate to have had some excellent teachers since my school days. Durga Rana, his son Dibyendu Rana, and our school headmaster, the late Panchanan sir, took great care to teach me the English language. Our math school teacher, Pradip sir, took great effort to help us grasp the basics of mathematics. Later, Debasish Roychoudhury (Deba da) helped me with the higher mathematics. I was first introduced to computer programming by Abhijit da (late Abhijit Banerjee) during high school. Abhijit da is and always will be my inspiration. Sudip da, my chemistry teacher, is the one who suggested me to pursue computer science after high school, which eventually brought me where I am today. I sincerely thank him for putting me on this path. During my bachelor's degree, Pijush sir, Sugata sir, and Indrajit sir helped me grasp core computer science subjects. Akinchan sir also helped me a lot to learn a few core subjects. I joined the Rajabajar Science College campus of Calcutta University for my master's, where I also had some excellent teachers such as Sanjit sir, Sankhayan sir, Nabendu sir, Rajat sir, Kashinath sir, Pritha mam, Banani mam, Sunirmal sir, and Rajib sir, who taught us some of the advanced topics of computer science in a memorable way. Later at ISI, I also had the fortune to undergo some courses, which have helped me in many ways to formulate the solutions presented in this thesis.

During my master's at Rajabajar Science College, I had the opportunity to meet some excellent batchmates who have now become family to me. This pseudo-family, named *Amra Sobai Raja* (which can be loosely translated as: every one is equal), comprises myself, Tania, Amit, Subharchana, Aritra, Chandrima, Sudeshna, Soumik, Rupash, Soumali, Monalisa,

Rajdip da, and Anupam. They have been my constant support system. I also met some of the best seniors one could have, Amit da, Debayan da, Kajari di, Dibyendu da to name a few. The members of *Haveli* (loosely described as a large accommodation) welcomed me into their group with their big hearts. It is where I met some new friends like Khairul, Anamitra, Saikat, Rajit, Rajarshi, etc. and reacquainted myself with some old ones such as Debraj and Sudipta. I was fortunate to spend the lockdown period during the COVID-19 pandemic with Amit, Debraj, and Khairul. They have been more like my own family, who pampered me during the pandemic and continue to do so.

During my leisure time, I like to help fellow students with their studies in computer science. While doing so, they sometimes ask some very basic, fundamental questions answering which have helped me clarify my own understanding of the topics. I am fortunate to have such interested students and/or friends, such as Romita, Pritha, Aditi, Madhura, Sahasrabdi, and Madhumita, to name a few. I also had the misfortune to get acquainted with some annoying people, whose harsh words, narrow-minded selfish attitudes, and/or continuous taunting have only strengthened my determination to do research. Due to obvious reasons, I deliberately omit their names and refer to them as AK-47S. I thank their annoying presence for motivating me in its own way and teaching me some important life lessons, especially about what not to do.

The availability of various online and/or open-source resources and tools has played a crucial role in shaping this thesis. I am grateful to Donald Knuth for developing T_EX; Leslie Lamport, and others for building the L^AT_EX ecosystem. It would have been a great pain if such open-source tools didn't exist for typesetting this thesis. All the drawings contained in this thesis are made using TikZ, which allows one to be very precise and programmatically manipulate the figures. Reading contemporary papers is crucial in research, and for this, I acknowledge many open science initiatives for providing easy access to literature. Stack Overflow and its sister communities have been lifesavers. Starting from doubts regarding syntax and example usage of even simple things such as dictionary enumeration in Python to nicely typesetting various parts of this thesis to resolving compilation errors, debugging simulation codes, and many other algorithmic puzzles, the online portals such as Stack Overflow, Stack Exchange, and others have answered many of these questions. I would like to contribute back to the community by making the source codes of the TikZ figures and other materials used in this thesis publicly available through my personal webpage: <https://ratcoinc.github.io/>.

I can only express my heartfelt gratitude to my parents for their uncountable sacrifices

for me. My parents were my first formal teachers in my life. My mother, who didn't get the chance to pursue any higher studies, has been able to give me a basic education during my school life, which has been the foundation of my higher studies. My father, who didn't even cross the 8th grade mark due to financial crisis, was my early math teacher. My maternal uncle, the late Prabir Dutta, also helped me with mathematics during my school life, especially for competitive exams. I also thank my other family members and my cousins, especially Pramita, for their unconditional support and love. I would also like to mention my childhood friends, namely Sayan, Roodraditya, Souvik, and Haimanti, among others, for being there when I needed them the most.

Lastly, I would like to mention Tania, my better half, for her many sacrifices and compromises to support me during my PhD. I cannot thank her enough for her never-diminishing love and care, despite my tantrums and negligence. I only hope to be worthy of being called her better half as well.



Rathindra Nath Dutta

December 2023

Abstract

Device-to-device (D2D) communication has been envisioned as the solution to the bandwidth scarcity problem in the era of exponentially growing smart handheld devices. In D2D communications, two or more user equipment (UEs) are allowed to directly communicate with each other with limited or no involvement of the base station (BS). Since the number of available frequency channels is limited, one must judiciously allocate the channel resources among the demanding UEs. In cases where the direct communication link between two UEs offers poor signal quality, an idle UE may be judiciously selected to establish a relay-aided indirect communication link. To cope with the high bandwidth demands of modern applications, D2D communication using millimeter-wave (mmWave) signals has been proposed due to its improved spectral efficiency, higher data rates, and lower delays. The major challenge of using mmWave signals is that they suffer from high penetration and propagation losses and thus require short-distance obstacle-free line-of-sight (LOS) communication.

The two problems, namely channel allocation and relay selection, have inherent interdependencies and thus must be jointly dealt with. To this end, in our first work of this thesis, we have tried to address the joint relay selection and channel assignment problem (JRSCAP) for D2D communications, and devised a near-optimal algorithm with polynomial time complexity.

Both user mobility and the presence of static as well as dynamic obstacles can severely affect an mmWave communication link. Next, in this thesis, we have investigated the JRSCAP for mobile UEs in the presence of obstacles. After proving the hardness of this joint problem, we provide a greedy solution along with its approximation bound.

For an energy-efficient green communication network, one must jointly allocate the frequency channel to requesting users as well as control their transmit power. As mentioned, the presence of obstacles can break an mmWave communication link, which may require a retransmission and contribute to wasteful energy consumption. While static obstacles are easier to avoid, dynamic obstacles pose the main hurdle, as they move independently

outside the purview of the BS. Here, we have proposed a [reinforcement learning \(RL\)](#) framework for the [joint power and channel allocation problem \(JPCAP\)](#) for maximizing energy efficiency in the presence of dynamic obstacles.

Information about dynamic obstacles can also be learned from link failures. To obtain a complete knowledge about the whole service area, sometimes we may be required to non-optimally allocate resources so that all requesting links get an equal chance of activation. Although such non-optimal allocations are undesirable, they help in acquiring information about all the links uniformly. This brings us to the infamous exploration–exploitation dilemma. To this end, we have proposed a systematic way of inducing non-optimality in [JPCAP](#). Given the hardness of this problem, we have devised a greedy solution and shown its effectiveness.

In many modern applications, such as video streaming, the same data packets may need to be delivered to a group of users. Multicasting these packets has a clear advantage over repeated unicasts. Due to the dynamic nature of wireless communication links, establishing a stable multicast communication route is a challenging task, especially in the presence of dynamic obstacles. We address the [multicast link selection problem \(MLSP\)](#) as our final work in this thesis and present an optimal algorithm for stable link selection in the presence of dynamic obstacles.

For all of our work in this thesis, we have performed extensive simulations and shown that our proposed solutions outperform existing state-of-the-art approaches.

Publications out of this Thesis

Journals

- [J1] **Rathindra Nath Dutta** and Sasthi C. Ghosh. “Mobility aware resource allocation for millimeter-wave D2D communications in presence of obstacles”. In: *Computer Communications (Elsevier)*, Vol. 200 (Feb. 2023), pp. 54–65. ISSN: 0140-3664. DOI: [10.1016/j.comcom.2022.12.025](https://doi.org/10.1016/j.comcom.2022.12.025).

Conferences

- [C1] **Rathindra Nath Dutta** and Sasthi C. Ghosh. “Resource Allocation for Millimeter Wave D2D Communications in Presence of Static Obstacles”. In: *Proceedings of the 35th International Conference on Advanced Information Networking and Applications (AINA-2021), Toronto, ON, Canada, 12-14 May, 2021*. Vol. 225. Lecture Notes in Networks and Systems (LNNS). Springer, 2021, pp. 667–680. ISBN: 978-3-030-75100-5. DOI: [10.1007/978-3-030-75100-5_57](https://doi.org/10.1007/978-3-030-75100-5_57).
- [C2] **Rathindra Nath Dutta** and Sasthi C. Ghosh. “Joint Relay Selection and Frequency Allocation for D2D Communications”. In: *Proceedings of the 17th EAI International Conference on Quality, Reliability, Security and Robustness in Heterogeneous Systems (QShine 2021), November 29-30, 2021*. Vol. 402. Lecture Notes of the Institute for Computer Sciences, Social Informatics and Telecommunications Engineering (LNICST). Springer, 2021, pp. 159–173. DOI: [10.1007/978-3-030-91424-0_10](https://doi.org/10.1007/978-3-030-91424-0_10).
- [C3] **Rathindra Nath Dutta** and Sasthi C. Ghosh. “Obstacle Aware Link Selection for Stable Multicast D2D Communications”. In: *Proceedings of the 3rd International Conference on Computer and Communication Engineering (CCCE 2023), Stockholm, Sweden, 10-12 March, 2023*. Vol. 1823. Communications in Computer and Information Science (CCIS). Springer, 2023, pp. 54–66. ISBN: 978-3-031-35299-7. DOI: [10.1007/978-3-031-35299-7_5](https://doi.org/10.1007/978-3-031-35299-7_5).
- [C4] **Rathindra Nath Dutta** and Sasthi C. Ghosh. “Energy Efficient Resource Allocation for D2D Communications using Reinforcement Learning”. In: *2023 IEEE 48th Conference on Local Computer Networks (LCN)*. Oct. 2023, pp. 1–7. DOI: [10.1109/LCN58197.2023.10223387](https://doi.org/10.1109/LCN58197.2023.10223387).
- [C5] **Rathindra Nath Dutta** and Sasthi C. Ghosh. “Non-optimal is Good! Resource Allocation in Presence of Dynamic Obstacles in D2D Networks”. In: *2023 IEEE 48th Conference on Local Computer Networks (LCN)*. Oct. 2023, pp. 1–7. DOI: [10.1109/LCN58197.2023.10223393](https://doi.org/10.1109/LCN58197.2023.10223393).

Table of Contents

Acknowledgements	v
Abstract	ix
Publications out of this Thesis	xi
Table of Contents	xiii
List of Acronyms	xvii
List of Symbols	xxi
List of Figures	xxiii
List of Tables	xxv
List of Algorithms	xxvii
1 Introduction	1
1.1 Background	2
1.1.1 Device-to-Device Communications	2
1.1.2 Wireless Communications	3
1.1.3 Millimeter-Wave Signal	6
1.1.4 Relay-Aided Communications	8
1.1.5 Multicast Communications	9
1.2 Challenges in D2D Communications	10
1.2.1 Channel Allocation	10
1.2.2 Relay Selection	11
1.2.3 User Mobility	11
1.2.4 Presence of Obstacles	12
1.2.5 Green Communications	13
1.2.6 Multicast Communications	13
1.3 Motivation and Contribution of this Thesis	14
1.4 Outline of this Thesis	20

2	Literature Review	21
I	Channel Allocation and Relay Selection	31
3	Joint Channel and Relay Selection for D2D Communications	33
3.1	A Motivating Example	34
3.2	System Model	36
3.3	Problem Formulation	40
3.4	Joint Relay Selection and Frequency Assignment	43
3.5	Simulation Results	46
3.6	Conclusion	50
4	Channel and Relay Selection for Mobile Users in Presence of Obstacles	51
4.1	System Model	54
4.2	Problem Formulation	59
4.2.1	Developing an SIP Model	59
4.2.2	Proving Hardness	61
4.2.3	Solving the SIP	62
4.3	Proposed Algorithm	64
4.3.1	Precomputation	64
4.3.2	Finding Candidate Relays	65
4.3.3	Critical Region of an mmWave Beam	67
4.3.4	Proposed Greedy Algorithm	67
4.3.5	Procedure APX_MIS()	72
4.3.6	Analysis of the Proposed Algorithms	73
4.4	Simulation Results	77
4.5	Conclusion	84
II	Obstacle Aware Green Communications	85
5	Joint Channel and Power Allocation Using Reinforcement Learning	87
5.1	System Model	89
5.2	Problem Formulation	92
5.3	Proposed Reinforcement Learning Framework	93
5.3.1	Basics of Q -learning	93
5.3.2	Frequency and Power Allocation Using Q -learning	95
5.3.3	Convergence and Optimality Guarantees	98
5.4	Simulation Results	101
5.5	Conclusion	104

6	Non-Optimal is Good: Towards Long Term Stable Link Allocation	107
6.1	System Model	109
6.2	Problem Formulation	111
6.3	Proposed Solution	113
6.3.1	Greedy Resource Allocation	113
6.3.2	Power Optimization using LP	114
6.3.3	Procedure <code>APX_WMIS()</code>	116
6.4	Estimating Link Stability	116
6.5	Simulation Results	118
6.6	Conclusion	122
III	Multicast D2D Communications	123
7	Obstacle Aware Multicasting for D2D Communications	125
7.1	System Model	127
7.2	Problem Formulation	129
7.3	Obstacle-Aware Multicast Link Selection Algorithm	130
7.4	Learning Blockage Probabilities	132
7.5	Simulation Results	135
7.6	Conclusion	139
8	Conclusion and Future Directions	141
	List of References	145

List of Acronyms

3GPP 3rd generation partnership project.

5G fifth-generation technology standard for broadband cellular networks.

5G-NR 5G new radio.

\mathcal{APX} -hard Complexity class for deterministic polynomial time solvable problems.

AR augmented reality.

BS base station.

CAP channel assignment problem.

CDN content delivery network.

CSI channel state information.

D2D Device-to-device communications.

dB decibel, a relative unit for measuring strength of a signal.

DVMRP distance vector multicast routing protocol.

EM electromagnetic.

eMBMS enhanced MBMS.

eNB evolved NodeB (LTE-A base station).

FDMA frequency-division multiple access.

gNB gNodeB (5G-NR base station).

IGMP internet group management protocol.

ILP integer linear program.

IoT internet of things.

IRS intelligent reflecting surface.

JPCAP joint power and channel allocation problem.

JRSCAP joint relay selection and channel assignment problem.

LOS line-of-sight.

LP linear program.

LTE long term evolution.

LTE-A LTE-advanced.

MBMS multimedia broadcasting multicast services.

MDP Markov decision process.

MILP mixed-integer linear program.

MIMO multiple-input multiple-output.

MIS maximum independent set.

MLSP multicast link selection problem.

mmWave millimeter-wave.

MOSPF multicast extension of open shortest path first routing.

MST minimum spanning tree.

\mathcal{NP} Complexity class for non-deterministic polynomial time solvable problems.

\mathcal{NP} -Complete Complexity class for the hardest problems in \mathcal{NP} .

OFDMA orthogonal frequency-division multiple access.

\mathcal{P} Complexity class for deterministic polynomial time solvable problems.

PIM protocol-independent multicast.

POMDP partially observable Markov decision process.

PTAS polynomial time approximation scheme.

Q-learning a model-free reinforcement learning algorithm.

QoS quality of service.

RL reinforcement learning.

RSS received signal strength.

Rx receiver.

SINR signal-to-interference-plus-noise ratio.

SIP stochastic integer program.

Tx transmitter.

UE user equipment.

V2X vehicle-to-anything.

VR virtual reality.

List of Symbols

- G_m Mainlobe gain of an antenna.
- G_s Sidelobe gain of an antenna.
- I Interference.
- M A suitably large (positive) constant.
- N_p Number of elements in an antenna array.
- P_{\max} Maximum transmit-power.
- P_{\min} Minimum transmit-power.
- Γ Signal-to-interference-plus-noise ratio (SINR).
- \Pr Probability of an event.
- \mathbb{E} Expected value.
- ρ Probability threshold.
- Rx** Receiver.
- Tx** Transmitter.
- ξ Energy efficiency.
- ζ SINR threshold.
- d_{\max} Maximum D2D communication distance.

List of Figures

1.1	Hexagonal cellular network architecture	2
1.2	An example scenario of D2D communication	4
1.3	Electromagnetic spectrum	4
1.4	Beamforming of a signal using antenna arrays	7
1.5	An example of a relay-aided communication avoiding an obstacle	8
1.6	A multicasting scenario	10
1.7	Different multicast trees	14
3.1	Motivation for joint relay selection and channel assignment	35
3.2	An example scenario	37
3.3	Slot reduction using network coding for two-way communication	39
3.4	Interference from other transmitters for the two time slots	40
3.5	Plot of active links and system throughput (without network coding)	48
3.6	Plot of comparison against optimal solution (with network coding)	49
4.1	Grid approximation of an obstacle	55
4.2	Relay-aided communication avoiding an obstacle	55
4.3	Obtaining Candidate Relays	66
4.4	Critical region	67
4.5	Plot of activated links count versus system load	78
4.6	Plot of average throughput versus system load	79
4.7	Plot of activated links count versus datarate threshold	79
4.8	Plot of links failures versus system load (with only static obstacles)	80
4.9	Plot of link failures versus the system load (with dynamic obstacles)	81
4.10	Plot of average system throughput versus system load (with obstacles)	82
4.11	Plot of fairness versus system load (with obstacles)	82
4.12	Plot of link failures versus system load (with user mobility and obstacles)	83
4.13	Plot of inaccuracy versus grid size with varying obstacle sizes	84
5.1	An example scenario	90
5.2	Plot of convergence of our proposed algorithm	103
5.3	Plot of turn-around time versus obstacle count	104
5.4	Plot of energy-efficiency versus obstacle count	104

5.5	Plot of energy-efficiency versus demand levels	105
5.6	Plot of running time versus user count	105
6.1	Plot of activated links versus k	120
6.2	Plot of link failures versus k	120
6.3	Plot of fairness versus k	121
6.4	Plot of energy-efficiency versus k	121
6.5	Plot of convergence of mean squared error	122
7.1	Discretization of the service area	128
7.2	Plot of convergence of the proposed learning framework	136
7.3	Plot of stability verses group size	137
7.4	Plot of stability verses obstacle count	138
7.5	Plot of effect of grid approximation	138

List of Tables

1.1	Attenuation against different obstacles for mmWave communications	12
3.1	Notations used throughout Chapter 3	39
3.2	Simulation Parameters	47
4.1	Notations used throughout Chapter 4	58
4.2	Simulation Parameters	77
5.1	Notations used throughout Chapter 5	91
5.2	Simulation Parameters	102
6.1	Simulation Parameters	119

List of Algorithms

3.1	Joint relay selection and channel allocation	45
3.2	Integer conversion of the relaxed variables	46
4.1	Precomputation of visibility and blockage matrices	65
4.2	Constructing candidate relay sets	67
4.3	Initial frequency class formation	70
4.4	Updating frequency classes	72
5.1	The Q -learning algorithm	95
5.2	Resource allocation using Q -learning	97
6.1	Greedy resource allocation	115
6.2	Updating blockage information	118
7.1	Stable multicast tree construction	131
7.2	Learning blockage probabilities	135

CHAPTER 1

Introduction

Due to recent technological advancements, number of smart handheld **user equipment (UE)** has seen an exponential growth over the past decade. The total number of internet users is expected to cross 5 billion mark by 2023 [1] of which 1.2 billion cell phone users are from India alone [2]. This has led to dramatic increase of bandwidth intensive mobile applications such as video calling, video streaming, mobile gaming and others, and has already saturated the capacities of traditional licensed frequency spectrum in **long term evolution (LTE)** networks. In **fifth-generation cellular networks (5G)**, datarate has been increased by at least 5 times over the earlier generation [3]. This is still inadequate, as modern applications tend to demand higher datarate and lower latency. In **5G new radio (5G-NR)**, several new technologies, such as direct device-to-device communication, millimeter-wave communication, beamforming and others, have been introduced to mitigate this bandwidth scarcity problem, and standardized by the **3rd generation partnership project (3GPP)**. **5G-NR** introduces new sub-6 GHz frequency bands [4], as well as unlicensed bands operating in 30-60 GHz frequency range [5], promising gigabit speeds [6].

In order to harness the full potential of a communication system, the limited channel resources must be carefully assigned among the devices. Relay-aided cooperative communication has also been considered which require proper selection of relays and also allocating channel resources to them. Due to device mobility and the presence of obstacles, the quality of a communication link may suffer significantly, which makes the resource allocation problem much harder. Furthermore, for battery-constrained smart devices, energy-efficient communication is a must, which demands optimal allocation of transmit power. Moreover, efficient distribution of a data packet to a group of devices is required by many modern applications (livestreaming, content delivery, and others). Due to the heterogeneous nature of wireless links, link selection for such multicast applications is more challenging compared to unicast ones. These are the issues that we have tried to address in this thesis and devised efficient algorithms for them.

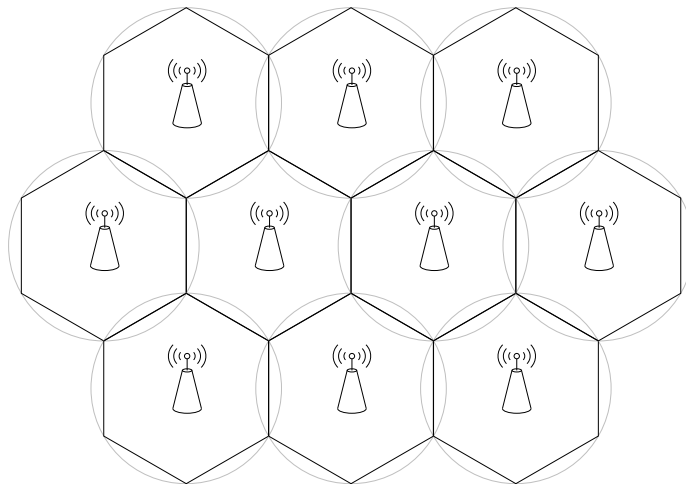


Figure 1.1: Hexagonal cellular network architecture

1.1 Background

Before delving any deeper, let us first lay out a few terminologies relevant to this thesis.

1.1.1 Device-to-Device Communications

In a traditional LTE network, the **base station (BS)**, also known as cell tower, is responsible for transmitting and receiving wireless signals to and from the mobile **UEs** within its coverage area. Typically, a geographical region is divided into regular hexagonal grids, and a **BS** is placed at the center of each such hexagon as depicted in [Figure 1.1](#). The available frequency channels are distributed among these **BSs** in such a way, that two nearby **BSs** do not share the same frequency channels [7]. In this centralized architecture, all communications between a pair of **UEs** must be routed via the **BS**, which incurs a significant communication delay. As the number of simultaneous communications grows, the limited capacity of the **BS** quickly becomes a bottleneck for the achievable end-to-end datarate. This has led to the conceptualization of direct communication between a proximal pair of devices, bypassing the **BS**.

The **device-to-device (D2D)** communication is the enabling technology that allows two nearby devices to directly communicate with each other with limited or no involvement of the **BS** [8]. Since the received signal strength decays with the transmission distance, communication over a close proximity promises higher datarate, lower delay, and reduced power

consumption. Furthermore, it allows same frequency channels to be simultaneously shared among multiple users, which increases the *spectral-efficiency* [9, 10]. The spectral-efficiency denotes how efficiently the limited frequency spectrum is being utilized and measured as the data transmission rate per unit bandwidth. The idea of direct communication is not a very contemporary concept, as it has already been realized through the standards like Bluetooth (IEEE 802.15.1), Zigbee (based on IEEE 802.15.4), and Wi-Fi Direct¹. Famous device-to-device wireless file transfer app services like Google’s Nearby Share² for Android/Windows, and Apple’s AirDrop³ for iOS/macOS are primarily based on Wi-Fi Direct and Bluetooth. Since these services use available frequency channels in the unlicensed band, and may suffer from uncontrolled interference from other users, the **quality of service (QoS)** of an end user may not be guaranteed. This brings us to the standardization of **D2D** communication in **5G-NR**.

For the purpose of this thesis, we consider a single cell with the **BS**, also called **evolved NodeB (eNB)**, placed at its center. Researchers have studied two modes of **D2D** communications, namely *underlay* mode and *overlay* mode [11]. In underlay mode, the same frequency channels that are being used for traditional cellular communications via **BS**, are reused for **D2D** communications. In contrast, **D2D** communications in overlay mode are done using a dedicated frequency band, which does not interfere with existing **LTE** communications. For the rest of this thesis, we consider only the overlay mode of **D2D** communications. Furthermore, we assume that the **BS** is responsible for controlling and scheduling the **D2D** communication links. A sample **D2D** communication scenario is depicted in **Figure 1.2**. As evident there are ten active users (UE_1 to UE_{10}) and six idle devices (UE_{11} to UE_{16} , colored in gray). The pairs UE_1 - UE_2 and UE_5 - UE_6 are sharing the frequency channel f_1 , and pairs UE_3 - UE_4 and UE_7 - UE_8 are using the channel f_2 , while the pair UE_9 - UE_{10} transmits using frequency f_3 . Note that, like any cellular communication, **D2D** communications also rely on wireless transmissions of data, which we describe next.

1.1.2 Wireless Communications

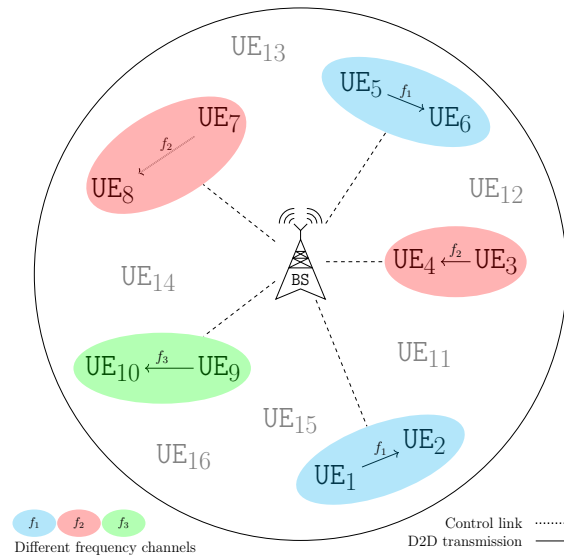
In wireless communication, information is transmitted without the use of any physical cables or wired connections. It typically uses the physical properties of an **electromagnetic**

Description of all terminologies is beyond the scope of this thesis; interested readers may refer to these:

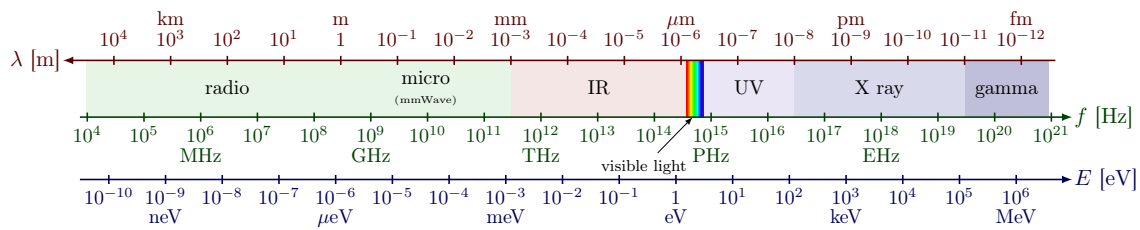
¹Wi-Fi Direct: <https://www.wi-fi.org/discover-wi-fi/wi-fi-direct>

²Nearby Share: <https://blog.google/products/android/nearby-share-windows/>

³AirDrop: http://ipad.about.com/od/iPad_Guide/ss/What-Is-Airdrop-How-Does-It-Work.htm

Figure 1.2: An example scenario of D2D communication¹

(EM) signal to carry the data through the air or space. The electromagnetic spectrum encompasses all types of EM signals ranging from radio waves to visible lights to X-rays, and gamma rays as depicted in Figure 1.3. According to the *dispersion relation*, the wavelength (λ) of a EM signal is inversely proportional to its frequency (f). In free space, we have $c = f\lambda$, where c is the speed of light in vacuum. As evident in Figure 1.3, the wavelength decreases with increasing frequency, while the energy (E) increases.

Figure 1.3: Electromagnetic spectrum²

A wireless signal propagating through the air or space, can experience various challenges, such as attenuation, reflection, diffraction, and interference. These factors affect

¹The TikZ code for BS is adapted from: <https://tex.stackexchange.com/a/110022>

²Modified the TikZ code available at: https://tikz.net/electromagnetic_spectrum/.

the quality of wireless communications. The signal quality of wireless communications depend on factors like transmit power, frequency, antenna characteristics, and environmental conditions. Researchers have developed several empirical models to capture the path-loss of a radio wave propagation [12–14]. For a **transmitter (Tx)**, **receiver (Rx)** pair, the power of the received signal at **Rx** can be expressed by [Equation \(1.1\)](#).

$$R_{\text{Tx,Rx}} = P_{\text{Tx}} h_{\text{Tx,Rx}} G_{\text{Tx}} G_{\text{Rx}} d_{\text{Tx,Rx}}^{-L} \quad (1.1)$$

where:

- P_{Tx} = transmit power at **Tx**
- $h_{\text{Tx,Rx}}$ = channel gain
- G_{Tx} = transmitter antenna gain
- G_{Rx} = receiver antenna gain
- $d_{\text{Tx,Rx}}$ = distance between the transmitter and the receiver
- L = pathloss exponent

Often the signal strength is expressed in **decibel (dB)** relative to one watt, or dBW. Thus, we have the following relation. Similarly, if the references point is in milliwatt we express the power in dBm.

$$P_{\text{dBW}} = 10 \log_{10}(P_{\text{watt}}/1\text{watt})$$

where:

- P_{dBW} = power in decibels
- P_{watt} = power in watt

Since multiple devices may communicate using the same frequency channel, they may get interferences from other devices. The interference is nothing but the sum of unwanted received signal powers from neighboring devices and can be calculated similarly. The effective signal quality is measured by the **signal-to-interference-plus-noise ratio (SINR)** as defined in [Equation \(1.2\)](#).

$$\text{SINR}_{\text{Tx,Rx}} = \frac{R_{\text{Tx,Rx}}}{I_{\text{Tx,Rx}} + \eta_0} \quad (1.2)$$

where:

- $R_{\text{Tx,Rx}}$ = (wanted) received power at **Rx** from **Tx**
- $I_{\text{Tx,Rx}}$ = (unwanted) received power at **Rx** from devices other than **Tx**
- η_0 = noise power of the system

The capacity of a communication link, commonly known as the datarate, is calculated by the Shannon's capacity formula as given in Equation (1.3) and measured in bits/sec.

$$\text{datarate}_{\text{Tx,Rx}} = B \log_2(1 + \text{SINR}_{\text{Tx,Rx}}) \quad (1.3)$$

where: $\text{SINR}_{\text{Tx,Rx}}$ = SINR value of the communication link
 B = bandwidth of the communication channel in Hz

One way to increase the datarate is to make the communication distance ($d_{\text{Tx,Rx}}$) shorter, which also reduces transmit-power requirements and thus minimizes interference, making it more energy-efficient. This is the key idea behind D2D communications. The other way of increasing the datarate is to select a communication channel having a wider bandwidth, which brings us to our next topic.

1.1.3 Millimeter-Wave Signal

Due to physical properties of wireless transmission, wider bands are easier to acquire and process at higher frequencies [15], which directly translates into higher datarate. Communication using gigahertz frequencies having small wavelength (typically measured in millimeters) is called millimeter-wave (mmWave) communication [16]. Experiments with mmWave signals date back to 1895, when Indian physicist Sir Jagadish Chandra Bose demonstrated 60 GHz mmWave transmission over a distance of 23 meters [15]. Although communications using mmWave signals offer more bandwidth [6], they require more transmission power and are also susceptible to high signal attenuation [17]. Thus, the traditional LTE BS can not be equipped with mmWave signals as their coverage area typically ranges up to a few kilometers [18]. With the advent of small cell BS having smaller coverage areas (up to a few hundred meters), the mmWave signals are being used for high speed communications [19–21]. Advancements in antenna technologies now allow devices to be equipped with multiple-input multiple-output (MIMO) antennas, where more than one transceiver¹ is present. Presence of such antenna arrays enables *beamforming* of the signal, which allows a transmitter to direct its signal (beam) towards its intended receiver as depicted in Figure 1.4. As evident, beamforming helps to reduce the interference for nearby users, which was not possible in traditional systems where the signal is broadcasted in all directions. The *mainlobe* of the signal beam is steered to the intended receiver either

¹A transceiver is a combination of a transmitter and a receiver.

mechanically (by physically moving the antenna) or electronically (with the help of phase shift and constructive/destructive interferences). Thereby, beamforming is the key technique to compensate for the severe channel attenuation and reduce interference in **mmWave** networks [22]. Nearby devices may still face some interference due to the small *sidelobes*, which can often be ignored [23, 24]. Thus, **mmWave** communication behaves like an optical signal with almost zero leakage interferences, and is often referred to as pseudo-wire communication [24, 25].

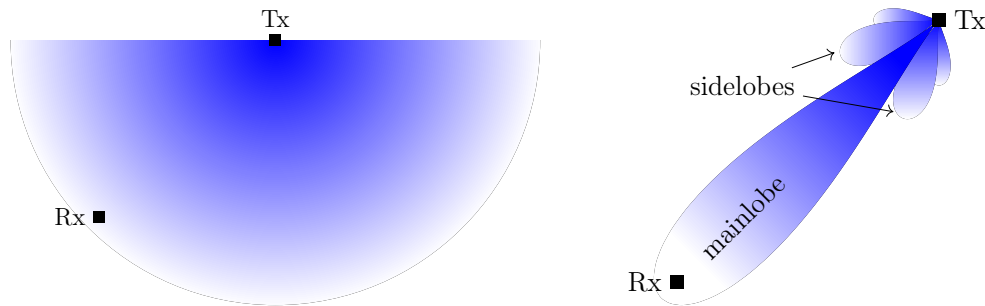


Figure 1.4: Beamforming of a signal using antenna arrays

Due to the pseudo-wire like communication characteristic of **mmWave**, a *flat-top* model of beamforming is often assumed, where interference due to the sidelobes are completely ignored [23, 24]. In flat-top model of communication, a nearby device faces interference only if it falls inside the mainlobe of any other device transmitting in the same frequency channel. The area of the mainlobe is defined by the beamwidth of the signal which depends on the number of antenna elements in the antenna array, and contributes unit gain. A more realistic model also considers the interference due to sidelobes. If there are $\sqrt{N_p} \times \sqrt{N_p}$ antenna elements present, we have the following: beamwidth $\phi = \sqrt{3/N_p}$, mainlobe gain $G_m = N_p$ and the sidelobe gain $G_s = 1/\sin^2(3\pi/2\sqrt{N_p})$ [9, 26]. Although even for a narrow beam it takes a few hundred microseconds for antenna alignment to steer the signal beam towards its intended receiver, this alignment overhead is negligible compared to actual data transmission time which is typically ranges in the order of seconds [27]. For the rest of this thesis, we thus assume that the signal beams are always aligned for a Tx-Rx pair.

Previously **mmWave** bands have been explored for backhaul communications between small cell base stations called **gNBs** [28–31]. New standards, such as WiGig¹, for **mmWave** communications in 60 GHz bands are being introduced [15, 32, 33]. The pseudo-wire

¹WiGig: <https://www.wi-fi.org/discover-wi-fi/wi-fi-certified-wigig>

like communication capability of **mmWave** signals, makes it a perfect candidate for short distance **D2D** communications [24], and has gained considerable interest over the past few years [34–36]. It has been reported that pairing **D2D** with **mmWave** provides massive capacity and even lower latency to unlock the full **5G** experience [37]. Evidently, in this thesis, we consider **D2D** communications happening over the 60 GHz **mmWave** channels.

1.1.4 Relay-Aided Communications

In cases where direct communication path is blocked by some obstacle or the channel is suffering from high interferences from neighboring devices, one may opt for a relay-aided communication. Here the source device routes its data via one or more intermediate relays to finally reach its destination. The full potential of cooperative communication can be unlocked by allowing device relaying; thus, for **D2D** communications, idle **UEs** may act as potential relays [8, 38]. Since relaying consumes computing and communication resources, it should be compensated by setting appropriate prices [39] or by some other incentives such as *energy harvesting* [40]. Recently **intelligent reflecting surfaces (IRSs)** are also being considered for signal relaying [40–43]. Since **IRS** are placed on fixed locations they serve as stationary relays. In this thesis, we therefore consider idle (possibly mobile) **UEs** to serve as relays. Thus, the solutions presented in this thesis can easily be extended for **IRS** aided **D2D** communications. A sample relay-aided **D2D** communication is depicted in **Figure 1.5**. Here, **UE₁** is using **UE₃** to relay its data to **UE₂** as the direct path between **UE₁** and **UE₂** is blocked by an obstacle.

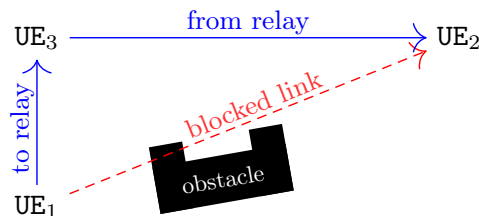


Figure 1.5: An example of a relay-aided communication avoiding an obstacle

Relaying via **UEs** typically uses the store-and-forward relaying [44] method, where the data is first cached at the relay node, then forwarded to the next hop or to the destination. Since the **UE** can have only limited buffer space, the received data is almost immediately sent out, which also minimizes the transmission delay. Since increasing the number of hops

(intermediate relays) increases the delay overhead, we therefore restrict ourselves only to single hop relay-aided communications for the purpose of this thesis. In such cases, the overall effective SINR is taken as the minimum of the two legs namely, source to relay link and the link from relay to destination.

1.1.5 Multicast Communications

Many modern applications such as video streaming, augmented reality (AR)/virtual reality (VR) gaming, content delivery networks (CDNs), automotive internet of things (IoT), public safety system, autonomous vehicles etc., require same data packets to be delivered among multiple users [45, 46]. One of the simplest (yet guaranteed) ways to distribute data packets among a set of users is *flooding*. In simple flooding, each node in the network, *broadcasts* each received packets to all its connected devices. Thus, the entire network is flooded with the copies of these data packets. Flooding the entire network therefore consumes significant power and network resources, and increases the network traffic which in turn increases the delay in packet delivery. Recently *gossip* protocol [47] is being considered to reduce the overhead in flooding.

In cases where the data packets may be actually needed to be delivered only among a handful of users (forming a group), flooding the entire network in order to broadcast some data packets is not desirable and gave rise to the study of *multicast* techniques [48]. In multicasting, a transmitter can simultaneously send data to more than one receiver [46]. The multicasting ability of a UE has already been considered in LTE-A. For efficient delivery in broadcast and multicast services, multimedia broadcasting multicast services (MBMS) [48, 49] was proposed in LTE networks, which was later upgraded to enhanced MBMS (eMBMS) [50, 51]. Many telecom operators now support eMBMS and it has been incorporated into major smartphone operating systems [52].

It is not surprising that the fusion of the two realms, namely D2D communications and multicasting, enables efficient data distribution and group communication among nearby users without relying on the conventional LTE network [53]. Thus multicast D2D communication has gained considerable interest for the scenarios such as public safety communications, local group collaboration, live event streaming, vehicle-to-anything (V2X) communications, among others [45, 46, 54]. A sample multicast scenario is depicted in Figure 1.6, where UE₀ is multicasting to UE₁, UE₂, UE₃, UE₄ and UE₅. Note that UE₆-UE₁₀ do not receive any data as they are not part of the considered multicast group.

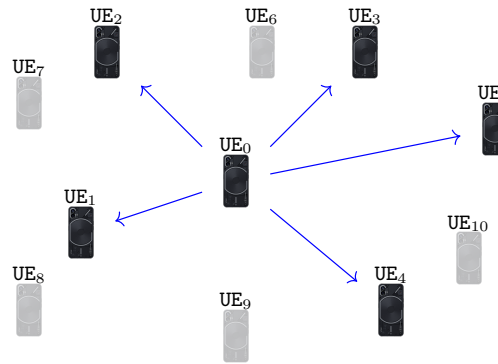


Figure 1.6: An example of D2D multicast scenario¹

1.2 Challenges in D2D Communications

In order to harness the full potential of **D2D** communications, one must judiciously schedule the requesting communication links. There are several challenges in **D2D** communications, such as resource scarcity, user mobility, presence of obstacles etc., which are subsequently described in greater detail.

1.2.1 Channel Allocation

As mentioned earlier, a wireless **D2D** communication requires a communication channel, for which a carrier frequency band (such as 60 GHz) is selected. Since there are multiple users simultaneously requesting for a communication channel, the frequency band must be shared among them. One way to share the available frequency band, is by using **frequency-division multiple access (FDMA)**, where the entire channel bandwidth is split into many non-overlapping *subchannels*. In **orthogonal frequency-division multiple access (OFDMA)**, co-channel interference is almost negligible, and thus it is now widely accepted [55]. For example, in 60 GHz band, we typically have a bandwidth of 2 GHz, which can be divided into 10 subchannels each of about 200 MHz wide [26]. Even with this subdivision of the available frequency band, it is still not adequate to assign each requesting user a dedicated subchannel. Therefore, these subchannels must be shared among these users. Two or more **D2D** links may share the same channel, only if their **SINR** levels are above some predetermined threshold. This **SINR** threshold, is dictated by the underlying application.

¹From now on, my current handset, *Nothing Phone (1)*, has been used as the model for the UEs.

Therefore, the objective of the **channel assignment problem (CAP)**, is to optimally allocate the subchannels among the requesting users by satisfying their **SINR** requirements, so as to maximize the overall resource utilization. It can be observed that the **CAP** has a close resemblance to the classical vertex coloring problem in graphs, and with a simple reduction it can be shown that **CAP** is also **\mathcal{NP} -Complete** [7]. Unless $\mathcal{P} = \mathcal{NP}$, it is computationally intractable to optimally solve the **CAP** for large input instances. This necessitates the study of efficient channel allocation algorithms for **D2D** communications which can produce near optimal solutions.

1.2.2 Relay Selection

A relay device can possibly be a relay candidate for many **D2D** pairs due to its spatial location. Similarly, a **D2D** pair may have many candidate relays available in its vicinity. Note that, here we are considering only device relaying, and the number of idle **UEs**, willing to act as relays, is limited. Moreover, each idle **UE** can participate in at most one relay-aided communication at a time. Therefore, the aim of the relay selection problem is to judiciously assign the relays to the requesting **D2D** pairs, so that the overall system utilization maximizes. Given a channel allocation scheme, the relay selection problem boils down to two-dimensional matching problem, which is in \mathcal{P} , and can be efficiently solved by the Hungarian¹ method [58]. We argue that solving relay selection and channel allocation in successive stages may lead to suboptimal utilization of the resources. Thus, it is desirable to deal with the two problems jointly. Although selecting relays in combination with channel allocation has the potential to yield greater system utilization, it no longer remains in \mathcal{P} . Therefore, the **joint relay selection and channel assignment problem (JRSCAP)** requires further investigation.

1.2.3 User Mobility

Mobility of the **UEs** makes the channel allocation as well as relay selection much harder. Since the devices are moving, their distance may increase or decrease over time which affects the received signal strength. Moreover, user mobility can dramatically change the neighborhood of a device, which heavily modifies interference values. Thus, a good communication link may no longer remain viable over time. Furthermore, changing neighborhood also affects the choice of a relay candidate. Therefore, the dynamic nature of **UE** locations,

¹The Hungarian method refers to Kuhn-Munkres algorithm for solving the assignment problem [56, 57].

only adds further complications to the already hard problem of channel allocation and relay selection. Even if some mobility model [59, 60] is assumed or the mobility patterns of the users are exactly known, the **JRSCAP** still remains nontrivial due to its stochastic nature.

1.2.4 Presence of Obstacles

Presence of any obstacle on the communication path attenuates the signal, which results into degradation in data rate. Here by obstacle we imply brick walls, buildings, large billboards, moving vehicle, or even humans [61, 62]. It becomes a severe problem in case of **mmWave** communications, as these obstacles may lead to link failures. Due to its small wavelength, a **mmWave** communication suffers from high propagation and penetration losses. To paint a vivid picture, we summarize the levels of attenuation caused by a few of the common obstacles into **Table 1.1**, as reported in [15, 63–69]. Therefore, **mmWave** communications strictly require obstacle free **line-of-sight (LOS)** links between the **Tx-Rx** pairs. This stringent requirement of **mmWave** links makes the channel allocation problem even more challenging.

Object	Thickness [cm]	Attenuation [dB]
Wooden panels	1.2	3.4-7.6
Drywall	4.8	5.2
Brick	11	16.9
Concrete	5	≥ 30
Clear Glass	1	4.3
Double-pane Tinted Glass	$0.4+1.5(\text{gap})+0.4$	≥ 30
Foliage	50-100	16-27
Human	28	20-40
Vehicle		15-40

Table 1.1: Attenuation against different obstacles for 60 GHz mmWave communications

Avoiding Static Obstacles

Since the static obstacles, such as buildings, walls, etc. do not change their positions, their location and sizes can be obtained from satellite images [70], open source databases like **OpenStreetMap**¹ buildings [71], or can even be learned through link failures [61]. Given

¹OpenStreetMap: <https://www.openstreetmap.org/about>

a perfect knowledge about the static obstacles, one still need to query this database for a potential link failure before any **mmWave** link can be established. Storing the obstacle information in a space efficient way, and querying that efficiently for establishing links avoiding any static obstacles, is a challenging task.

Avoiding Dynamic Obstacles

The dynamic obstacles, such as moving vehicles, pedestrians etc., move independently outside the purview of the **BS**. The mobile nature of dynamic obstacles poses a serious concern for **mmWave** links. Even if one activates a **mmWave** link avoiding the static obstacles, the link can still abruptly break due to a blockage by some dynamic obstacle. This very mobile nature of dynamic obstacles makes it hard to acquire any information about them, and subsequently use that to predict/avoid link blockages [61, 72]. Even when we have perfect information about the dynamic obstacles, the problem of efficient storage and querying still persists, not to mention that acquiring such knowledge is itself a challenging task.

1.2.5 Green Communications

Recently, it has been observed that wireless communications contributed up to 10% of the global energy consumption and about 2% of carbon emissions world-wide [73]. Thus, such energy consumption must be reduced for a sustainable smart environment and promote *green communications* [10, 74]. In green communications, the resource utilization metric is typically its *energy-efficiency* [73, 74], which is defined as the number of bits transmitted per unit time using unit transmit-power and is measured in bits/sec/joule. Due to massive **IoT** devices connectivity, energy-efficiency poses a critical concern in modern application scenarios [75]. Although increasing the transmit-power should translate into increase in data rate, it consumes higher energy, which is not desirable for battery constrained portable smart devices. Increased transmit-power also contributes to the interference; therefore, optimizing the power level while allocating the channels for energy-efficient green communication is not a trivial task.

1.2.6 Multicast Communications

So far, we have only considered unicast communication scenarios. Since multicasting has the potential to improve spectral-efficiency over repeated unicasts, it is only natural to

explore the realm of multicasting in context of D2D communications. Multicasting over IP was first standardized back in 1986 [76]. Traditional multicasting uses [internet group management protocol \(IGMP\)](#) to manage group formations and their memberships. A family of routing protocols, commonly referred to as [protocol-independent multicast \(PIM\)](#), has been developed for multicast routing. Many routing protocols, including [multicast extension of open shortest path first routing \(MOSPF\)](#) [77], [distance vector multicast routing protocol \(DVMRP\)](#) [78], and others, have been developed for multicast routing. The multicast route is typically a *spanning tree* of underlying network topology [79, 80]. Recall that, a spanning tree of a graph is a connected subgraph that spans over all the nodes and does not contain any cycle. Depending upon the connectivity, there might exist more than one spanning tree for a given topology as depicted in [Figure 1.7](#). In such cases, we are interested in optimizing some *cost function* associated with the spanning tree, where the costs can be distance, transmission delay, link capacity etc. Several protocols [77–81] have been proposed for optimizing different multicast metrics. But these solutions may not readily work for a [mmWave](#) multicasting scenario, as they do not consider the presence of any obstacles while selecting the links. Furthermore, different links in a multicast route may suffer from different channel conditions which makes it harder to select an optimal set of links for multicasting [45, 53, 82]. Therefore, creating an obstacle-aware efficient multicast D2D route is a difficult task that merits additional investigation.

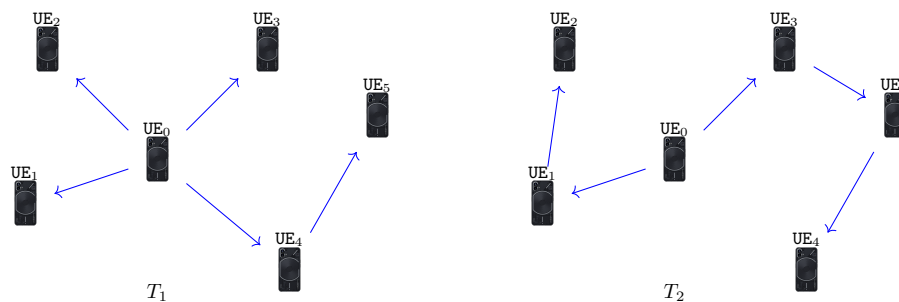


Figure 1.7: Two different multicast trees T_1 and T_2

1.3 Motivation and Contribution of this Thesis

With the aforesaid challenges of D2D communications, we are now ready to present our contributions in this thesis, which are broadly divided into three parts as presented below.

Joint Relay Selection and Channel Allocation

The channel allocation for D2D communication has been well investigated in the literature [11, 36, 73, 83–109]. Some authors have also considered relay-aided D2D communications where the problem of optimal relay selection has been explored [61, 70, 72, 110–118]. Although, relay selection and channel allocation both have considered in [58, 119–124], these works solve the two problem separately in successive stages. With a motivating example, we argue that such a two-step solution can be highly suboptimal. Even if one solves the two problems optimally independently in each step, we argue that the combined solution may still be suboptimal. Furthermore, most of the existing works do not share the frequency channels among multiple users simultaneously, which significantly diminishes the spectral-efficiency. With that in mind, we design a joint framework for relay selection and channel allocation for D2D communications, where multiple D2D links may share same frequency channel as long as their required SINR level is satisfied. This brings us to our first work, where the following contributions have been reported.

[Contribution 1.1] We consider the joint problem of relay selection and channel allocation (JRSCAP) for D2D communications. Given its computational hardness [58], we employ a linear program (LP) relaxation based greedy rounding scheme for JRSCAP, where we try to maximize the number of links activated with the available resources. The greedy rounding has been performed iteratively such that it maintains the feasibility of the final solution.

[Contribution 1.2] Furthermore, we utilize a network coding scheme for two-way relay-aided D2D communications to reduce the communication time by a factor of two. The said coding scheme allows a relay UE to simultaneously receive data from two D2D users and then relay them back again simultaneously.

[Contribution 1.3] Through simulations, we show the near optimal performance of our proposed algorithm in terms of the number of links activated. We also show that our proposed algorithm outperforms a state-of-the-art classical algorithm [58] as well as a recent one [124] in terms of number of links activated and overall system throughput.

The limitation of the above work is that it assumes a static environment with no obstacles present. Recall that mmWave D2D communications requires obstacle-free strict LOS communication links, as the presence of static as well as dynamic obstacles can result

in link failures. Furthermore, device mobility also affects the stability of a link and may also lead to a link breakage. Mobility-aware link selection for D2D communications has been dealt in [61, 72, 111, 117, 118], while few authors [61, 72, 112–118] have investigated obstacle-aware link selection. Both user mobility and the presence of dynamic obstacles make both the channel allocation and relay selection problems stochastic, as the network topology can change rapidly over time. To the best of our knowledge, none of the existing works, including the aforementioned ones, have dealt with device mobility while considering the presence of obstacles for joint relay selection and channel assignment problem. This brings us to our second work, which includes the following contributions.

[Contribution 2.1] We formally prove that joint relay selection and channel assignment problem is not only \mathcal{NP} -Complete but also \mathcal{APX} -hard, which eliminates the possibility of finding any constant factor polynomial time approximation scheme (PTAS) unless $\mathcal{P}=\mathcal{NP}$.

[Contribution 2.2] By directly incorporating device mobility and knowledge of obstacles, we pose the joint problem as a stochastic integer program (SIP), which has probabilistic constraints.

[Contribution 2.3] As dealing with the probabilistic constraints is hard, we convert our proposed SIP into an equivalent deterministic mixed-integer linear program (MILP). We utilize a standard concentration inequality, namely the Chebyshev–Cantelli inequality, for this conversion.

[Contribution 2.4] Given the computational cost of MILP for large instances, we propose a greedy solution for this. We construct an interference graph of the requesting links, where we capture the user mobility and blockages due to the presence of obstacles. We then use the notion of *defective-coloring* [125] to jointly allocate channels and select relays for the requesting users.

[Contribution 2.5] Furthermore, we derive an approximation bound of our proposed greedy solution.

[Contribution 2.6] Our proposed solution has been compared against a recent work [105], and with extensive simulations, we have shown the superiority of our proposed solution in terms of activated links, system throughput, link failures and fairness.

Channel and Power Allocation for Green Communications

Existing works, including the ones mentioned above, either assume a fixed power for all transmitting devices or allocate channels resources, namely frequency channels and transmit-powers, in separate stages. Since channel allocation and power assignment have inherent interdependencies, the two problems must be dealt with jointly to maximize energy-efficiency for green communications. Obstacle-aware resource allocation has been gaining interest over the past few years. Existing works, such as [114], assume some known distribution of the dynamic obstacles. These distributions are typically based of historical data and may not reflect the present scenario accurately. Researchers have studied the use of specialized hardware such as radar and cameras to track the dynamic obstacles [66, 72, 126], which can then be used to obtain and update these distributions. Use of such specialized hardware not only are expensive but also raises some privacy concerns [127]. Recently, researchers have proposed link failure based learning approaches to directly capture the obstacle distributions without resorting to any specialized hardware [61, 112, 115, 116, 128]. Motivated by this, we present our third work that tries to maximize the energy-efficiency by solving the [joint power and channel allocation problem \(JPCAP\)](#) in presence of dynamic obstacles. Our contributions in this work are listed below.

[Contribution 3.1] Since [JPCAP](#) in presence of dynamic obstacles involves stochastic variables, here also we formulate an [SIP](#), which involves probabilistic constraints.

[Contribution 3.2] Blockages due to the dynamic obstacles can be learned by doing trials and taking feedback from the system, which brings us to the realm of [reinforcement learning \(RL\)](#). We thus pose our joint channel and power allocation problem as an [RL](#) framework and propose a solution based on [Q-learning](#).

[Contribution 3.3] A formal proof has been crafted to show that our choice of reward function maximizes overall energy-efficiency.

[Contribution 3.4] We establish the convergence of our proposed algorithm both theoretically and experimentally. For the theoretical proof of convergence, we use the standard tool of stochastic approximation, namely the Robbins–Monro method [129].

[Contribution 3.5] Using extensive simulations, we show the effectiveness of our proposed algorithm over an existing baseline approach [107] in terms of energy-efficiency.

One major drawback of the previous approach is that it is not very scalable. Although there are methods such as function approximation, deep learning, and others for mitigating this scalability issue, they usually tend to slow down the convergence and do not provide any theoretical guarantees. Motivated by this, we went looking for other, possibly much simpler ways to address the joint power and channel allocation problem in presence of dynamic obstacles. One obvious yet simple solution is to learn from mistakes, that is, to do an optimistic link allocation and then learn the blockages from link failures [61]. One major drawback of such link failure-based learning mechanisms is that they require links to be activated infinitely often over the entire service region. Most of the existing works, including our first two works in this thesis, try to optimize some metric such as active link count, system throughput, link stability, energy efficiency, and others. With limited resources, only a subset of the requesting links can be activated. This results in skewed knowledge about the environment as the bad links are never explored and only the good ones are repeatedly exploited. To explore these deprived bad links once in a while, we are to essentially perform some non-optimal resource allocation. This brings us to our fourth work, where we address this exploration-exploitation dilemma by systematically inducing a controlled amount of non-optimality. The contributions in this work are as follows.

[Contribution 4.1] To address the aforementioned exploration-exploitation dilemma, we ensure that all requesting links are to be activated at least k number of times, where k is an input parameter. Subsequently, the joint power and channel allocation problem has been mathematically formulated.

[Contribution 4.2] We prove that the considered problem is \mathcal{NP} -Complete using a simple reduction, and propose a greedy solution for the same. We construct a weighted interference graph where the weights are used to capture the notion of k time activation of a link as well as its stability. An approximation algorithm for weighted **maximum independent set (MIS)** construction and a power control **LP** have been used to solve the joint problem. The said **LP**, checks the admissibility of a new link by solving an energy-efficient power assignment problem for a group of **D2D** links.

[Contribution 4.3] The proposed greedy solution require stability estimates for each of the requesting **D2D** links. We thus develop a *reservoir sampling* [130] based method to compute these stability values from the link failure information.

[Contribution 4.4] With extensive simulations, the effectiveness of our proposed frame-

work is validated against the standard metrics, namely active links, link failures, fairness, and energy-efficiency. We show how the choice of the parameter k affects the performance of our algorithm in terms of these metrics and compare the performance of our proposed method against existing approaches [96, 105].

Link Selection for Multicasting

Many modern applications may need the same data packets to be distributed among a group of users where multicasting is required. The previous works in this thesis, as stated above, consider only unicast D2D communications, where each communication link is treated independently of each other, which is no longer possible in multicasting. As stated earlier, one of the major challenges in multicasting is that different links may observe different channel conditions, which can dramatically vary, especially in the presence of dynamic obstacles. Armed with the capability of learning the link stability values in the presence of dynamic obstacles, we investigate the **multicast link selection problem (MLSP)** as our fifth and final work in this thesis. More specifically, we explore the MLSP for stability maximization. The contributions in this work are summarized below.

[Contribution 5.1] Given the link stability values, we present the MLSP as an optimization problem. We have formulated an **integer linear program (ILP)** where we utilize the spanning tree formulation given by Martin [131].

[Contribution 5.2] We provide an efficient algorithm to obtain the desired stable multicast route based on the standard **minimum spanning tree (MST)** finding algorithm.

[Contribution 5.3] Given the knowledge of link stability values, we prove the optimality of our proposed solution.

[Contribution 5.4] Our proposed solution requires the stability estimates of the candidate links. We use an *evidential theory* framework [132, 133] to estimate these stability values in presence of dynamic obstacles.

[Contribution 5.5] Through simulations, we demonstrate the effectiveness of our proposed method over baseline approaches namely a random allocation scheme and a fixed distribution scheme [62].

1.4 Outline of this Thesis

This thesis contains eight chapters which are summarized below.

Chapter 1: This chapter sets the stage for this thesis and outlines its key contributions.

Chapter 2: Here, we take a deep dive into the existing works to get a feel for the current state of the art and identify prospective research gaps.

Chapter 3: This chapter deals with the joint problem of relay selection and channel allocation in **D2D** communications.

Chapter 4: Here we extend the above for **mmWave** communications, and have developed a mobility-aware framework to jointly select relays and allocate channels in the presence of both static and dynamic obstacles.

Chapter 5: An energy-efficient resource allocation scheme for **mmWave D2D** communications using **RL** has been presented here, which can directly learn the blockage patterns due to dynamic obstacles through the implicit feedback mechanism of **RL**.

Chapter 6: Here we revisit the problem of channel resource allocation in the presence of dynamic obstacles and present a much simpler but effective framework that can learn the blockage probabilities by inducing a controlled amount of non-optimality.

Chapter 7: Multicast stable route selection problem for **mmWave D2D** communications in presence of obstacles has been studied in this chapter.

Chapter 8: Finally, in this chapter, we conclude our thesis by summarizing our contributions once more and indicating some future extensions of them.

Furthermore, we arrange the contributing chapters of this thesis into three parts. **Part I**, which contains **Chapters 3** and **4**, focuses on the **JRSCAP** (joint relay selection and channel assignment problem). In **Part II**, which comprises **Chapters 5** and **6**, we discuss the **JPCAP** (joint power and channel allocation problem). Lastly, **Chapter 7** of **Part III** explores the **MLSP** (multicast link selection problem).

CHAPTER 2

Literature Review

This chapter provides a detailed insight into the existing literature relevant to this thesis. Recall that this thesis primarily deals with the resource allocation problem in context **device-to-device (D2D)** communications, where each requesting link is to be allocated some frequency channel and their transmit power also needs to be decided. In cases where relay-aided communication is chosen, appropriate relays are to be selected. For **millimeter-wave (mmWave)** communication, the presence of obstacles (both static and dynamic) and user mobility poses a serious challenge. Furthermore, to enable energy-efficient green communication networks, optimal power allocation must also be decided. Lastly, due to heterogeneous wireless links, the problem of link selection for **D2D** multicasting is non-trivial, especially in the presence of dynamic obstacles. These are aspects that we have tried to address in this thesis. What follows are the existing developments related to these problems. To make it more convenient and emphasize the research gap addressed in this thesis, we divide our discussion into the following sections:

Channel Allocation

The **channel assignment problem (CAP)** is a fundamental problem in the context of cellular communications, and several techniques have been developed for it. As mentioned earlier, **CAP** is **\mathcal{NP} -Complete** [7] and requires efficient allocation algorithms to be devised. Ghosh, Sinha, and Das [7] summarized the existing works on channel allocation for cellular networks and presented a novel channel assignment framework that optimally solves the well-known benchmark instances. The problem of optimal channel assignment naturally comes up in **D2D** communications with new challenges that require the existing solutions to be redesigned [8]. The **CAP** in **D2D** communication has also been extensively studied in the existing literature. In **D2D** communications, users can communicate in one of the three modes: traditional cellular mode, **D2D** reuse mode, or dedicated **D2D** mode [93].

In cellular mode, users communicate via the **base station (BS)** through conventional cellular spectrum. In D2D reuse mode, more commonly known as *underlay* mode, a **D2D** pair opportunistically reuses cellular channels while keeping the interference under control. For dedicated **D2D** mode, also known as *overlay* mode, a dedicated channel spectrum is reserved for **D2D** communications.

Most of the initial work on channel allocation for **D2D** communications considered the underlay mode, where the **D2D** users reuse the uplink or downlink channels of the cellular users. Moreover, researchers have favored uplink channel resources over downlink ones due to better interference management and possibly to avoid any restrictions imposed by the operators [87]. Mach, Becvar, and Vanek [134] have given a very detailed survey of **D2D** communications in **orthogonal frequency-division multiple access (OFDMA)** cellular networks. The early push in D2D communications can be attributed to Doppler et al. Doppler et al. [83] proposed **D2D** communication by reusing the uplink resources to facilitate local peer-to-peer communications. In [11, 84], Doppler et al. present an architecture for integrating **D2D** communications into existing **LTE-advanced (LTE-A)** networks and discuss interference coordination. Doppler, Yu, Ribeiro, and Jänis [85] consider the throughput maximization problem for underlay **D2D** communications. They consider a simple case where there is only one **D2D** pair reusing the channel resource of a cellular user. They devise an optimization problem that controls the transmit-power and chooses the communication mode that gives the maximum throughput. In [86], Yu, Doppler, Ribeiro, and Tirkkonen extend the previous work and derive the optimal power control mechanism based on feasibility region analysis. A Stackelberg game [135] has been considered by Wang et al. [89] for power and uplink channel allocation for **D2D** communications. Feng et al. [90] have also considered the channel and power allocation problems. Here they apply the feasibility region analysis for power control, and following this, they solve the weighted bipartite matching using the Kuhn–Munkres algorithm [56, 57] for uplink channel allocation. Zhang et al. [91, 92] have proposed an interference graph based channel allocation scheme, where they used the said graph to group the users that may share the same frequency channel. Yu et al. [93] have considered the channel and power allocation as two subproblems. The power allocation problem is solved similarly to [90], whereas the channel allocation problem is formulated as a 0–1 integer program that can be solved using the branch-and-bound method [136]. Zhao and Wang [95] have considered a sum rate maximization problem. They have given a two-step solution where, in the first step they greedily allocate the channels. Given the channel assignment, in the second step the

power optimization problem has been posed as a non-linear program. They have shown that it satisfies the KKT conditions [137, 138], and the optimal solution is found using a bisection search. Nguyen, Hasegawa, and Hwang [139] have considered a pricing scheme for interference management. They have proposed a non-cooperative power control game with a distributed update rule to reach Nash equilibrium. Chen, Kao, Ciou, and Lin [97] have considered the throughput maximization problem and presented a **maximum independent set (MIS)** based [140] channel allocation scheme. They have also applied a Stackelberg game to allocate powers, similar to [89]. Mondal, Neogi, Chaporkar, and Karandikar [103] have addressed the fairness in resource allocation problem. To make the allocation fair, they allow multiple resource blocks to be allocated to a single **D2D** user. They have analytically derived closed-form expressions for power allocation, whereas bipartite matching is employed for resource allocation. A full-duplex scenario has been considered by Yang, Zhang, Cheng, and Yang [104], where they have tried to maximize the system throughput. They have considered many-to-many sharing of the resource blocks and proposed a graph coloring based solution. Kim, Karim, and Cho [141] have divided the service area into four zones for interference mitigation. A fair uplink resource allocation has also been considered by Mukherjee and Ghosh [142, 143], where they have used a game-theoretic model to maximize the throughput. A randomized joint channel and power allocation scheme has been proposed by Ghosal and Ghosh [106, 107]. They also consider multiple reuses of the same frequency channel.

Many authors have also explored the downlink resource sharing problem. Xu et al. [88] have studied the channel allocation problem from a game theoretic perspective, where they apply a reverse iterative combinatorial auction method to allocate downlink resources. Li, Kaleem, and Chang [82] have used an interference alignment [144] technique to group users that may share the same downlink channel. Chang, Jau, Su, and Lee [98] have also considered downlink channel sharing, where they create a priority list for each user based on the channel gains. They then apply the Gale–Shapley algorithm [145] to obtain the required resource allocation solution. Downlink resource sharing has also been considered by Wu, Atat, Mastronarde, and Liu [9], where they use stochastic geometry to derive expressions for downlink coverage and utilize relays to further improve spectral-efficiency.

Some researchers have considered a **D2D** communication model where **D2D** communications happen in overlay mode either in the sub-6 GHz band or using **mmWave** bands. Lai, Wang, Lin, and Li [105] have considered the joint channel and power allocation problem where multiple users can share the same channel resource. They have used vertex coloring

with branch-and-bound to assign channels, while power control and throughput maximization have been performed using linear programming. Tan, Liang, Zhang, and Feng [108] have considered weighted sum rate maximization as their objective and have proposed a fractional programming [146] approach. They then criticized this centralized approach due to imperfect channel state information and scalability, and presented a distributed scheme using deep reinforcement learning (RL). Yang et al. [109] have devised a multiagent dueling deep RL where they apply distributed coordinated learning to solve the joint channel and power allocation problem.

Rappaport et al. pioneered the early development of mmWave communications [16, 17, 65, 67, 68] with thorough experiments on the propagation of mmWave signals and their attenuation against various obstacles. A thorough description of mmWave wireless communications can be found in the text book [15]. Pi and Khan [147] introduce a mmWave mobile broadband system to facilitate Gbps data rates. Qiao et al. [24] have proposed D2D communications in mmWave signals and given a design for the MAC layer. They have considered sharing the same frequency channel among multiple users to increase network capacity by taking advantage of high propagation losses and the use of directional antennas for mmWave communications. Deng and Haenggi [26] have given a signal-level analysis on the feasibility of mmWave D2D communication. Li, Zhou, Peng, and Shan [36] have considered the joint beamwidth and resource optimization for sum rate maximization in mmWave D2D communications. Sarkar and Ghosh [61, 113, 118] have considered the stable link selection problem for mmWave communications.

Relay Selection

Fixed terminal relaying through small BS has already been considered in LTE networks. Hoymann et al. [148] have provided an overview of the challenges and solutions for the design of relay stations in LTE networks. The proposal to use idle UEs as relays to increase coverage in D2D communications is due to Vanganuru, Ferrante, and Sternberg [38]. The resource allocation and relay selection for D2D communications have been considered by Kim and Dong [58]. They have shown that the joint problem is \mathcal{NP} -Complete and proposed a 3D matching framework for it. They solve the 3D matching problem with the iterative Hungarian method [56, 57]. As for power control, they have derived closed-form expressions. Congiu, Shokri-Ghadikolaei, Fischione, and Santucci [27] present a discussion about the relay-fallback trade-off in mmWave communications. Biswas, Vuppala, Xue, and

Ratnarajah [110] have considered the relay selection problem in **mmWave** networks. They have derived closed-form expressions for selecting the best relay as well as the best path. Hu and Blough [70] have considered relay-aided communication for avoiding obstacles. They maximize the throughput by selecting an appropriate relay-aided path. A probabilistic model for relay selection has been presented by Singh and Ghosh [72], where they choose the best relay depending on their expected data rate. A mobility-aware relay selection strategy for delay minimization has been presented by Singh and Ghosh [111]. Meng and Wang [39] have discussed the pricing scheme for relays. Singh, Chattopadhyay, and Ghosh [112, 116, 128] have considered a **partially observable Markov decision process (POMDP)** for relay selection. Sarkar and Ghosh [61, 113] have dealt with the relay selection problem in the presence of obstacles. A relay-disjoint stable path-finding problem has been considered by Sarkar, Ghosal, Bandyopadhyay, and Ghosh [117] in the presence of obstacles. A stable maximum capacity path finding problem has been considered by Sarkar and Ghosh [118], where they used the widest path algorithm [149] to obtain the required solution. Shukla and Ghosh [114] have used a game-theoretic (auction) framework for selecting relays such that throughput is maximized and also proposed a distributed relay switching mechanism to minimize packet losses. Ganesan and Ghosh [115] have constructed a visibility graph for selecting the relays.

Relay selection and channel allocation have also been dealt with simultaneously in a few works. Ma, Yin, Yu, and Zhang [150] consider the distributed interference-aware channel and relay selection problem. They present a local greedy selection scheme based on the **signal-to-interference-plus-noise ratio (SINR)**. Zhengwen, Su, and Shixiang [119] first allocate uplink resources to the relays based on **SINR**; following this, they employ a timer-based greedy relay selection strategy similar to [150]. Zhao, Li, Chen, and Ge [120] have presented a hardness proof by reducing the relay and channel allocation problem to a 0–1 knapsack problem. The formulated binary integer program is then solved using the branch-and-cut method [138]. Wei, Hu, Qian, and Wu [99] have considered a two-way, multihop **D2D** communication scenario. With thorough analysis, they have obtained closed-form expressions for the mode and relay selection criteria. A throughput maximization problem for relay-aided communications has been considered by Hoang, Le, and Le-Ngoc [100]. They apply fractional programming with the Dinkelbach method [146] to obtain a power allocation, while for the channel allocation they apply the Hungarian method [56, 57]. Deng et al. [121] have devised a distributed interference coordination scheme based on graph coloring to allocate resources in a relay-aided overlay network. Gu et al. [122]

have formulated the relay and channel allocation problem as weighted bipartite matching and solved it using the Kuhn–Munkres algorithm [56, 57]. They have also formulated a throughput-balancing mechanism for relay-aided communications. Liu and Zhang [123] have also considered the resource and relay allocation problems and proposed heuristic algorithms for sum rate maximization. Throughput maximization has also been considered by Sun, Zhang, Xing, and Xiao [124], where they sectorized the service area into five zones and decomposed the problem into four subproblems. They first fix the power allocation, select relays, decide communication mode, and finally allocate uplink channels.

Mobility-Aware Communications

Almost all the works stated above assume that users are stationary. User mobility makes the resource allocation problem much harder, as the links may fail due to rapid SINR changes over time. Verdone and Zanella [151] discuss the effect of user mobility on resource association. Both Cowling [59] and Keshav [60] present a nice excerpt on location management in cellular networks and discuss different mobility models to capture user mobility. Ghosal and Ghosh [107] have considered devices to be pseudo-stationary and generated different snapshots of the system using a random waypoint mobility model. The mobility of the users is usually captured into some metric, which is then used to evaluate the link quality. More specifically, in [152], Han, Wu, Yang, and Li defined ‘contact time’ as the duration in which transmitter-receiver pairs stay in the communication range and solved the routing problem using this metric. A received signal strength based distance threshold has been derived by Omri and Hasna [153] for mode selection for mobile users. Singh and Ghosh [111] define a metric called ‘connectivity factor’ to denote link stability for mobile users. They use that to construct a network graph, and apply the widest path algorithm [149] to obtain a minimum-delay relay-aided path. Both Singh and Ghosh [72] and Shukla and Ghosh [114] have considered simple geometry to capture the device mobility in order to detect potential link failures.

Obstacle-Aware Communications

There have been a few studies on obstacle-aware communications as well. Park and Heath [126] have demonstrated the use of radars for blockage sensing in high frequency mmWave communications. On the other hand, Koda, Yamamoto, Nishio, and Morikura [66] have

proposed the use of cameras to track pedestrian movements, using which they have formulated an **RL** framework for minimizing handoffs. Kumar and Ohtsuki [62] have used historical link failures to learn the blockage probabilities due to pedestrians, which are then used to predict handoffs. Singh, Chattopadhyay, and Ghosh [112, 116, 128] have considered a **POMDP** to model obstacles for relay selection, where they have used successive acknowledgement failures to infer the presence of a dynamic obstacle. They derive a threshold policy for selecting relays in order to minimize the delay due to retransmissions. Sarkar and Ghosh [61, 113] have argued that small static obstacles, such as trees, signboards, and others, are not well captured by the satellite imagery but can be gradually learned from the link failure information. They further point out that the same can also be used for avoiding dynamic obstacles. Sarkar, Ghosal, Bandyopadhyay, and Ghosh [117] have shown that such link failure based blockage prediction can be used to construct relay-disjoint stable paths. Obstacle-Aware solutions for indoor scenarios have been considered by Brown et al. [154]. Ganesan and Ghosh [115] have used the evidential framework [132, 133] to learn the spatial correlation of the obstacles in order to build an occupancy map. Sarkar and Ghosh [118] have attempted to track a dynamic obstacle in order to avoid link failures.

Green Communications

Most of the above works considered throughput maximization as their objective, which may not result in an energy-efficient resource allocation. A thorough survey on energy-efficient communications has been conducted by Feng et al. [74]. Chih-Lin et al. [10] report many initiatives towards energy-efficient (green) communications. Huang, Zhong, and Ding [155] also document many such green initiatives.

Reider and Fodor [87] consider the power minimization problem while satisfying the **SINR** constraints in an uplink resource sharing scenario. Hoang, Le, and Le-Ngoc [94] have considered a weighted energy-efficiency maximization problem with guaranteed **SINR**. They solve it in two steps: first, they resolve the power allocation by solving a linear program, and then they apply relaxation and fractional programming [146] to allocate channels. Jiang et al. [96] have formulated a non-convex optimization problem for uplink resource allocation. They also solve it in two steps: first, they obtain a power allocation, and then they allocate the channel resources. They use the Dinkelbach method [146] along with a penalty function based constraint removal method to obtain the required solutions. Zhou, Ota, Dong, and Xu [101] have presented non-cooperative game based preference modeling

for energy-efficient resource allocation using stable matching. They have also formulated a distributed iterative power control mechanism. Penda, Fu, and Johansson [102] have formulated an integer non-linear program for the channel and power allocation, which can be solved using the branch-and-bound method [136]. They have also given a heuristic algorithm that scales better. A distributed iterative power control mechanism has also been considered in their work. Energy efficiency in uplink resource sharing has been considered by Kai et al. [73], where they have solved two subproblems separately. They have devised a heuristic solution for channel allocation, while power control has been performed using standard tools of convex optimization. Ansere et al. [75] have raised the issue of green resource allocation for [internet of things \(IoT\)](#) networks. Ghosal and Ghosh [106, 107] have considered a randomized approach for channel allocation and a linear programming approach for power control for resource-efficient communication.

Multicast Communications

The link selection for multicasting has also been extensively studied by the researchers. Xie, Talpade, McAuley, and Liu [156] have proposed protocol-independent multicast tree construction for heterogeneous networks. In the case of wireless networks with varying link quality and user mobility, multicasting is a challenging task. Wang, Liang, and Wang [157] have highlighted some of these issues and discussed state-of-the-art algorithms. Perkins [79] and Basagni, Conti, Giordano, and Stojmenovic [80] document some standard multicast routing algorithms. Wang and Crowcroft [158] and Shacham [159] have considered multicast routing, where they opt for the widest paths. Seppälä, Koskela, Chen, and Hakola [160] present a nice motivation for studying multicasting in the context of [D2D](#) communications. Rubin, Tan, and Cohen [161] have presented a heuristic algorithm for resource allocation in a multicast network. Huang, Zhong, and Ding [155] have raised the issue of green communication in multicast services. Chiti, Fantacci, and Pierucci [45] have considered multicasting within a social community of [D2D](#) users with a focus on minimizing end-to-end delay. Han, Wu, Yang, and Li [152] have also considered delay-constrained multicast [D2D](#) communications. Hou [162] has studied [D2D](#) relay-assisted multicasting and tried to minimize the multicast delay. The trade-off between energy and spectral efficiency in [D2D](#) multicast networks has been highlighted by Bhardwaj and Agnihotri [163]. A meta-heuristic tabu search [164] method for throughput maximization has been studied by Ningombam and Shin [46]. Gupta, Khan, and Ngo [54] have presented an architecture for

D2D multicasting. Li et al. [81] have addressed routing delay minimization in multicasting trees. Bhardwaj and Agnihotri [53] have given an overview of various multicast protocols for D2D communications. Ji et al. [165] have explored intelligent reflecting surface assisted multicast D2D communications.

Research Gap and Contributions

Most of the existing work on channel allocation considers the single reuse of a frequency channel. The advent of **multiple-input multiple-output (MIMO)** antennas with **mmWave** beamforming enables multiple reuse of the same frequency channel within the same service area, which hugely improves the spectral efficiency. Designing an efficient channel-sharing scheme that takes advantage of this is a challenging task. Furthermore, in a relay-aided communication scenario, both the relays and frequency channels are to be assigned to the requesting users. Unlike most existing works, which deal with the relay and frequency allocation successively in separate stages, the two problems must be dealt with jointly due to their inherent interdependencies, which have been addressed in **Chapter 3**. It becomes more difficult when devices are mobile and/or there are static as well as dynamic obstacles present in the area. Designing a mobility and obstacle aware joint resource allocation and relay selection framework is a more challenging task, which has been addressed in **Chapter 4**. Moreover, for sustainable, green communication networks, energy efficiency must be prioritized. Although energy-efficient resource allocation has been extensively studied, the effect of dynamic obstacles has not been adequately addressed in this context. We deal with energy-efficient resource allocation in **Chapters 5 and 6**, where we primarily focus on the presence of dynamic obstacles. Lastly, the multicast link selection problem in the presence of dynamic obstacles is also a challenging task, as links may exhibit different stability due to varying channel conditions. In **Chapter 7**, we devise an obstacle-aware stable multicast link selection mechanism. These are the areas that we have tried to address in this thesis, as detailed in the following five contributory chapters.

Part I

Channel Allocation and Relay Selection

CHAPTER 3

Joint Channel and Relay Selection for D2D Communications*

High demand for bandwidth has been a primary motivation for **device-to-device (D2D)** communications. In cases where direct communication suffers from poor link quality, two **D2D** devices are allowed to communicate via a relay node. Both the number of available frequency channels and candidate relays are scarce resources and thus must be judiciously allocated among the requesting users. The relay selection problem is concerned with the selection of a suitable relay device for each such **D2D** pair, while the frequency assignment problem aims to optimally share the available spectrum resources among the active devices, satisfying their **signal-to-interference-plus-noise ratio (SINR)** requirements. The relay selection problem has several inherent challenges and interdependencies with other problems like frequency channel assignment, making it a computationally hard problem to deal with. More precisely, the combined problem of relay selection and frequency allocation has been shown to be NP-complete [58].

Both the channel allocation and relay selection problems in context of **D2D** communications have been studied extensively in the literature. The channel allocation problem for **D2D** communication has been studied by [11, 36, 73, 83–109]. Some authors have also considered relay-aided **D2D** communications where the problem of optimal relay selection has been explored [61, 70, 72, 110–118]. Although, relay selection and channel allocation both have considered in [58, 119–124], these works solve the two problem separately in successive stages. With a motivating example, we argue that such a two-step solution can

*This chapter is based on the following publication:

- [C2] **Rathindra Nath Dutta** and Sasthi C. Ghosh. “Joint Relay Selection and Frequency Allocation for D2D Communications”. In: *Proceedings of the 17th EAI International Conference on Quality, Reliability, Security and Robustness in Heterogeneous Systems (QShine 2021)*, November 29-30, 2021. Vol. 402. Lecture Notes of the Institute for Computer Sciences, Social Informatics and Telecommunications Engineering (LNICST). Springer, 2021, pp. 159–173. DOI: [10.1007/978-3-030-91424-0_10](https://doi.org/10.1007/978-3-030-91424-0_10)

be highly suboptimal. Even if one solves the two problems optimally independently in each step, we argue that the combined solution may still be suboptimal. Furthermore, most of the existing works do not share the frequency channels among multiple users simultaneously, which significantly diminishes the spectral-efficiency. With that in mind, we consider the joint problem of relay selection and channel allocation for D2D communications, where multiple D2D links may share same frequency channel as long as their required SINR level is satisfied. This brings us to our first work, which includes the following contributions.

[Contribution 1.1] We consider the joint relay selection and channel assignment problem (JRSCAP) for D2D communications. Given its computational hardness [58], we employ a linear program (LP) relaxation based greedy rounding scheme for JRSCAP, where we aim to maximize the number of links activated with the available resources. The greedy rounding has been performed iteratively such that it maintains the feasibility of the final solution.

[Contribution 1.2] Furthermore, we utilize a network coding scheme for two-way relay-aided D2D communications to reduce the communication time by a factor of two. The said coding scheme allows a relay user equipment (UE) to simultaneously receive data from two D2D users and then relay them back again simultaneously.

[Contribution 1.3] Through simulations, we show the near optimal performance of our proposed algorithm in terms of the number of links activated. We also show that our proposed algorithm outperforms a state-of-the-art classical algorithm [58] as well as a recent one [124] in terms of number of links activated and overall system throughput.

The rest of this chapter is organized as follows. A motivating example for joint formulation is given in Section 3.1. Section 3.2 presents the system model and states various assumptions. The joint problem formulation is given in Section 3.3 and our proposed solution is given in Section 3.4 followed by its simulation results in Section 3.5. We conclude this chapter with Section 3.6.

3.1 A Motivating Example

The problems of relay selection and frequency allocation must be dealt with jointly; otherwise, like in any multistage strategy, the result of a former stage will heavily influence the

quality of the solution obtained at the end of the subsequent stages. Even if one solves the one stage optimally, there is no guarantee that it will be part of the overall optimal solution of the joint problem. One can easily construct an instance where doing relay selection independent of frequency allocation in two stages produces non-optimal results.

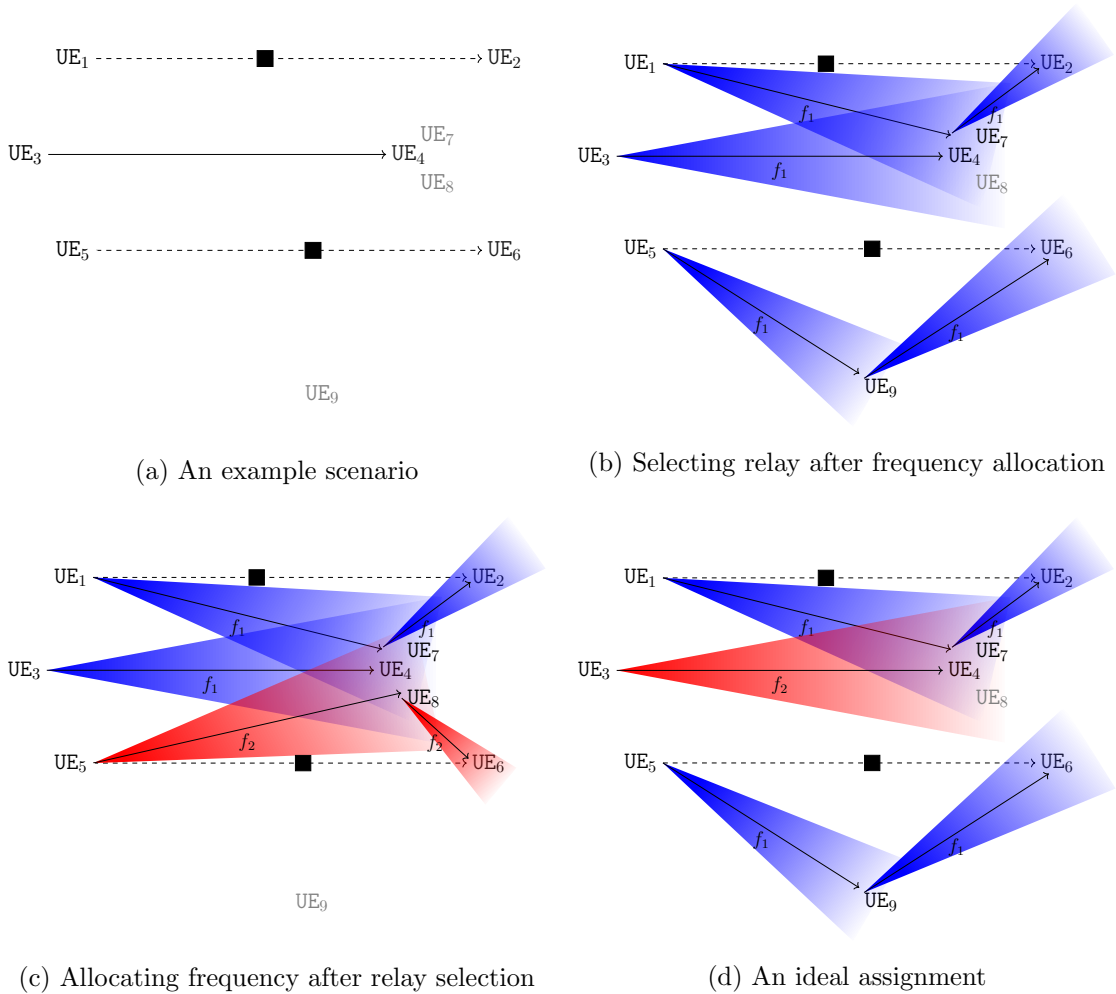


Figure 3.1: Motivation for joint relay selection and channel assignment

Consider the scenario depicted in Figure 3.1a. Suppose only two frequency channels, f_1 and f_2 , are available, and there are three requesting D2D pairs, $UE_1 \rightarrow UE_2$ ¹, $UE_3 \rightarrow UE_4$,

¹ $UE_i \rightarrow UE_j$ indicates that UE_i is the transmitter and UE_j is the receiver

and $\text{UE}_5 \rightarrow \text{UE}_6$, which are to be served. Furthermore, there are three idle users, namely UE_7 , UE_8 , and UE_9 , which may serve as relays. Let us first consider the case where frequency assignment is done first, followed by relay selection. **Figure 3.1b** depicts a frequency assignment where all three pairs $\text{UE}_1 \rightarrow \text{UE}_2$, $\text{UE}_3 \rightarrow \text{UE}_4$, and $\text{UE}_5 \rightarrow \text{UE}_6$ have been assigned the same channel f_1 , as they do not interfere with each other. Now suppose that the links $\text{UE}_1 \rightarrow \text{UE}_2$ and $\text{UE}_5 \rightarrow \text{UE}_6$ are blocked by obstacles (denoted by black squares), thus opting for relay-aided communication. Now there is only one relay candidate, UE_7 , in the vicinity of the link $\text{UE}_1 \rightarrow \text{UE}_2$, while the link $\text{UE}_5 \rightarrow \text{UE}_6$ has two relay candidates, UE_8 and UE_9 . As seen in **Figure 3.1b**, links $\text{UE}_1 \rightarrow \text{UE}_7$ and $\text{UE}_3 \rightarrow \text{UE}_4$ cause significant interference to each other and thus cannot be activated with the same frequency f_1 , while $\text{UE}_5 \rightarrow \text{UE}_6$ can communicate using frequency f_1 via relay UE_9 . Thus, at most two requesting **D2D** pairs can be served in this case. Now consider the case where relay selection is performed first, followed by frequency allocation, as shown in **Figure 3.1c**. In this case, one would choose UE_7 as the relay for the blocked link $\text{UE}_1 \rightarrow \text{UE}_2$ as it is the only relay candidate available, and relay UE_8 for the blocked link $\text{UE}_5 \rightarrow \text{UE}_6$ as it would give better **SINR** being closer than relay UE_9 . Since links $\text{UE}_1 \rightarrow \text{UE}_7 \rightarrow \text{UE}_2$, $\text{UE}_3 \rightarrow \text{UE}_4$, and $\text{UE}_5 \rightarrow \text{UE}_8 \rightarrow \text{UE}_6$ interfere with each other, at most two of them can be served with f_1 and f_2 . **Figure 3.1d** depicts the optimal solution where frequency allocation and relay selection have been performed jointly. Here UE_7 and UE_9 are chosen as the relays for the blocked links $\text{UE}_1 \rightarrow \text{UE}_2$ and $\text{UE}_5 \rightarrow \text{UE}_6$, respectively, and frequency f_1 is assigned to both the relay-aided links $\text{UE}_1 \rightarrow \text{UE}_7 \rightarrow \text{UE}_2$ and $\text{UE}_5 \rightarrow \text{UE}_9 \rightarrow \text{UE}_6$, whereas, frequency f_2 is assigned to the direct link $\text{UE}_3 \rightarrow \text{UE}_4$. Thus, all three requesting pairs can be served in this case. This ascertains that doing relay selection and frequency allocation independently of each other may not give an optimal solution, and thus a joint approach is required.

3.2 System Model

We assume a single-cell **base station (BS)** controlled **D2D** overlay scenario where we have M pairs of **D2D UEs** who are willing to partake in two-way communications (have some data traffic to transmit) and N idle **UEs**. Let us denote \mathcal{D} as the set of requesting **D2D** pairs. Some of these **D2D** pairs can directly communicate with each other, whereas others need an intermediate relay device for their communication. In such cases, we are only considering one-hop relay-assisted **D2D** communications. **Figure 3.2** depicts such a scenario. All the requesting devices need to be allocated spectrum resources where we have an F number of

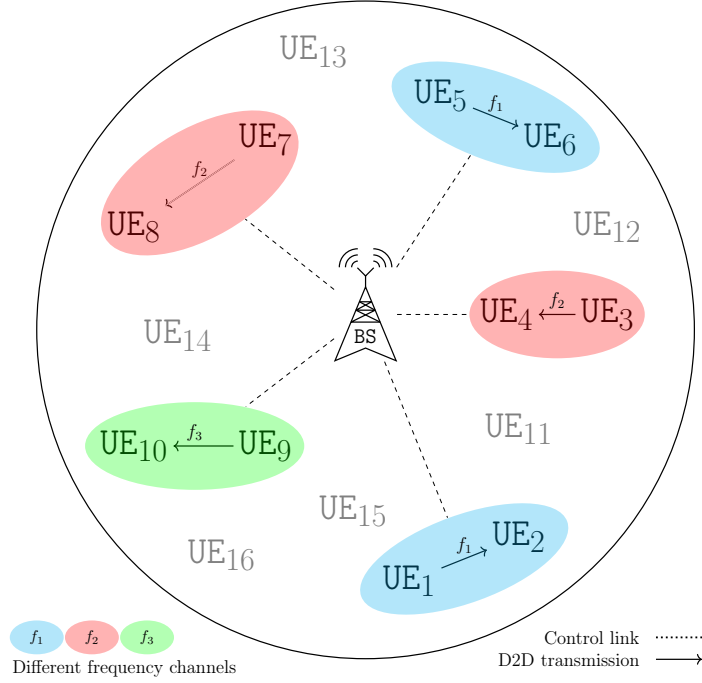


Figure 3.2: An example scenario

dedicated orthogonal sub-channels available for D2D communications. We assume time is discretized into time slots $\{t_0, t_1, t_2, \dots\}$ with small Δt time span for each time slot. We denote a pair of successive time slots as a *superslot*. Notations used in this chapter are summarized in Table 3.1.

Mobility Consideration

We consider the nodes to be pseudo-stationary, that is, they do not change their position for the duration of a superslot. As we solve the problem for each superslot independently, their movement in between superslots does not affect our proposed solution. For a particular superslot, the position of an UE can be determined with great accuracy (about 30 centimeters) [166] and is available to the BS.

Candidate Relays

Similar to [38, 122], we assume all idle D2D UEs are capable and willing to participate in device relaying. Furthermore, we assume that a D2D pair can communicate with each

other via a single relay, making a one-hop relay-assisted communication possible in cases where the direct communication link is poor or does not exist. For a D2D pair, all idle devices within its vicinity, thus possibly having good SINR values, are eligible to be a candidate relay for that pair. An idle device can be on more than one such candidate list but can only be assigned to a single D2D pair for relaying. We denote \mathcal{R} to be the set of all such candidate relay nodes in the service area.

Communication Channel

We need to allocate frequency channels to each of the D2D links and also to their relay links (if any). Long term evolution (LTE) allows 12 subcarrier channels to be used, which is also adapted in the simulations in the existing literature [124]. With a limited number of frequency channels, we need to employ frequency reuse while keeping the SINR values above the required threshold. We denote \mathcal{F} as the set of available orthogonal frequency channels. We assume all transmitter devices are transmitting at a fixed power P . As in [11], for the pathloss model, we consider both fast fading due to multi-path propagation and slow fading due to shadowing. Thus, the channel gain between two devices is expressed by Equation (1.1).

Slot Reduction

In [167], it is shown that for two-way communication, it is possible to reduce the number of required time slots by using a network coding technique. System requirements to support such channel coding are given in [167] and also its implementation and usability has been demonstrated in [168–173]. As shown in Figure 3.3a, it would take two time slots to send UE_A 's data to UE_B via relay UE_R and another two time slots to send UE_B 's data to UE_A via relay UE_R . The data transmissions are denoted by directed arrows, marked with slot numbers, in the figure. But with proper network coding, UE_R can receive from both UE_A and UE_B simultaneously in one time slot and send back the combined received data in the next time slot, as depicted in Figure 3.3b. Here, both UE_A and UE_B receive the combined data simultaneously from UE_R and decode the required data from it. This shows a clear benefit in the reduction of the number of time slots from four to two, which supersedes the small overheads incurred for the use of this network coding [167]. The usability of this channel coding scheme requires proper synchronization between the two senders, as mentioned in [169–171]. We assume relay nodes have limited memory, so the data in one

time slot must be sent out in the next time slot. Our task thus reduces to solving the problem just for a single superslot.

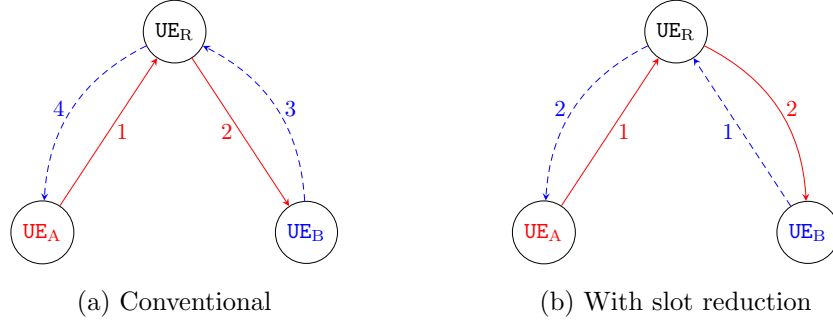


Figure 3.3: Slot reduction using network coding for two-way communication

Notation	Meaning
\mathcal{D}	Set of D2D pairs
\mathcal{R}	Set of idle UEs who can relay
\mathcal{F}	Set of orthogonal frequency channels
t	Discrete time slots
Δt	Duration of a time slot
P	Transmit power
$R(a, b)$	Received signal power from a to b
η_0	Noise
I	Interference
Γ	SINR
ζ	SINR threshold
\mathcal{C}_f	Frequency class f
X, Y	Optimization variables

Table 3.1: Notations used throughout Chapter 3

Interference consideration

Consider a D2D pair UE_A - UE_B communicating via a relay UE_R . As shown in Figure 3.4a, in the first time slot, both UE_A and UE_B will act as transmitters, and UE_R will act as a receiver. Both UE_A and UE_B will contribute to the interference of all other devices, such as UE_P , receiving using the same frequency in which both UE_A and UE_B transmit. Similarly,

all other devices, such as UE_Q , transmitting on the same frequency channel will cause interference at UE_R . Whereas in the second time slot, the receiving and transmitting roles of the devices reverse. As shown in figure 3.4b, UE_R now becomes a transmitter and relays back the data to UE_B and UE_A , both of which are now in receiving mode. Thus, UE_A and UE_B get interference from all other devices, such as UE_P , transmitting using the same frequency. Similarly, UE_R causes interference to all other devices, such as UE_Q , receiving on the same frequency channel.

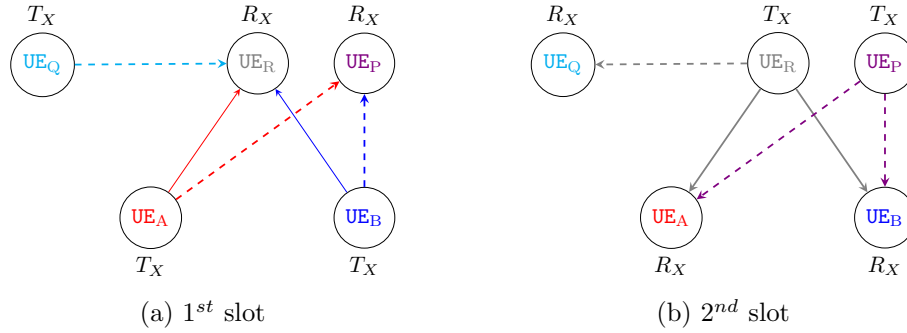


Figure 3.4: Interference from other transmitters for the two time slots

3.3 Problem Formulation

Assuming all devices transmit using fixed power P , we define received power from device a to device b as $R(a,b)$. We define binary allocation matrices $X \in \{0,1\}^{|\mathcal{D}|\times|\mathcal{F}|}$ and $Y \in \{0,1\}^{|\mathcal{D}|\times|\mathcal{R}|\times|\mathcal{F}|}$ of which entries $X_{i,f}$ and $Y_{k,r,f}$ are defined as follows.

$$X_{i,f} = \begin{cases} 1 & \text{if } i\text{-th D2D pair communicates directly using frequency } f \\ 0 & \text{otherwise} \end{cases}$$

$$Y_{i,r,f} = \begin{cases} 1 & \text{if } i\text{-th D2D pair communicates via relay } r \text{ using frequency } f \\ 0 & \text{otherwise} \end{cases}$$

We denote $i = (i_1, i_2)$ for a directly communicating **D2D** pair i consisting of devices i_1 and i_2 . Let us now derive the **SINR** expressions for a **D2D** pair i communicating via the relay r . In the first time slot, both i_1 and i_2 act as transmitters, and r acts as the receiver, as depicted in **Figure 3.4a**. Even with all transmitters transmitting with the same fixed

power P , the received signal strength will vary due to different gains obtained at different positions. Thus, to ensure no buffering is needed at the receiver r , the effective received power at r is set as the minimum of the received powers from the two transmitters i_1 and i_2 , that is, $\min(R(i_1, r), R(i_2, r))$. The total interference at the relay r (associated with **D2D** pair i) from all other **D2D** pairs $j = (j_1, j_2) \in \mathcal{D}$ operating on the same frequency channel f is given by equation (3.1).

$$I_{i,r,f} = \sum_{\substack{j \in \mathcal{D} \\ j \neq i}} R(j_1, r) X_{j,f} + \sum_{\substack{j \in \mathcal{D} \\ j \neq i}} \sum_{\substack{r' \in \mathcal{R} \\ r' \neq r}} (R(j_1, r) + R(j_2, r)) Y_{j,r',f} \quad (3.1)$$

Therefore, in the first time slot, **SINR** for the **D2D** pair i communicating via relay r using frequency channel f can be given as

$$\Gamma_{i,r,f} = \frac{\min(R(i_1, r), R(i_2, r))}{\eta_0 + I_{i,r,f}}$$

where η_0 is the thermal noise. Furthermore, for **D2D** pair i the **SINR** value must be larger than or equal to the required **SINR** threshold ζ_i whenever $Y_{i,r,f} = 1$. We can write this as linear inequalities (3.2) and (3.3), where M is a suitably large constant value, representing positive infinity.

$$(1 - Y_{i,r,f})M + R(i_1, r) \geq (\eta_0 + I_{i,r,f})\zeta_i \quad (3.2)$$

$$(1 - Y_{i,r,f})M + R(i_2, r) \geq (\eta_0 + I_{i,r,f})\zeta_i \quad (3.3)$$

In the second slot, the role of transmitters and receivers reverses. That is, both i_1 and i_2 act as the receivers and r acts as a transmitter. We calculate the interference at i_1 and i_2 in equations (3.4) and (3.5) respectively.

$$I'_{i_1,r,f} = \sum_{\substack{j \in \mathcal{D} \\ j \neq i}} R(j_2, i_1) X_{j,f} + \sum_{\substack{j \in \mathcal{D} \\ j \neq i}} \sum_{\substack{r' \in \mathcal{R} \\ r' \neq r}} R(r', i_1) Y_{j,r',f} \quad (3.4)$$

$$I'_{i_2,r,f} = \sum_{\substack{j \in \mathcal{D} \\ j \neq i}} R(j_2, i_2) X_{j,f} + \sum_{\substack{j \in \mathcal{D} \\ j \neq i}} \sum_{\substack{r' \in \mathcal{R} \\ r' \neq r}} R(r', i_2) Y_{j,r',f} \quad (3.5)$$

Thus effective SINR in second time slot is given as:

$$\Gamma'_{i,r,f} = \min \left(\frac{R(r, i_1)}{\eta_0 + I'_{i_1,r,f}}, \frac{R(r, i_2)}{\eta_0 + I'_{i_2,r,f}} \right).$$

This SINR value must also be larger than ζ_i whenever $Y_{i,r,f} = 1$. We can similarly write this as linear inequalities (3.6) and (3.7).

$$(1 - Y_{i,r,f})M + R(r, i_1) \geq (\eta_0 + I'_{i_1,r,f})\zeta_i \quad (3.6)$$

$$(1 - Y_{i,r,f})M + R(r, i_2) \geq (\eta_0 + I'_{i_2,r,f})\zeta_i \quad (3.7)$$

For a D2D pair $i = (i_1, i_2)$ communicating directly using frequency f , interference at i_2 in slot 1 and at i_1 in slot 2 are given in equations (3.8) and (3.9) respectively.

$$I'''_{i_2,f} = \sum_{\substack{j \in \mathcal{D} \\ j \neq i}} R(j_1, i_2)X_{j,f} + \sum_{\substack{j \in \mathcal{D} \\ j \neq i}} \sum_{r \in \mathcal{R}} (R(j_1, i_2) + R(j_2, i_2))Y_{j,r,f} \quad (3.8)$$

$$I'''_{i_1,f} = \sum_{\substack{j \in \mathcal{D} \\ j \neq i}} R(j_2, i_1)X_{j,f} + \sum_{\substack{j \in \mathcal{D} \\ j \neq i}} \sum_{r \in \mathcal{R}} R(r, i_2)Y_{i,r,f} \quad (3.9)$$

Similarly, linear inequalities in (3.10) and (3.11) ensure SINR value for the D2D pair i communicating using frequency f is larger or equal to threshold ζ_i whenever $X_{i,f} = 1$.

$$(1 - X_{i,f})M + R(i_1, i_2) \geq (\eta_0 + I'''_{i_2,f})\zeta_i \quad (3.10)$$

$$(1 - X_{i,f})M + R(i_2, i_1) \geq (\eta_0 + I'''_{i_1,f})\zeta_i \quad (3.11)$$

Inequality (3.12) ensures that a relay device can be used for at most one D2D pair and can transmit using a single frequency.

$$\sum_{i \in \mathcal{D}} \sum_{f \in \mathcal{F}} Y_{i,r,f} \leq 1 \quad \forall r \in \mathcal{R} \quad (3.12)$$

A D2D pair can have at most one relay and can transmit using a single frequency. This gives us the inequality (3.13). A D2D pair can communicate either in direct mode or in relay-aided mode and can transmit using a single frequency channel. This can be written

as inequality (3.14).

$$\sum_{r \in \mathcal{R}} \sum_{f \in \mathcal{F}} Y_{i,r,f} \leq 1 \quad \forall i \in \mathcal{D} \quad (3.13)$$

$$\sum_{f \in \mathcal{F}} X_{i,f} + \sum_{r \in \mathcal{R}} \sum_{f \in \mathcal{F}} Y_{i,r,f} \leq 1 \quad \forall i \in \mathcal{D} \quad (3.14)$$

Finally, we have the integrality constraints (3.15) and (3.16).

$$X_{i,f} \in \{0, 1\} \quad \forall i \in \mathcal{D}, f \in \mathcal{F} \quad (3.15)$$

$$Y_{i,r,f} \in \{0, 1\} \quad \forall i \in \mathcal{D}, r \in \mathcal{R}, f \in \mathcal{F} \quad (3.16)$$

In order to maximize the number of links that can be activated together the following integer linear program (ILP) can be formulated.

$$\text{maximize : } \sum_{i \in \mathcal{D}} \sum_{f \in \mathcal{F}} X_{i,f} + \sum_{i \in \mathcal{D}} \sum_{r \in \mathcal{R}} \sum_{f \in \mathcal{F}} Y_{i,r,f} \quad (3.17)$$

Here the objective function is given by (3.17) subject to the constraints (3.2), (3.3), (3.6), (3.7), and (3.10) through (3.16).

3.4 Joint Relay Selection and Frequency Assignment

We begin with elimination of the allocation matrix X by introducing a dummy virtual relay node r_i for each D2D pair $i = (i_1, i_2)$ in \mathcal{D} in order to simplify the equations. While calculating SINR values, we consider position of r_i is same as transmitter i_1 for the first slot and the position is same as transmitter i_2 for the second slot. Thus, we update $\mathcal{R} = \mathcal{R} \cup \{r_i \mid i \in \mathcal{D}\}$. We also update the definition of received power such that $R(a, b) = \infty$ whenever $a = r_b$ or $b = r_a$, in all other cases it remains as defined earlier. Interference calculations in (3.1), (3.4), and (3.5) thus reduce to (3.18), (3.19), and (3.20), respectively, and the objective function simplifies to (3.21).

$$I_{i,r,f} = \sum_{\substack{j \in \mathcal{D} \\ j \neq i}} \sum_{\substack{r' \in \mathcal{R} \\ r' \neq r}} [R(j_1, r) + R(j_2, r)] Y_{j,r',f} \quad (3.18)$$

$$I'_{i_1,r,f} = \sum_{\substack{j \in \mathcal{D} \\ j \neq i}} \sum_{\substack{r' \in \mathcal{R} \\ r' \neq r}} R(r', i_1) Y_{j,r',f} \quad (3.19)$$

$$I'_{i_2,r,f} = \sum_{\substack{j \in \mathcal{D} \\ j \neq i}} \sum_{\substack{r' \in \mathcal{R} \\ r' \neq r}} R(r', i_2) Y_{j,r',f} \quad (3.20)$$

$$\text{maximize : } \sum_{i \in \mathcal{D}} \sum_{r \in \mathcal{R}} \sum_{f \in \mathcal{F}} Y_{i,r,f} \quad (3.21)$$

We devise a LP relaxation based greedy algorithm to near-optimally solve the problem. We start by relaxing the integrality constraints in (3.16) to allow the indicator variables to have fractional values in the closed interval between 0 and 1, as defined in (3.22).

$$Y_{i,r,f} \in [0, 1] \quad \forall i \in \mathcal{D}, r \in \mathcal{R}, f \in \mathcal{F} \quad (3.22)$$

We thus have an LP with the objective function given in (3.21) subject to constraints (3.2), (3.3), (3.6), (3.7), (3.12), (3.13), and (3.22). Solving this relaxed LP, we obtain an allocation matrix Y with fractional entries. We apply a simple rounding mechanism to change these fractional values to 0–1 integral values satisfying constraints (3.12) and (3.13), which is given in Algorithm 3.2. The resultant solution might not be a valid one with respect to the SINR constraints (3.2), (3.3), (3.6), and (3.7). Nevertheless, this gives us $|\mathcal{F}|$ frequency classes, $\mathcal{C} = \{\mathcal{C}_1, \mathcal{C}_2, \dots, \mathcal{C}_{|\mathcal{F}|}\}$, where \mathcal{C}_f represents a set of links that are to be activated with frequency f . More precisely, we store (i, r) pairs in a \mathcal{C}_f , denoting that the i -th D2D pair is assigned relay r and transmits using frequency f . The admissibility of each such frequency class can be tested independently of other frequency classes using the SINR constraints (3.2), (3.3), (3.6), and (3.7). For each such \mathcal{C}_f , disabling a few links might just satisfy the SINR constraints of the remaining links and thus can be activated with the same frequency f . We mark a link in \mathcal{C}_f as a *victim link*, which causes maximum interference to all other links in \mathcal{C}_f . We move this victim link into a common *discarded pool* of links \mathcal{L} for later consideration. This removal of links is done iteratively until all links in \mathcal{C}_f can be activated with the same frequency f without violating SINR constraints. By repeating the same process for all frequency classes, we can activate all the remaining links in $\bigcup_{f \in \mathcal{F}} \mathcal{C}_f$ together.

Now a link $l \in \mathcal{L}$ may be accommodated back into some frequency class \mathcal{C}_f such that $\mathcal{C}_f \cup \{l\}$ satisfies the SINR constraints. We should note that the order in which the links are

Algorithm 3.1: Joint relay selection and channel allocation

```

1  $\tilde{X} \leftarrow$  solve the relaxed LP and obtain the solution vector
2  $Y \leftarrow$  apply integer conversion scheme on  $\tilde{X}$  using Algorithm 3.2
3 Create the frequency classes  $\mathcal{C} = \{\mathcal{C}_1, \mathcal{C}_2, \dots, \mathcal{C}_{|\mathcal{F}|}\}$  based on  $Y$ 
4 Set  $\mathcal{L} \leftarrow \emptyset$  // initialize the discard pool
5 foreach class  $\mathcal{C}_f \in \mathcal{C}$  do
6   while  $\mathcal{C}_f$  not satisfying QoS constraints (3.2), (3.3), (3.6) and (3.7) do
7     foreach link  $(i, r) \in \mathcal{C}_f$  do
8        $I_{i,r} \leftarrow I_{i,r,f} + I'_{i_1,r,f} + I'_{i_2,r,f}$ 
9       Set  $(\hat{i}, \hat{r}) \leftarrow \arg \max_{(i,r) \in \mathcal{C}_f} \{I_{i,r}\}$ 
10      Set  $\mathcal{C}_f \leftarrow \mathcal{C}_f \setminus \{(\hat{i}, \hat{r})\}$  and  $\mathcal{L} \leftarrow \mathcal{L} \cup \{(\hat{i}, \hat{r})\}$ 
11 while  $\mathcal{L} \neq \emptyset$  do
12   foreach link  $(i, r) \in \mathcal{L}$  do
13     foreach  $f \in \mathcal{F}$  do
14       if  $\mathcal{C}_f \cup \{(i, r)\}$  satisfies QoS constraint then
15          $I_{i,r,f} \leftarrow I_{i,r,f} + I'_{i_1,r,f} + I'_{i_2,r,f}$ 
16       else
17          $I_{i,r,f} \leftarrow \infty$ 
18   Set  $(\hat{i}, \hat{r}, \hat{f}) \leftarrow \arg \min_{(i,r) \in \mathcal{L}, f \in \mathcal{F}} \{I_{i,r,f}\}$  // most economical assignment
19   if  $I_{\hat{i}, \hat{r}, \hat{f}} \neq \infty$  then
20     Update  $\mathcal{C}_{\hat{k}} \leftarrow \mathcal{C}_{\hat{k}} \cup \{(\hat{i}, \hat{r})\}$ 
21   Update  $\mathcal{L} \leftarrow \mathcal{L} \setminus \{(\hat{i}, \hat{r})\}$ 
22 return  $\mathcal{C}$ 

```

reinserted has a significant impact on the number of links that can be activated together. Here again, we employ a simple greedy scheme by iteratively finding the most *economical link* in \mathcal{L} and inserting it into its most *economical frequency class*, satisfying the SINR constraints. For a given link $l \in \mathcal{L}$, we say $\mathcal{C}_f \in \mathcal{C}$ is the most economical frequency class for l , if assigning l into \mathcal{C}_f incurs the minimum possible interference in comparison to assigning l to some other class $\mathcal{C}_{f'} \in \mathcal{C}$ with $f' \neq f$. We call (l, f) the most economical link-class pair if link l incurs minimum interference into frequency class \mathcal{C}_f for all such (l, f) pairs, where $l \in \mathcal{L}, \mathcal{C}_f \in \mathcal{C}$. If, for some link l , no such accommodating frequency class satisfying the SINR constraints can be found, we permanently discard this link and

Algorithm 3.2: Integer conversion of the relaxed vector \tilde{X}

```

1 Create a binary vector  $Y$ 
2 Loop
3    $\hat{i}, \hat{r}, \hat{f} \leftarrow \arg \max_{i,r,f} \{\tilde{X}_{i,r,f}\}$  // pick the one closest to 1
4   if  $\tilde{X}_{\hat{i},\hat{r},\hat{f}} = 0$  then
5     break // no more round-ups are possible
6    $Y_{\hat{i},\hat{r},\hat{f}} \leftarrow 1$  and  $\tilde{X}_{\hat{i},\hat{r},\hat{f}} \leftarrow 0$ 
7   foreach  $i \in \mathcal{D}$  and  $f \in \mathcal{F}$  do
8      $Y_{i,\hat{r},f} \leftarrow 0$  and  $\tilde{X}_{i,\hat{r},f} \leftarrow 0$  // ensures constraint (3.12) is satisfied
9   foreach  $r \in \mathcal{R}$  and  $f \in \mathcal{F}$  do
10     $Y_{\hat{i},r,f} \leftarrow 0$  and  $\tilde{X}_{\hat{i},r,f} \leftarrow 0$  // ensures constraint (3.13) is satisfied
11 return  $Y$ 

```

move onto the next economical link. We continue this process until no new links can be admitted. The formal description of this proposed scheme is given in [Algorithm 3.1](#).

Lemma 3.1. *Algorithm 3.1 terminates with a solution as good as any single frequency reuse algorithm.*

Proof. After the rounding-off, we check the admissibility of each of the frequency classes and make the necessary changes. This ensures that each frequency class must contain at least one link, if not more. Thus, at this point, in terms of the number of D2D links activated, the solution obtained by our proposed method must be as large as any solution produced by any algorithm that considers only the single use of a frequency channel. Furthermore, next we try to pack more links in the frequency classes, which can only improve the solution and bring it closer to the optimal one. This iterative improvement process must terminate as we consider each of the remaining links only once. ■

3.5 Simulation Results

In this section we present the simulation results to demonstrate the performance of our proposed scheme. We have considered a single cell scenario similar to [124]. We take 5-20 D2D pairs and 200 idle D2D devices eligible for device relaying within a cell of 500 m. The maximum distance between a D2D pair is 50 m. Other channel parameters are also

adapted from [124]. The maximum transmission power is 25 dBm, SINR threshold is 5 dB, thermal noise is -174 dBm/Hz and the pathloss exponent is 4. The various simulation parameters are summarized in Table 3.2.

Parameter	Value
D2D pairs	5-20
idle D2D UEs	200
max D2D distance	50 m
channel bandwidth	200 MHz
frequency channels	10
transmit power	25 dBm
noise	-174 dBm/Hz
pathloss exponent	4
SINR threshold	5 dB

Table 3.2: Simulation Parameters

For the comparison we choose two other algorithms namely iterative Hungarian method (IHM) [58] and uplink resource allocation (ULRA) [124] described in Chapter 2. Since both IHM and ULRA do not deal with network coding, for a fair comparison, we have considered a version of our algorithm which does not use the network coding for slot reduction. We slightly modify our approach similar to [124] by halving the available bandwidth for a time slot in case of a relay aided communication. Since both IHM and ULRA reuse a channel allocated to a cellular user (CU) we consider the presence of 10 active CUs each using a unique orthogonal frequency channel similar to [124]. We assume the base station is placed at the center of the cells and CUs are distributed uniformly at random in the cell. For accurate measurements we ran these algorithms on 1000 random instances and took the average of them. Furthermore, to enable two-way communication we run these algorithms twice, once for the forward direction and on this result we run the algorithm a second time for the other direction. We only activate those links which are still feasible after the second round of execution. We compare the performance of our approach with these two algorithms in terms of number of links activated and total system throughput achieved with varying system load. By system load we imply the number of requesting D2D pairs. For throughput calculations we only select the links outputted by an algorithm for activation and apply the Shannon capacity formula. As depicted in figure 3.5 our proposed scheme outperforms both of these algorithms. This improvement can be attributed to the fact that

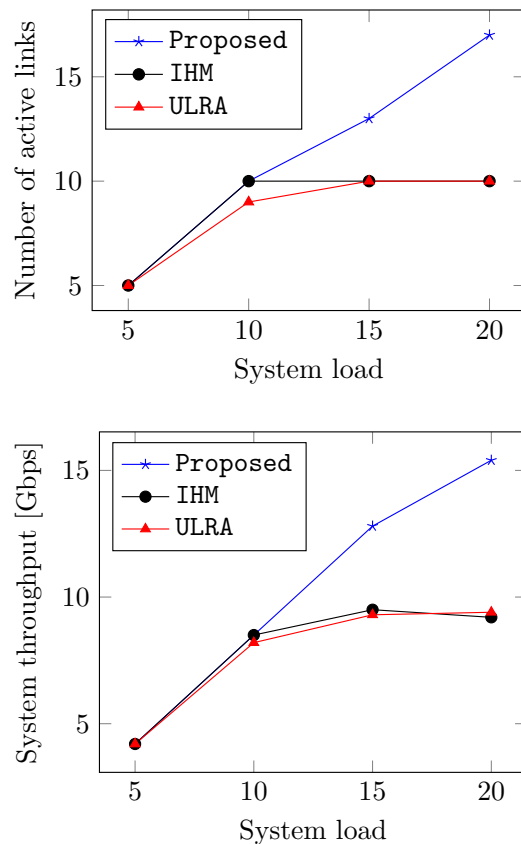


Figure 3.5: Plot of active link count and total system throughput (without network coding)

we have considered the two problems jointly and allowed multiple frequency reuse.

The true potential of our algorithm is observed when the network coding is enabled. For reference, we also consider the *optimal* scheme where we directly solve the formulated ILP. Modern optimization solvers like Gurobi [174] can solve an ILP efficiently within reasonable amount of time for smaller instances. Figure 3.6 shows how well our proposed algorithm perform to achieve a near optimal solution in comparison to the optimal scheme.

The IHM algorithm has a running time of $O(jB^3)$, where $B = \max(|\mathcal{D}|, |\mathcal{R}|, |\mathcal{F}|)$ and j is the number of iterations in IHM and the time complexity for ULRA is $O(|\mathcal{D}||\mathcal{R}||\mathcal{F}|)$. While our algorithm has a running time of $O(L)$ where L is the time complexity for solving the LP with $|\mathcal{D}||\mathcal{R}||\mathcal{F}|$ variables. Our algorithm has higher time complexity due to the fact that it allows multiple frequency reuse, while both IHM and ULRA allow only single reuse. On an Intel i7-11700 CPU running Kubuntu 22.04 with 32 GB of main memory, we measured the

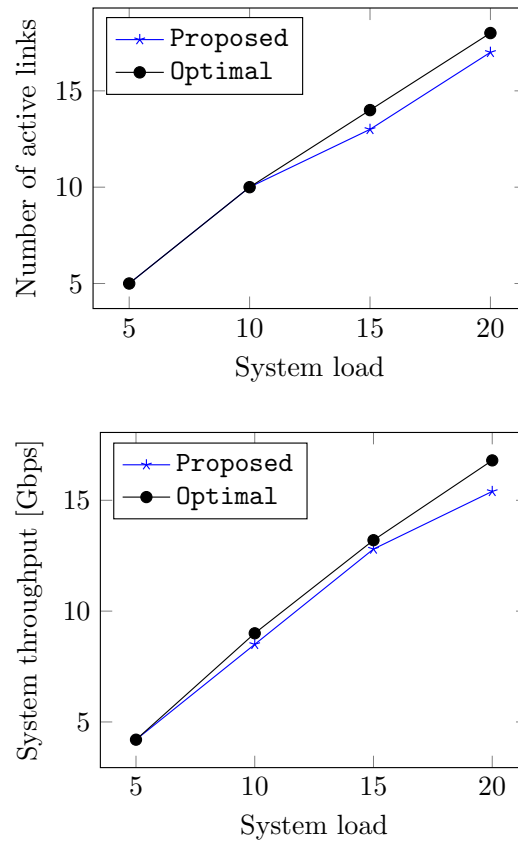


Figure 3.6: Plot of comparison against **Optimal** (with network coding)

running time of the aforementioned solutions. The Gurobi solver took about 6 ms to find the optimal solution, while our proposed approach obtained a near-optimal solution within 3 ms. Both IHM and ULRA take less than 1 ms to find a solution, which is much worse than the one obtained via our proposed method, as demonstrated above.

Thus, by jointly dealing the relay selection and frequency allocation problem with multiple frequency reuse our proposed algorithm results into improved system throughput. The use of network coding for slot reduction also plays a significant role in the throughput improvement.

3.6 Conclusion

In this chapter, we have addressed the joint relay selection and frequency allocation problem in relay-aided D2D communication and devised an LP relaxation based greedy strategy for this \mathcal{NP} -Complete problem. The simulation results show that our proposed scheme solves the problem near-optimally. Moreover, our algorithm outperforms the IHM [58] and ULRA [124] algorithms in terms of activated links and system throughput. This improvement can be attributed to the fact that we have jointly dealt with the two problems, unlike solving them in successive stages like in the IHM or ULRA algorithms. Moreover, using the network coding scheme [167] for slot reduction also contributes to the said improvements. Lastly, instead of single reuse of frequencies, our proposed scheme allows multiple reuse to further improve the spectral-efficiency, which is reflected in the system throughput. One obvious limitation of this work is that it assumes an obstacle-free environment with stationary UEs. Addressing these two issues can be a possible extension of this work.

CHAPTER 4

Joint Channel and Relay Selection for Mobile Users in Presence of Obstacles*

The exponential growth of portable handheld devices, along with their bandwidth-hungry applications, has already saturated traditional wireless communication systems. In next generation wireless communication, new strategies such as **device-to-device (D2D)** communication using **millimeter-wave (mmWave)** signals have been proposed to satisfy the high bandwidth requirements [8]. Recall that **D2D** communication is the enabling technology that allows two nearby **user equipment (UEs)** to communicate directly with each other with limited or no involvement of the **base station (BS)**. Such short-distance communication using **mmWave** not only provides good received signal strength but also limits interference to and from other **UEs** communicating in the same frequency channel [8]. Using beamforming, we can send highly directed **mmWave** signals to a receiver and have pseudowire-like communication [23]. Since **D2D** communication using **mmWave** signals incurs very limited interference, it allows us to activate two or more **D2D** communication links in the same frequency channel, which improves the spectral efficiency and in turn improves the overall system throughput, as demonstrated in **Chapter 3**. Furthermore, the recent IEEE 802.11ay standard, which operates in the **mmWave** spectrum, also supports spatial sharing and interference mitigation technologies [175, 176].

*This chapter is based on the following publications:

- [C1] **Rathindra Nath Dutta** and Sasthi C. Ghosh. “Resource Allocation for Millimeter Wave D2D Communications in Presence of Static Obstacles”. In: *Proceedings of the 35th International Conference on Advanced Information Networking and Applications (AINA-2021)*, Toronto, ON, Canada, 12-14 May, 2021. Vol. 225. Lecture Notes in Networks and Systems (LNNS). Springer, 2021, pp. 667–680. ISBN: 978-3-030-75100-5. DOI: [10.1007/978-3-030-75100-5_57](https://doi.org/10.1007/978-3-030-75100-5_57)
- [J1] **Rathindra Nath Dutta** and Sasthi C. Ghosh. “Mobility aware resource allocation for millimeter-wave D2D communications in presence of obstacles”. In: *Computer Communications (Elsevier)*, Vol. 200 (Feb. 2023), pp. 54–65. ISSN: 0140-3664. DOI: [10.1016/j.comcom.2022.12.025](https://doi.org/10.1016/j.comcom.2022.12.025)

One downside of using high-frequency signals like **mmWave** is that they are highly susceptible to propagation and penetration losses due to their smaller wavelengths. Therefore, we need short, obstacle-free **line-of-sight (LOS)** communication path [24] between the transmitter-receiver pair to achieve high data rates. By obstacles, we mean anything from a brick wall or signboard to moving objects like vehicles or even humans. The **UEs** that are not communicating on their own may act as relays. In cases where the direct **LOS** communication path offers poor signal quality due to the presence of some obstacles, one can opt for relay-aided communications [70, 100]. Before going any further, we make the following remark: The slot reduction technique used in **Chapter 3** relies on the fact that a receiver can simultaneously receive two signals that may come from completely opposite directions. This is no longer feasible for **mmWave** communication using directed antennas. Furthermore, the technique is applicable only when two-way communication is taking place, which may not be the case in general. Thus, from this chapter onwards, we can no longer use the slot reduction technique, and we consider only one-way D2D communications.

Usually, the number of available frequency channels is limited and significantly smaller than the number of requesting **D2D** pairs. The available relay devices are also limited in number, and each relay device can participate in at most one relay-aided communication at a time. Now the resource allocation problem in relay-aided communications needs to deal with two types of resources, namely channel resources and relay resources. The *channel allocation problem* is concerned with allocating frequency channels to the **D2D** links so that their datarate requirements are satisfied. On the other hand, the aim of the *relay selection problem* is to assign relay devices to the **D2D** pairs that wish to establish relay-aided communications. Given the number of frequency channels and the relay resources, the aim is to activate the maximum possible number of requesting **D2D** pairs.

As motivated in **Section 3.1**, the two problems, namely resource allocation and relay selection, have inherent interdependencies, and thus they must be dealt with jointly. Most of the existing works on resource allocation have considered a snapshot of the system where the users are stationary, as mentioned in **Chapter 2**. User mobility makes it much harder to optimally allocate resources, as the measured **signal-to-interference-plus-noise ratio (SINR)** at the current time instant may dramatically change in the next time instant. Moreover, the presence of static and dynamic obstacles may severely degrade the expected **SINR** between two **D2D** devices communicating using a **mmWave** signal. Therefore, one must incorporate user mobility and the presence of obstacles into the problem formulation to make the solution more practical. Existing works, including our own work presented

in [Chapter 3](#), assume an obstacle-free environment with stationary UEs. Thus, in this chapter, we consider the [joint relay selection and channel assignment problem \(JRSCAP\)](#) for mobile users in the presence of static as well as dynamic obstacles. Basically, here we try to predict the SINR by considering user mobility and the presence of obstacles. We use this information to judge the quality of the links. This is captured by probabilistic constraints with stochastic random variables in our proposed problem formulation. Later, these probabilistic constraints are converted into deterministic ones to make them more tractable. More specifically, our contributions can be summarized as follows:

[Contribution 2.1] We formally prove that joint relay selection and channel assignment problem is not only \mathcal{NP} -Complete but also \mathcal{APX} -hard, which eliminates the possibility of finding any constant factor polynomial time approximation scheme (PTAS) unless $\mathcal{P}=\mathcal{NP}$.

[Contribution 2.2] By directly incorporating device mobility and knowledge of obstacles, we pose the joint problem as a [stochastic integer program \(SIP\)](#), which has probabilistic constraints.

[Contribution 2.3] As dealing with the probabilistic constraints is hard, we convert our proposed SIP into an equivalent deterministic [mixed-integer linear program \(MILP\)](#). We utilize a standard concentration inequality, namely the Chebyshev–Cantelli inequality, for this conversion.

[Contribution 2.4] Given the computational cost of MILP for large instances, we propose a greedy solution for this. We construct an interference graph of the requesting links, where we capture the user mobility and blockages due to the presence of obstacles. We then use the notion of *defective-coloring* [125] to jointly allocate channels and select relays for the requesting users.

[Contribution 2.5] Furthermore, we derive an approximation bound of our proposed greedy solution.

[Contribution 2.6] Our proposed solution has been compared against a recent work [105], and with extensive simulations, we have shown the superiority of our proposed solution in terms of activated links, system throughput, link failures and fairness.

The rest of this chapter is organized as follows: [Section 4.1](#) outlines the system model and various assumptions. In [Section 4.2](#), we show the hardness of JRSCAP and develop a

SIP formulation, which is then converted into an MILP. Our proposed algorithm, along with its analysis, is presented in Section 4.3, followed by the simulation results in Section 4.4. Finally, Section 4.5 concludes this chapter.

4.1 System Model

We consider a service area to be one that is controlled by a single BS, and all the decisions are taken in a centralized way by the BS. We assume a D2D overlay communication scenario where static as well as dynamic obstacles are present in the environment. The UEs are classified as either requesting or idle, depending on their intention to communicate. Suppose there are M requesting UE pairs who are willing to communicate and N idle UEs that can provide relaying services to them. We assume all communication to be in half-duplex mode, and hence a UE cannot receive and transmit simultaneously. Time is discretized into slots t_0, t_1, \dots , each with a small Δt time span. We also discretize the entire region as a grid of small squared cells of size $g \times g$, as done in [61]. Notations used in this chapter are summarized in Table 4.1.

Static Obstacle Modelling

We assume that the approximate sizes and locations of the static obstacles are known a priori. One possible way to acquire this information is through satellite imagery [61]. A grid cell that contains even a portion of an obstacle is considered to be fully *blocked*. Figure 4.1 shows the blocked cells (shaded in gray) due to the presence of an obstacle (shaded in black). We maintain a binary matrix called `visibility` that indicates whether a pair of nearby grid cells has a LOS path free of static obstacles or not, and we call two grid cells nearby if they are within a distance d_{\max} . Let us abuse the notation a little and write `visibilitya,b` to indicate the existence of a static obstacle-free LOS path between the grid cells containing the devices a and b . The efficient computation of this matrix is discussed in Section 4.3.1.

Direct and Relay-Aided Communications

For a requesting D2D pair, if there is an obstacle-free LOS path, they may communicate directly. Whereas, if their LOS path is blocked due to the presence of some static or dynamic obstacles or the direct link has poor signal quality due to severe interference, the

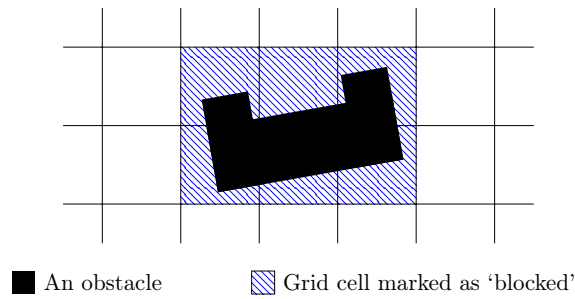


Figure 4.1: Grid approximation of an obstacle

concerned **D2D** pair may communicate via an intermediate relay node. For simplicity, we are considering only one-hop relay-assisted **D2D** communication in such cases. We further assume that an idle **UE** can serve as a relay for only one **D2D** pair. We denote \mathcal{D} to be the set of all requesting **D2D** pairs. As shown in Figure 4.2, the direct **LOS** path is blocked for the requesting pair UE_1 - UE_2 , so they communicate via relay UE_3 . Since the idle **UEs** are acting as relays and have limited resources, we assume they can only hold one data packet at a time. Thus, with store-and-forward relaying, the one-hop relay-aided communication must be completed within a superslot. Here we denote a pair of successive time slots (t_{2i}, t_{2i+1}) as a superslot. Here, we assume that a relay device that receives data in slot t_{2i} forwards it in the next slot t_{2i+1} . This is a reasonable assumption, as buffering more data packets would anyway introduce delays, which should be avoided.

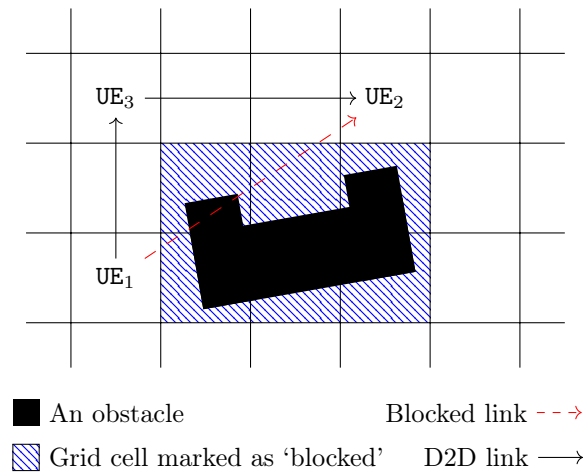


Figure 4.2: Relay-aided communication avoiding an obstacle

Candidate Relays

For a requesting D2D pair $i = (i_1, i_2)$, all the idle UE r within its vicinity, having LOS paths with both UE i_1 and UE i_2 , form the set of candidate relays for the pair i . In other words, r is a candidate relay for D2D pair i if and only if r is within d_{\max} distance from both i_1 and i_2 , and both $\text{visibility}_{i_1, r} = 1$ and $\text{visibility}_{r, i_2} = 1$. An idle UE can be present in more than one such candidate relay set but can be selected for at most one D2D pair for relaying. We denote \mathcal{R}_i to be the set of candidate relays for the D2D pair i , and the set of all such relay nodes is thus defined as $\mathcal{R} = \bigcup_{i \in \mathcal{D}} \mathcal{R}_i$. An efficient computation of these \mathcal{R}_i sets is described in Section 4.3.2.

Modelling User Mobility

We consider that the UEs are moving following some known mobility pattern that is known to the BS. For convenience, we also assume that the UEs do not cross the boundary of the considered service area during a superslot and that no new UE enters the area. We make this assumption to keep the number of UEs in the service area during a superslot unchanged. This is not a very hard assumption because the length of a superslot is very short compared to the average velocities of the UEs and the size of the service area considered. This assumption actually simplifies the computation of the interference from different UEs. Further, we assume that the location of each UE is approximated to the center of its containing grid cell (as also evident in Figure 4.2), and this information is available to the BS at the beginning of each superslot. BS leverages this information to predict the SINR values for the next time instant and intelligently choose a link for activation.

Modelling Dynamic Obstacles

Suppose the grid cell (x, y) contains a dynamic obstacle with probability $b_{x,y}$. Similar to [114], we assume that BS knows these probabilities, where the dynamic obstacles are uniformly distributed over the service area. We maintain a matrix called **blockage**, where $\text{blockage}_{(x_s, y_s), (x_e, y_e)}$ denotes the blockage probability of an LOS link between grid cells (x_s, y_s) and (x_e, y_e) . Note that this **blockage** matrix incorporates the presence of both static and dynamic obstacles. Thus, if there exists a static obstacle in between two grid cells, the corresponding entry in the **blockage** matrix is 1. The efficient computation of this matrix is discussed in Section 4.3.1.

Communication Channel

We assume that directional antenna arrays are being used for mmWave D2D communications. To compensate for high propagation losses, devices use beamforming with these directional antennas [23, 26], where mainlobe and sidelobe antenna gains are given by $G_m = N_p$ and $G_s = 1/\sin^2(3\pi/2\sqrt{N_p})$ respectively. Here, N_p denotes the size of the antenna array. The beamwidth is given as $\sqrt{3/N_p}$. We assume a fixed beamwidth throughout this work. We also assume the directional antennas of a communicating D2D pair are automatically aligned to each other based on the device positions. In other words, we ignore the alignment overhead that ranges around a few hundreds of microseconds even for extremely narrow beams, and it can be considered negligible compared to actual data transmission, which is in the order of seconds [27, 111, 114]. Similar to Chapter 3, following [23, 26, 111], the received power with transmit power P can be computed as $R_{\text{Tx,Rx}} = \kappa \phi G_{\text{Tx}} G_{\text{Rx}} P d_{\text{Tx,Rx}}^{-L}$, where $d_{\text{Tx,Rx}}$ is the distance between the transmitter (Tx) and the receiver (Rx), L is the pathloss exponent, $\kappa = (\frac{\lambda}{4\pi d_0})^2$ with d_0 and λ being the reference distance for the antenna far-field and the wavelength, respectively, ϕ is the shadowing random variable, G_{Tx} and G_{Rx} are the antenna gains at the transmitter and the receiver, respectively. If the receiver falls within the beamwidth of the transmitter, we set $G_{\text{Tx}} = G_m$, and $G_{\text{Tx}} = G_s$ otherwise. Similarly, if the transmitter falls within the beamwidth of the receiver, we set $G_{\text{Rx}} = G_m$ and $G_{\text{Rx}} = G_s$ otherwise. An efficient determination of G_{Tx} and G_{Rx} is detailed in Section 4.3.3.

Interference Consideration

Consider a relay-aided D2D pair $i \in \mathcal{D}$ consisting of two UEs, denoted as (i_1, i_2) , where UE i_1 sends some data to UE i_2 via some relay UE $r \in \mathcal{R}_i$. In the first time slot of a superslot, i_1 plays the role of a transmitter, r becomes the receiver, and i_2 stays idle. In the second slot, r becomes the transmitter, i_2 plays the role of a receiver, and i_1 does not take part. Whereas for a D2D pair $i \in \mathcal{D}$ with UE i_1 directly transmitting to UE i_2 , i_1 plays the role of a transmitter while i_2 receives. Such a D2D pair can be opportunistically scheduled in either of the two time slots of a superslot. In a specific time slot where a transmitter-receiver pair Tx-Rx is scheduled for transmission, Tx may cause interference to all active receivers other than Rx receiving in the same frequency channel.

Notation	Meaning
\mathcal{D}	Set of D2D pairs
\mathcal{R}	Set of idle UEs who can relay
\mathcal{F}	Set of orthogonal frequency channels
t	Discrete time slots
Δt	Duration of a time slot
g	Grid size
G_m, G_s	Mainlobe and sidelobe antenna gain
θ	beamwidth of the signal
d_{\max}	maximum D2D transmission distance
P	Transmit power
$R(a, b, c)$	Received signal power from a to c while directed towards b
η_0	Noise
I	Interference
Γ	SINR
ζ	SINR threshold
ρ	probability threshold
\mathcal{G}_f	Frequency class f
n_{OPT}	Optimum number of activated links
n_{APX}	Number of activated links with our approach
β	Approximation ratio for maximum independent set problem
Δ	Maximum degree of a graph
X, Y	Optimization variables
$\text{blockage}_{a,b}$	Probability of not having LOS between grid a and grid b

Table 4.1: Notations used throughout Chapter 4

4.2 Problem Formulation

Here we first develop a **SIP** for the considered problem, followed by its hardness proof, and then present a mechanism to deterministically solve our proposed **SIP**. Here, we solve the problem independently for every superslot. Therefore, for notational brevity, we conveniently drop the time index and simply represent a superslot as slot 1 and slot 2.

4.2.1 Developing an SIP Model

Each **D2D** pair can be activated in direct communication mode or relay-aided mode; thus, we define two sets of binary decision variables $\forall i \in \mathcal{D}, r \in \mathcal{R}_i, f \in \mathcal{F}, f' \in \mathcal{F}, s \in \{1, 2\}$:

$$X_{i,f,s} = \begin{cases} 1 & \text{if } i\text{-th D2D pair communicates directly using frequency } f \text{ in slot } s \\ 0 & \text{otherwise} \end{cases}$$

$$Y_{i,r,f,f'} = \begin{cases} 1 & \text{if } i\text{-th D2D pair communicates via relay } r \text{ using frequencies } f \text{ and } f' \\ 0 & \text{otherwise} \end{cases}$$

The two frequency indices f and f' in the subscript of the binary indicator variable $Y_{i,r,f,f'}$ denote that the communication in the first slot from i_1 to r happens via frequency channel f , while in the second slot, r relays the data to i_2 over frequency channel f' . For notational convenience, let us define $R(a, b, c)$ as the received signal strength from device a to device c while the signal is directed towards device b . For a **D2D** pair $i \in \mathcal{D}$ transmitting directly using a frequency channel $f \in \mathcal{F}$, the interferences during the two slots 1 and 2 of a superslot are given in (4.1) and (4.2), respectively.

$$I_{i,f,1} = \sum_{j \in \mathcal{D}, j \neq i} R(j_1, j_2, i_2) X_{j,f,1} + \sum_{j \in \mathcal{D}, j \neq i} \sum_{r \in \mathcal{R}_j} \sum_{f' \in \mathcal{F}} R(j_1, r, i_2) Y_{j,r,f,f'} \quad (4.1)$$

$$I_{i,f,2} = \sum_{j \in \mathcal{D}, j \neq i} R(j_1, j_2, i_2) X_{j,f,2} + \sum_{j \in \mathcal{D}, j \neq i} \sum_{r \in \mathcal{R}_j} \sum_{f' \in \mathcal{F}} R(r, j_2, i_2) Y_{j,r,f',f} \quad (4.2)$$

The corresponding expected **SINR** value is given in (4.3), where η_0 denotes thermal noise.

$$\Gamma_{i,f,s} = \frac{(1 - \text{blockage}_{i_1, i_2}) R_{i_1, i_2}}{\eta_0 + I_{i,f,s}}, \quad \forall i \in \mathcal{D}, f \in \mathcal{F}, s \in \{1, 2\} \quad (4.3)$$

Similarly, for a **D2D** pair $i \in \mathcal{D}$ transmitting via relay $r \in \mathcal{R}_i$ using a frequency channel $f \in \mathcal{F}$, the interferences during the two slots 1 and 2 of a superslot are given in (4.4) and (4.5), respectively.

$$\widehat{I}_{i,r,f,1} = \sum_{j \in \mathcal{D}, j \neq i} R(j_1, j_2, r) X_{j,f,1} + \sum_{j \in \mathcal{D}, j \neq i} \sum_{r' \in \mathcal{R}_j} \sum_{f' \in \mathcal{F}} R(j_1, r', r) Y_{j,r',f,f'} \quad (4.4)$$

$$\widehat{I}_{i,r,f,2} = \sum_{j \in \mathcal{D}, j \neq i} R(j_1, j_2, i_2) X_{j,f,2} + \sum_{j \in \mathcal{D}, j \neq i} \sum_{r' \in \mathcal{R}_j} \sum_{f' \in \mathcal{F}} R(r', j_2, i_2) Y_{j,r',f',f} \quad (4.5)$$

For each $i \in \mathcal{D}$, $r \in \mathcal{R}_i$, $f \in \mathcal{F}$ the **SINR** values for the two slots 1 and 2 are given in (4.6).

$$\widehat{\Gamma}_{i,r,f,1} = \frac{(1 - \text{blockage}_{i_1,r}) R_{i_1,r}}{\eta_0 + \widehat{I}_{i,r,f,1}} \quad \text{and} \quad \widehat{\Gamma}_{i,r,f,2} = \frac{(1 - \text{blockage}_{r,i_2}) R_{r,i_2}}{\eta_0 + \widehat{I}_{i,r,f,2}} \quad (4.6)$$

For each **D2D** link $i \in \mathcal{D}$ communicating via relay $r \in \mathcal{R}_i$ using some frequency channels f and f' , respectively, for the two slots 1 and 2, the effective **SINR** is computed as the minimum over the two slots as given by the equation (4.7).

$$\widehat{\Gamma}_{i,r,f,f'} = \min \left(\widehat{\Gamma}_{i,r,f,1}, \widehat{\Gamma}_{i,r,f',2} \right) Y_{i,r,f,f'} \quad (4.7)$$

Note that the measured **SINR** can change significantly between successive time instants due to user mobility and the presence of dynamic obstacles. At time instant t , a link is considered for activation in slot $s \in \{1, 2\}$ if its **SINR** value remains above some threshold ρ during the entire time span between t and $t + s$. To capture this, we reintroduce the time index t as a superscript to all the variables and expressions involving $\Gamma_{i,f,s}$ and $\widehat{\Gamma}_{i,r,f,s}$ to denote the corresponding time instant t . To formalize this, we write the data rate constraints involving $\Gamma_{i,f,s}$ and $\widehat{\Gamma}_{i,r,f,s}$ as follows:

$$\Pr \left[\Gamma_{i,f,s}^{(t+s)} \geq \zeta_i \mid \Gamma_{i,f,s}^{(t)} \geq \zeta_i \right] \geq (1 - \rho) X_{i,f,s} \quad \forall i \in \mathcal{D}, f \in \mathcal{F}, s \in \{1, 2\} \quad (4.8)$$

$$\Pr \left[\widehat{\Gamma}_{i,r,f,1}^{(t+1)} \geq \zeta_i \mid \widehat{\Gamma}_{i,r,f,1}^{(t)} \geq \zeta_i \right] \geq (1 - \rho) \sum_{f' \in \mathcal{F}} Y_{i,r,f,f'} \quad \forall i \in \mathcal{D}, r \in \mathcal{R}_i, f \in \mathcal{F} \quad (4.9)$$

$$\Pr \left[\widehat{\Gamma}_{i,r,f,2}^{(t+2)} \geq \zeta_i \mid \widehat{\Gamma}_{i,r,f,2}^{(t)} \geq \zeta_i \right] \geq (1 - \rho) \sum_{f' \in \mathcal{F}} Y_{i,r,f',f} \quad \forall i \in \mathcal{D}, r \in \mathcal{R}_i, f \in \mathcal{F} \quad (4.10)$$

Here ζ_i is the SINR threshold required for link i . Furthermore, we must also have the following constraints on the binary variables:

$$\sum_{f \in \mathcal{F}} \sum_{s \in \{1,2\}} X_{i,f,s} + \sum_{r \in \mathcal{R}_i} \sum_{f \in \mathcal{F}} \sum_{f' \in \mathcal{F}} Y_{i,r,f,f'} \leq 1, \quad \forall i \in \mathcal{D} \quad (4.11)$$

$$\sum_{i \in \mathcal{D}} \sum_{f \in \mathcal{F}} \sum_{f' \in \mathcal{F}} Y_{i,r,f,f'} \leq 1, \quad \forall r \in \mathcal{R} \quad (4.12)$$

Constraint (4.11) ensures that a requesting link can be scheduled in direct mode at either slot 1 or slot 2 or can be scheduled in relay-aided mode. Constraints (4.11) and (4.12) together ensure that for relay-aided communication, a pair can choose only one relay and a particular relay can be chosen by at most one pair. We aim to maximize the total number of links activated, as expressed below.

$$\text{maximize : } \left\{ \sum_{i \in \mathcal{D}} \sum_{f \in \mathcal{F}} \sum_{s \in \{1,2\}} X_{i,f,s} + \sum_{i \in \mathcal{D}} \sum_{r \in \mathcal{R}_i} \sum_{f \in \mathcal{F}} \sum_{f' \in \mathcal{F}} Y_{i,r,f,f'} \right\} \quad (4.13)$$

Throughput obtained from the active links can be computed using Shannon's capacity formula as given in Equation (1.3). Thus, we have an SIP formulation where the objective function is given by (4.13) and the constraints are given by Equations (4.8) to (4.12).

4.2.2 Proving Hardness

Lemma 4.1 (Approximation hardness). *The JRSCAP is \mathcal{APX} -hard.*

Proof. Consider a special case of JRSCAP where we are given an input instance I with n requesting D2D links and only one available frequency channel. Moreover, assume that all devices are stationary and that their positions and data rate requirements are such that they cannot tolerate even a small amount of interference. One can model any graph G as an interference graph, where vertices denote the D2D links and edges encode the interference relationship among the links. Any algorithm that maximizes the number of activated links of this special input instance I essentially outputs a maximum independent set (MIS) of the underlying interference graph G . Now the MIS problem is a well-known \mathcal{NP} -Complete problem; moreover, it is \mathcal{APX} -hard [177], i.e., it cannot be approximated to a constant factor by any deterministic polynomial time algorithm unless $\mathcal{P} = \mathcal{NP}$. Since JRSCAP is at least as hard as MIS, it is not only \mathcal{NP} -Complete but also \mathcal{APX} -hard. ■

4.2.3 Solving the SIP

A classical way of solving an SIP problem is to first convert the probabilistic constraints into their equivalent deterministic ones and then solve the problem involving only deterministic constraints [111]. This conversion process can be briefly explained next.

For this purpose, let us consider a probabilistic constraint, as shown in (4.14), which actually generalizes the three probabilistic constraints (4.8), (4.9), and (4.10) present in the above SIP formulation.

$$\Pr \left[\Gamma^{(t+1)} \geq \zeta \mid \Gamma^{(t)} \geq \zeta \right] \geq (1 - \rho) \quad (4.14)$$

Since devices are moving independently of each other the SINR value of a link at time t and $t + 1$ is independent of each other. Thus, we can rewrite inequality (4.14) as (4.15).

$$\Pr \left[\Gamma^{(t+1)} \geq \zeta \right] \geq (1 - \rho) \quad (4.15)$$

We can rewrite (4.15) as follows:

$$\Pr \left[\Gamma^{(t+1)} < \zeta \right] \leq 1 - (1 - \rho) = \rho$$

This can further be rewritten as (4.16):

$$\Pr \left[\frac{1}{\Gamma^{(t+1)}} > \frac{1}{\zeta} \right] \leq \rho \quad (4.16)$$

Recall that for a random variable X having mean μ and variance σ^2 , Chebyshev–Cantelli inequality gives the following upper bound for any constant $c > 0$:

$$\Pr [X - \mu \geq c] \leq \frac{\sigma^2}{\sigma^2 + c^2}$$

Now putting $X = \frac{1}{\Gamma^{(t+1)}}$ and $c = \frac{1}{\zeta} - \mu^{(t+1)}$ into this concentration inequality, we get (4.17).

$$\Pr \left[\frac{1}{\Gamma^{(t+1)}} > \frac{1}{\zeta} \right] \leq \frac{(\sigma^{(t+1)})^2}{(\sigma^{(t+1)})^2 + \left(\frac{1}{\zeta} - \mu^{(t+1)} \right)^2} \quad (4.17)$$

Here, $\mu^{(t+1)}$ and $\sigma^{(t+1)}$ respectively denote the mean and standard deviation of the inverse

SINR value $\frac{1}{\Gamma^{(t+1)}}$ at time $t+1$, and are computed at time t . Comparing the two inequalities (4.16) and (4.17), we obtain the following deterministic constraint, which ensures that probabilistic constraint (4.14) is satisfied.

$$\frac{(\sigma^{(t+1)})^2}{(\sigma^{(t+1)})^2 + \left(\frac{1}{\zeta} - \mu^{(t+1)}\right)^2} \leq \rho$$

The above can be simplified to (4.18).

$$\mu^{(t+1)} + \sigma^{(t+1)} \sqrt{\frac{1-\rho}{\rho}} \leq \frac{1}{\zeta} \quad (4.18)$$

Using the above conversion process, the probabilistic constraints given in (4.8), (4.9), and (4.10) can be written as the following deterministic constraints:

$$\mu_{i,f,s}^{(t+1)} + \sigma_{i,f,s}^{(t+1)} \sqrt{\frac{1-\rho}{\rho}} \leq \frac{1}{\zeta_i} + (1 - X_{i,f,s}) M \quad \forall i \in \mathcal{D}, f \in \mathcal{F}, s \in \{1, 2\} \quad (4.19)$$

$$\mu_{i,r,f,1}^{(t+1)} + \sigma_{i,r,f,1}^{(t+1)} \sqrt{\frac{1-\rho}{\rho}} \leq \frac{1}{\zeta_i} + \left(1 - \sum_{f' \in \mathcal{F}} Y_{i,r,f,f'}\right) M \quad \forall i \in \mathcal{D}, r \in \mathcal{R}_i, f \in \mathcal{F} \quad (4.20)$$

$$\mu_{i,r,f,2}^{(t+1)} + \sigma_{i,r,f,2}^{(t+1)} \sqrt{\frac{1-\rho}{\rho}} \leq \frac{1}{\zeta_i} + \left(1 - \sum_{f' \in \mathcal{F}} Y_{i,r,f',f}\right) M \quad \forall i \in \mathcal{D}, r \in \mathcal{R}_i, f \in \mathcal{F} \quad (4.21)$$

Here, M is a suitably large positive quantity. The μ and σ values can be computed as mentioned in [111] by solving four-dimensional integrals, which is computationally intensive. Instead, one can opt for the Monte-Carlo estimation method for computing them. By law of large numbers we know that, $\lim_{n \rightarrow \infty} \frac{1}{n} \sum_{i=1}^n X_i = \mathbb{E}[X]$. Thus, by drawing enough samples of $\Gamma_{i,f,s}^{(t+1)}$, we can estimate the value of $\mu_{i,f,s}^{(t+s)}$. The Monte-Carlo estimation is done by repeatedly drawing random samples and taking an average of their values. Now $\sigma_{i,f,s}^{(t+s)}$ can be estimated using the equation $\text{Var}(X) = \mathbb{E}[X^2] - (\mathbb{E}[X])^2$. Similarly, we can estimate $\mu_{i,r,f,1}^{(t+1)}$, $\sigma_{i,r,f,1}^{(t+1)}$, $\mu_{i,r,f,2}^{(t+1)}$, and $\sigma_{i,r,f,2}^{(t+1)}$.

Thus, the SIP formulation can be converted into the following MILP, where the objective function is given by the Equation (4.13) and the constraints are given by the Equations (4.11), (4.12) and (4.19) to (4.21). As solving MILP is computationally expensive, especially for larger instances, we next develop an efficient greedy algorithm for the same.

4.3 Proposed Algorithm

Here we first discuss how the **visibility** and **blockage** matrices can be precomputed efficiently, followed by an efficient way of shortlisting candidate relays for a requesting **D2D** link and an efficient way of deciding antenna gains. Finally, we present our greedy algorithm along with its analysis.

4.3.1 Precomputation of visibility and blockage Matrices

Recall that we have discretized the entire service region into a grid of small square cells of size $g \times g$. Moreover, the positions and sizes of the static obstacles are known to the **BS**, which has been used to mark each grid cell containing a static obstacle as ‘blocked’, as depicted in [Figure 4.1](#). Since the status of each grid remains unchanged for a service region, we do some precomputation and produce a lookup table in order to reduce the actual runtime cost. Consider two grid cells, (x_s, y_s) and (x_e, y_e) , which we refer to as ‘start’ (s) and ‘end’ (e), respectively. Let l be the line segment joining the center of these two grid cells. We say these two grid cells are *visible* to each other if and only if there exists a static obstacle-free **LOS** path between them. In other words, (x_s, y_s) and (x_e, y_e) are visible to each other whenever the line segment l does not go through a ‘blocked’ cell. The grid cells through which a line segment passes can be efficiently obtained using Bresenham’s line drawing algorithm [178], which avoids floating point multiplication and division and instead uses only integral operations. Since we set d_{\max} as the maximum possible **D2D** transmission distance, we may need to cache the visibility information for all the grid cells within a circle of radius d_{\max} centered around each grid cell. The entire **visibility** matrix can be computed in this manner. The size of the **visibility** matrix is $\lceil \frac{w}{g} \rceil \times \lceil \frac{h}{g} \rceil \times \lceil \frac{d_{\max}}{g} \rceil \times \lceil \frac{d_{\max}}{g} \rceil$, where w and h are the width and height of the service area, respectively.

As discussed in [Section 4.1](#), given a grid cell (x, y) , how likely it is to contain a dynamic obstacle, is known to the **BS**. Let us denote this blocking probability as $b_{x,y}$. Note that, for a grid cell (x, y) containing a static obstacle, we simply assume $b_{x,y} = 1$. We initialize the **blockage** matrix with 0s. Now for each pair of grid cells (x_s, y_s) and (x_e, y_e) , not more than d_{\max} distance apart, we obtain the intermediate grid cells through which the **LOS** link between (x_s, y_s) and (x_e, y_e) passes. These intermediate grid cells can be efficiently computed using Bresenham’s line drawing algorithm, as stated above. Suppose the **LOS** link l between (x_s, y_s) and (x_e, y_e) goes through $\{(x_1, y_1), (x_2, y_2), \dots, (x_n, y_n)\}$, then the

blockage probability of the link l is given as follows:

$$\text{blockage}_{(x_s, y_s), (x_e, y_e)} = 1 - [(1 - b_{x_1, y_1})(1 - b_{x_2, y_2}) \dots (1 - b_{x_n, y_n})].$$

The size of the **blockage** matrix is the same as the **visibility** matrix, that is $\lceil \frac{w}{g} \rceil \times \lceil \frac{h}{g} \rceil \times \lceil \frac{d_{\max}}{g} \rceil \times \lceil \frac{d_{\max}}{g} \rceil$. [Algorithm 4.1](#) formalizes the described precomputation process.

Algorithm 4.1: Precomputation of **visibility** and **blockage** matrices

```

1 Allocate the visibility and blockage matrices
2 for  $x_s = 1$  to  $\lceil h/g \rceil$  do
3   for  $y_s = 1$  to  $\lceil w/g \rceil$  do
4     for  $x_e = x_s - d_{\max}$  to  $x_s + d_{\max}$  do
5       for  $y_e = y_s - d_{\max}$  to  $y_s + d_{\max}$  do
6         Let  $l$  be the line, joining  $(x_s, y_s)$  and  $(x_e, y_e)$ 
7         Compute  $\mathcal{P}$ , the set of grid cells on  $l$ , using Bresenham's algorithm
8         if  $\exists (x, y) \in \mathcal{P}$  such that grid cell  $(x, y)$  is 'blocked' then
9            $\text{visibility}_{(x_s, y_s), (x_e, y_e)} = \text{visibility}_{(x_e, y_e), (x_s, y_s)} = 0$ 
10          else
11             $\text{visibility}_{(x_s, y_s), (x_e, y_e)} = \text{visibility}_{(x_e, y_e), (x_s, y_s)} = 1$ 
12             $\text{blockage}_{(x_s, y_s), (x_e, y_e)} = 1 - \prod_{(x, y) \in \mathcal{P}} (1 - b_{x, y})$ 
13 return visibility and blockage matrices

```

4.3.2 Finding Candidate Relays

An idle device r may act as a potential relay for a **D2D** pair $i = (i_1, i_2) \in \mathcal{D}$ if and only if r is within the d_{\max} distance from both i_1 and i_2 as mentioned in [Section 4.1](#). Therefore, in order to act as a potential relay for this **D2D** pair, r must reside in the intersection region of the two d_{\max} radius circles centered around i_1 and i_2 , as depicted in [Figure 4.3a](#). As evident, r_1 and r_2 are the only candidates for relaying between i_1 and i_2 .

To reduce the search space for finding such candidate relay devices, we consider the minimum enclosing rectangle containing this intersection region of these two circles and perform a two-dimensional range search with respect to this rectangle. A two-dimensional range tree with fractional cascading [179, 180] can be used to answer this type of rectangular range query efficiently. Such an axis-parallel rectangle can be uniquely identified by any of

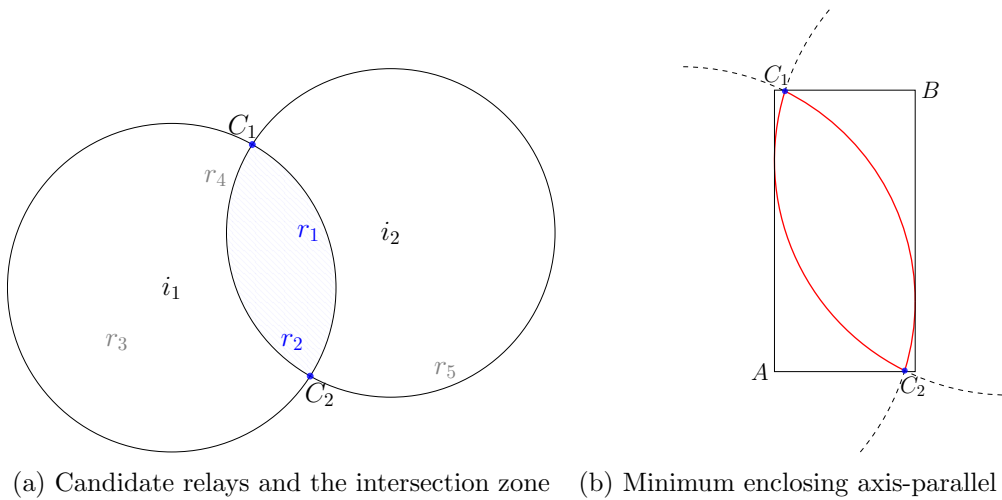


Figure 4.3: Obtaining Candidate Relays

its two opposite corners. [Figure 4.3b](#) depicts this idea. In this figure, A and B are two such corners such that $A.x \leq B.x$ and $A.y \leq B.y$, where $A.x$ and $A.y$ denote row and column indices of the grid cell containing some point A . Let C_1 and C_2 be the cut points where the two circles intersect with each other, which can be obtained from the two equations of the corresponding circles. We can compute $A.x$, $A.y$, $B.x$, and $B.y$ as follows:

$$A.x = \begin{cases} \max(i_1.x, i_2.x) - d_{\max} & \text{if } \min(C_1.y, C_2.y) < i_1.y < \max(C_1.y, C_2.y) \\ \min(C_1.x, C_2.x) & \text{otherwise} \end{cases}$$

$$A.y = \begin{cases} \max(i_1.y, i_2.y) - d_{\max} & \text{if } \min(C_1.x, C_2.x) < i_1.x < \max(C_1.x, C_2.x) \\ \min(C_1.y, C_2.y) & \text{otherwise} \end{cases}$$

$$B.x = \begin{cases} \min(i_1.x, i_2.x) + d_{\max} & \text{if } \min(C_1.y, C_2.y) < i_1.y < \max(C_1.y, C_2.y) \\ \max(C_1.x, C_2.x) & \text{otherwise} \end{cases}$$

$$B.y = \begin{cases} \min(i_1.y, i_2.y) + d_{\max} & \text{if } \min(C_1.x, C_2.x) < i_1.x < \max(C_1.x, C_2.x) \\ \max(C_1.y, C_2.y) & \text{otherwise} \end{cases}$$

The candidate relay set \mathcal{R}_i for each [D2D](#) pair can be obtained by using [Algorithm 4.2](#).

Algorithm 4.2: Constructing candidate relay sets

```

1 Store current locations of all idle devices  $r \in \mathcal{R}$  into a 2D range tree  $T_{\mathcal{R}}$ 
2 foreach  $i \in \mathcal{D}$  do
3   Compute the cut points  $C_1$  and  $C_2$ 
4   Compute the points  $A$  and  $B$  as per above equations
5    $\mathcal{R}_i \leftarrow$  Run a rectangular range query  $[(A.x, B.x), (A.y, B.y)]$  on  $T_{\mathcal{R}}$ 
6   foreach  $r \in \mathcal{R}_i$  do
7     if  $r$  is not within  $d_{\max}$  distance from both  $i_1$  and  $i_2$  then
8        $\mathcal{R}_i \leftarrow \mathcal{R}_i \setminus \{r\}$ 
9 return  $\{\mathcal{R}_i \mid \forall i \in \mathcal{D}\}$ 

```

4.3.3 Critical Region of an mmWave Beam

Consider a transmitter Tx is transmitting with a beamwidth θ to a receiver Rx, as depicted in Figure 4.4. Here the region of the beamwidth is shaded in light blue. Now some other nearby device a may get interference from Tx. Recall that the antenna gains will depend on the position and the beamwidth of the signal; that is, a mainlobe gain will apply if the device a is in the shaded zone, otherwise a sidelobe gain is applicable. This can be determined efficiently with only integral operations as detailed in [181].

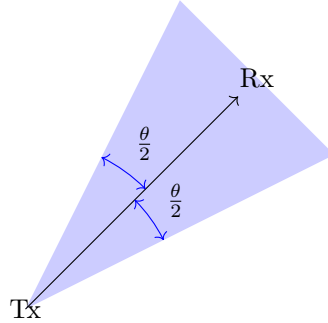


Figure 4.4: Critical region

4.3.4 Proposed Greedy Algorithm

As discussed earlier, we need to solve the considered problem for each superslot. We simplify our problem with the introduction of some *virtual relays* and unify direct communication with relay-aided ones. A direct link from i_1 to i_2 for requesting D2D pair

$i = (i_1, i_2)$, can be considered a relay-aided one by considering a virtual relay co-located either at i_1 or at i_2 . We denote the virtual relay as \hat{i}_2 when it is co-located at i_2 . Here, we assume that the actual transmission happens from i_1 to \hat{i}_2 in the first slot, and a dummy instantaneous transmission happens from \hat{i}_2 to i_2 in the second slot. Similarly, we denote the virtual relay as \hat{i}_1 when it is co-located at i_1 . Here, the dummy transmission from i_1 to \hat{i}_1 happens during the first slot, and the actual transmission from \hat{i}_1 to i_2 happens during the second slot. Note that the dummy links effectively stay idle and hence do not cause interference to any other devices. Thus, all requesting D2D links have now become relay-aided links. We consider that an idle device r can act as a relay for link $i = (i_1, i_2)$ if r is within the distance d_{\max} from both i_1 and i_2 . For each requesting link i , the candidate relay set \mathcal{R}_i can efficiently be computed in sublinear time by making orthogonal range queries which exploits the positional geometry of the devices using Algorithm 4.2. Due to the above unification, we also put two virtual relays, \hat{i}_1 and \hat{i}_2 into each candidate relay set, \mathcal{R}_i . Here, dummy virtual relays are used purely as an algorithmic tool for the unification of direct and relay-aided communications. These dummy relays are nothing but some virtual nodes, having no physical existence, and are considered in an intermediate step in our proposed solution. Any communication using such a virtual relay is finally substituted with its actual real counterpart at the end of our solution.

Let us begin by obtaining an initial frequency assignment for the requesting D2D pairs. For that, we shall try to assign frequencies in a non-interfering way. Let us define a *frequency class* \mathcal{G}_f^s consisting of the links that will be associated with a particular frequency channel $f \in \mathcal{F}$ during slot $s \in \{1, 2\}$. We will now create a graph $G_1 = (V_1, E_1 \cup E'_1)$ for the first slot, where each link (i_1, r) represents a vertex $v_{i_1, r}$ and E_1 encodes the interference relationship among the vertices for the first slot. That is,

$$V_1 = \{v_{i_1, r} \mid i \in \mathcal{D}, r \in \mathcal{R}_i\} \text{ and}$$

$$E_1 = \{(v_{i_1, r}, v_{j_1, s}) \mid \text{link } (i_1, r) \text{ and link } (j_1, s) \text{ interfere with each other}\}.$$

Since for each link i , we can choose only one relay in \mathcal{R}_i , we add an edge between two vertices $v_{i_1, r}$ and $v_{i_1, s}$ into E'_1 where $r, s \in \mathcal{R}_i, r \neq s$. Similarly, as r can be chosen as a relay only for one link i , we also add an edge between two vertices $v_{i_1, r}$ and $v_{j_1, r}$ into E'_1 where $i, j \in \mathcal{D}, i \neq j$. Note that here $i \neq j$ implicitly implies $i_1 \neq j_1$ and vice versa. Thus,

$$E'_1 = \{(v_{i_1, r}, v_{j_1, s}) \mid (i_1 = j_1 \wedge r \neq s) \vee (i_1 \neq j_1 \wedge r = s)\}.$$

Note that an MIS \mathcal{I} of G_1 would contain the links such that for each link, only one relay is chosen, each relay is chosen by only one link, and no two links interfere with each other during the first slot. This implies that all such links can be activated with the same frequency channel in the first slot and thus constitute a frequency class. It is evident that picking an MIS \mathcal{I} in G_1 not only assigns a frequency to the corresponding links but also selects relays for each of them. In this way, we are jointly dealing with the frequency allocation and relay selection problems, as motivated earlier.

Since we are dealing with relay-aided communications, we need to assign a pair of frequencies $f_1, f_2 \in \mathcal{F}$ to (i_1, r) and (r, i_2) for each requesting pair i communicating via relay r . Suppose \mathcal{I} contains a vertex $v_{i_1, r}$, which indicates that the link (i_1, r) is scheduled in the first slot with some frequency. But we have yet to schedule the link (r, i_2) in the second slot. If frequencies for both slots are available, only then the D2D pair i can be associated with the relay r . Now, the next frequency class can be obtained by taking another MIS of the residual graph, which is obtained by deleting the vertices in \mathcal{I} from G_1 . Therefore, all the frequency classes for the first slot can be obtained by iteratively picking MISs from the successive residual graphs. We initialize the residual graph G_r as G_1 itself. During the f -th iteration, the MIS of the residual graph G_r represents the frequency class \mathcal{G}_f^1 . For each vertex $v_{i_1, r} \in \mathcal{G}_f^1$ we define A_i as the set of all vertices $v_{i_1, s}$ of G_r , where $s \in \mathcal{R}_i$ and B_r as the set of all vertices $v_{j_1, r}$ of G_r , where $j \in \mathcal{D}$. Thus, for each vertex $v_{i_1, r}$ picked in \mathcal{G}_f^1 , we need to remove all vertices in A_i and B_r from G_r to ensure that the pairing of i and r is exclusive, i.e., no other relay s for i is chosen and r is not chosen for any other pair j , in successive iterations. Note that not all requesting D2D pairs may have been served in this manner; the remaining pairs are dealt with at a later stage.

At this point, we have already selected the relays for each D2D pair during the frequency assignment for the first slot. Thus, we only need to pick the links and assign frequencies to them for the second slot, corresponding to the relays selected in the first slot. Here again, we consider another graph, $G_2 = (V_2, E_2)$, where V_2 includes each link (r, i_2) such that (i_1, r) is picked and assigned with a frequency in the first slot. We put an edge between two vertices if the corresponding links interfere with each other. That is,

$$V_2 = \{v_{r, i_2} \mid \exists f \in \mathcal{F} \text{ such that } (i_1, r) \in \mathcal{G}_f^1\} \text{ and}$$

$$E_2 = \{(v_{r, i_2}, v_{s, j_2}) \mid (r, i_2) \text{ and } (s, j_2) \text{ interfere with each other}\}.$$

Similarly, by iteratively picking successive MISs and deleting the chosen vertices, we get the frequency classes for the second slot. The final residual graph may still contain a few vertices, which corresponds to the links having no frequency class assigned to them in the second slot. For each such remaining link (r, i_2) , the corresponding link (i_1, r) is removed from its respective frequency class in the first slot. These remaining pairs are dealt at a later stage. We note that the selected relay for a D2D pair could also be a virtual one, making the link operate in direct mode, and its scheduled slot depends on the location of the virtual node, whether it is co-located at i_1 or at i_2 , as discussed earlier. This process is formalized in Algorithm 4.3. Since finding the optimal MIS is \mathcal{NP} -Complete, we thus use an approximation algorithm as described in Section 4.3.5.

Algorithm 4.3: Initial frequency class formation

```

1 Construct the graph  $G_1$ 
2  $G_r \leftarrow G_1$  // initialize residual graph as  $G_1$ 
3 foreach  $f \in \mathcal{F}$  do
4    $\mathcal{G}_f^1 \leftarrow \text{APX.MIS}(G_r)$ 
5    $\mathcal{L}_1 \leftarrow \emptyset$ 
6   foreach  $v_{i_1, r} \in \mathcal{G}_f^1$  do
7     Let  $A_i = \{v_{i_1, s} \mid s \in \mathcal{R}_i\}$ 
8     Let  $B_r = \{v_{j_1, r} \mid j \in \mathcal{D}\}$ 
9      $\mathcal{L}_1 \leftarrow \mathcal{L}_1 \cup (A_i \cup B_r)$ 
10   $G_r \leftarrow G_r \setminus \mathcal{L}_1$  // remove vertices in  $\mathcal{L}_1$ 
11 Construct the graph  $G_2$ 
12  $G'_r \leftarrow G_2$  // initialize residual graph as  $G_2$ 
13 foreach  $f \in \mathcal{F}$  do
14    $\mathcal{G}_f^2 \leftarrow \text{APX.MIS}(G'_r)$ 
15    $G'_r \leftarrow G'_r \setminus \mathcal{G}_f^2$  // remove vertices in  $\mathcal{G}_f^2$ 
16 Let  $\mathcal{L}_2 = \{v_{i_1, r} \mid v_{r, i_2} \in G'_r\}$ 
   /* discard slot 1 links that do not get any frequency in slot 2 */
17 foreach  $\forall f \in \mathcal{F}$  do
18    $\mathcal{G}_f^1 \leftarrow \mathcal{G}_f^1 \setminus \mathcal{L}_2$ 
   /* return initial frequency and relay assignment */
19 return  $\{\mathcal{G}_f^1 \mid \forall f \in \mathcal{F}\}$  and  $\{\mathcal{G}_f^2 \mid \forall f \in \mathcal{F}\}$ 

```

We now consider the remaining D2D pairs that have not been assigned any frequency class in the first or second slots by Algorithm 4.3. Let us denote the set of these remaining

D2D pairs as \mathcal{D}_R . We define $\mathcal{L} = \{(i, r) \mid i \in \mathcal{D}_R \text{ and } r \in \mathcal{R}_i\}$. Suppose (i, r) is chosen from \mathcal{L} . We need to assign two frequencies, f_1 and f_2 , to the links (i_1, r) and (r, i_2) for slots 1 and 2, respectively. We now make a greedy choice over \mathcal{L} and assign two frequencies such that the interference is minimal. If we consider all possible choices of f_1 to (i_1, r) and f_2 to (r, i_2) for each (i, r) in \mathcal{L} , we would need to explore $|\mathcal{L}| \times 2|\mathcal{F}|$ possibilities. For each such possibility, the SINR values need to be reevaluated for all the links activated with the corresponding frequencies in the first and second slots. Thus, it would incur a very high time complexity of $|\mathcal{L}| \times 2|\mathcal{F}| \times |\mathcal{D}|$. Instead, we rank each element (i, r) in \mathcal{L} based on the number of devices that could be interfered with by activating this particular D2D pair i with relay r . For this, we consider an interference graph $\mathcal{G}_3 = (V_3, E_3)$ where

$$\begin{aligned} V_3 &= \{v_{i,r} \mid \text{pair } i \in \mathcal{D} \text{ is already assigned with a relay } r \in \mathcal{R}_i\} \\ &\quad \cup \{v_{i,r} \mid (i, r) \in \mathcal{L}\} \\ \text{and } E_3 &= \{(v_{i,r}, v_{j,s}) \mid ((r \neq \hat{i}_1) \wedge (i_1 \text{ interferes } s) \wedge (s \neq j_1)) \\ &\quad \vee ((r \neq \hat{i}_2) \wedge (r \text{ interferes } j_2) \wedge (s \neq j_2))\}. \end{aligned}$$

We sort the elements in \mathcal{L} in ascending order of the degrees of their corresponding vertices in \mathcal{G}_3 and break ties with the number of candidate relays. We now consider the elements from \mathcal{L} one by one in that order and try to accommodate the corresponding links into the existing frequency classes returned by Algorithm 4.3. A link (a, b) can only be accommodated into some frequency class \mathcal{G}_f^s if and only if all links of $\mathcal{G}_f^s \cup \{(a, b)\}$ satisfy the SINR constraints given by Equations (4.20) and (4.21). Since we are dealing with relay-aided communications, for each D2D pair i associated with relay r , we must find two such frequencies, $f_1, f_2 \in \mathcal{F}$, for the two slots. The order in which the frequency classes are inspected also plays a crucial role. Here we inspect the frequency classes in ascending order of their current sizes, which serves as a *load balancer* and helps to minimize the overall interference in the system. For this, we maintain a min-heap where we arrange the frequency classes by their sizes and update whenever a new link is added. Here we define the size of the frequency class \mathcal{G}_f^s as the number of links selected for activation using frequency f during slot $s \in \{1, 2\}$. This procedure is formalized as Algorithm 4.4.

Algorithm 4.4: Updating frequency classes

```

1  $\mathcal{L} = \{(i, r) \mid i \in \mathcal{D}_R \text{ and } r \in \mathcal{R}_i\}$ 
2 Construct the interference graph  $G_3$ 
3 Sort  $\mathcal{L}$  in ascending order of their degrees in  $G_3$ 
4 Construct  $\mathcal{H}_1 = \text{BUILD\_MIN\_HEAP}(\{\mathcal{G}_f^1 \mid \forall f \in \mathcal{F}\})$ 
5 Construct  $\mathcal{H}_2 = \text{BUILD\_MIN\_HEAP}(\{\mathcal{G}_f^2 \mid \forall f \in \mathcal{F}\})$ 
6 foreach  $(i, r) \in \mathcal{L}$  do
7   Set  $f_1 \leftarrow \text{NULL}$  and  $f_2 \leftarrow \text{NULL}$ 
8   foreach  $\mathcal{G}_f^1 \in \mathcal{H}_1$  do
9     if  $\mathcal{G}_f^1 \cup \{i_1, r\}$  satisfies constraint (4.20) then
10       Set  $f_1 \leftarrow f$ 
11       break
12   foreach  $\mathcal{G}_f^2 \in \mathcal{H}_2$  do
13     if  $\mathcal{G}_f^2 \cup \{r, i_2\}$  satisfies constraint (4.21) then
14       Set  $f_2 \leftarrow f$ 
15       break
16   if  $f_1 \neq \text{NULL}$  and  $f_2 \neq \text{NULL}$  then           // groups found for both slots
17      $\mathcal{G}_{f_1} \leftarrow \mathcal{G}_{f_1} \cup \{i_1, r\}$ 
18      $\mathcal{G}_{f_2} \leftarrow \mathcal{G}_{f_2} \cup \{r, i_2\}$ 
19     Update  $\mathcal{H}_1$  and  $\mathcal{H}_2$                                // heapify as per new group sizes
20     Let  $A_i = \{(i, s) \mid s \in \mathcal{R}_i\}$ 
21     Let  $B_r = \{(j, r) \mid j \in \mathcal{D}_R\}$ 
22      $\mathcal{L} \leftarrow \mathcal{L} \setminus (A_i \cup B_r)$ 
23 return  $\{\mathcal{G}_f^1 \mid \forall f \in \mathcal{F}\}$  and  $\{\mathcal{G}_f^2 \mid \forall f \in \mathcal{F}\}$ 

```

4.3.5 Procedure APX_MIS()

The best known approximation algorithm for **MIS** is based on a greedy selection policy and has an approximation ratio of $\beta = \frac{\Delta+2}{3}$ [177], where Δ is the maximum degree of the considered graph. Here, the algorithm iteratively picks one critical vertex from the graph, deletes its neighbors, and continues with the residual graph. A critical vertex is one whose degree is no more than the average degree of its neighbors. A minimum-degree vertex is always critical, so such a vertex will always exist. The procedure **APX_MIS()** applies this scheme to the given input graph and returns a maximal independent set with the approximation ratio β .

4.3.6 Analysis of the Proposed Algorithms

Let us first analyze the running time of our proposed algorithm. Thereafter, we provide an approximation ratio for the same.

Time Complexity Analysis

Lemma 4.2. *The running time of Algorithms 4.3 and 4.4 together is $O(n^2rf(n+r))$, where $n = |\mathcal{D}|$, $r = |\mathcal{R}|$, and $f = |\mathcal{F}|$.*

Proof. As specified here, $n = |\mathcal{D}|$ is the number of requesting D2D pairs, $r = |\mathcal{R}|$ is the total number of relay devices, and $f = |\mathcal{F}|$ is the number of frequency channels available. Furthermore, let us assume that Δ is the maximum degree of the underlying interference graph, i.e., any UE can interfere with at most Δ number of other UEs. In Algorithm 4.3, the graph G_1 has at most nr vertices and at most $nr\Delta$ edges, so its construction takes $O(nr\Delta)$ time. As indicated in [177], APX_MIS() procedure can be implemented with a running time linear to the number of edges and vertices of the corresponding graph. In each iteration, construction of the set \mathcal{L}_1 takes at most $nr\Delta$ time. Therefore, Lines 3 to 10 take a total of $O(nrf\Delta)$ time. On the other hand, the number of vertices in G_2 is at most n ; therefore, by a similar argument, we can say that the remaining lines take total $O(nf\Delta)$ time. Thus, Algorithm 4.3 has a total running time of $O(nrf\Delta)$.

Now in Algorithm 4.4, both the size of the set \mathcal{L} and the number of vertices in G_3 are at most nr . The construction of G_3 takes $O(nr\Delta)$ time. Line 3 can be performed in $O(nr \log(nr))$ time. A binary min-heap can be constructed by calling BUILD_MIN_HEAP in linear time with respect to the number of elements [182]. Now that there can be a total of at most n elements in the frequency groups, Lines 4 to 5 can be performed in $O(n)$ time. Line 9 requires validation of the SINR constraint given in equation (4.20) for a link in a frequency group. Now for each link, the equation (4.20) can be evaluated in $O(\tau\Delta)$ time, where τ is the number of random samples drawn for Monte-Carlo estimation. Since each frequency group can have at most n links, Line 9 requires $O(n\tau\Delta)$ time in the worst case. A similar argument holds for Line 13. The Lines 16 to 22 take at most $O(n)$ time. Thus, the loop spanning over Lines 6 to 22 takes a total of $O(n^2rf\tau\Delta)$ time in the worst case. Thus, the overall time complexity of Algorithm 4.4 is $O(n^2rf\tau\Delta)$. Since τ is a constant, we can drop it and get the overall time complexity of Algorithms 4.3 and 4.4 combined as $O(n^2rf\Delta)$. ■

Approximation Ratios for Algorithms 4.3 and 4.4

Lemma 4.3. *For a superslot, Algorithm 4.3 has an approximation ratio of $\beta + |\mathcal{F}|\Delta$ when only interference-free direct communications are considered.*

Proof. Suppose Algorithm 4.3 activates n_{APX} many links in the first slot for some input instance, while a maximum of n_{OPT} many links could have been activated by an optimal algorithm under interference-free direct communications. Since Algorithm 4.3 induces a proper coloring, each of the frequency classes must be independent sets of the underlying network graph G_1 considered in the first slot. Suppose m_{G_1} denotes the maximum number of links that could belong to a single frequency class without any interference among each other, which is essentially the size of the maximum independent set of G_1 . Since \mathcal{G}_1^1 is obtained by calling `APX-MIS()` on G_1 , we must have $n_1 = |\mathcal{G}_1^1| \geq m_{G_1}/\beta$. Now \mathcal{G}_2^1 is obtained by calling `APX-MIS()` on the residual graph $G_1 \setminus \mathcal{L}_1$ as indicated in Line 10. It is evident that $|\mathcal{L}_1| \leq n_1\Delta$. Therefore, we have the following inequality.

$$n_2 = |\mathcal{G}_2^1| \geq \frac{m_{G_1 \setminus \mathcal{L}_1}}{\beta} \geq \frac{m_{G_1} - n_1\Delta}{\beta}$$

Proceeding similarly, we can write

$$n_3 = |\mathcal{G}_3| \geq \frac{m_{G_1} - n_1\Delta - n_2\Delta}{\beta}$$

In general, we have

$$n_i = |\mathcal{G}_i| \geq \frac{1}{\beta} \left(m_{G_1} - \Delta \sum_{j=1}^{i-1} n_j \right)$$

Therefore, we can write

$$\begin{aligned} n_{\text{APX}} &= \sum_{i=1}^{|\mathcal{F}|} n_i \geq \frac{1}{\beta} \sum_{i=1}^{|\mathcal{F}|} \left(m_{G_1} - \Delta \sum_{j=1}^{i-1} n_j \right) = \frac{|\mathcal{F}|m_{G_1}}{\beta} - \frac{\Delta}{\beta} \sum_{i=1}^{|\mathcal{F}|} \sum_{j=1}^{i-1} n_j \\ &\geq \frac{|\mathcal{F}|m_{G_1}}{\beta} - \frac{\Delta}{\beta} \sum_{i=1}^{|\mathcal{F}|} n_{\text{APX}} \geq \frac{|\mathcal{F}|m_{G_1}}{\beta} - \frac{\Delta}{\beta} |\mathcal{F}| n_{\text{APX}} \end{aligned}$$

Now, with some algebraic manipulation, we can write

$$n_{\text{APX}} \geq m_{G_1} \times \frac{|\mathcal{F}|}{\beta + |\mathcal{F}|\Delta} \tag{4.22}$$

Using an optimal algorithm, suppose one can activate at most n_{OPT} many links with $|\mathcal{F}|$ frequencies without any interference. Now, by the pigeonhole principle, we must have at least $n_{\text{OPT}}/|\mathcal{F}|$ links in one of the frequency classes. Since each frequency class is an independent set of G_1 , by definition, we get $m_{G_1} \geq n_{\text{OPT}}/|\mathcal{F}|$. Plugging this into Equation (4.22), we get

$$n_{\text{APX}} \geq \frac{n_{\text{OPT}}}{|\mathcal{F}|} \times \frac{|\mathcal{F}|}{\beta + |\mathcal{F}|\Delta} = \frac{n_{\text{OPT}}}{\beta + |\mathcal{F}|\Delta}$$

Since for direct communications, the two slots are essentially treated independently of each other, the same approximation bound applies to the second slot as well. Therefore, combining the two slots, the approximation ratio for the superslot is also $\beta + |\mathcal{F}|\Delta$. ■

Next, we will derive an approximation bound for the case when two interfering links may be allowed to communicate using the same frequency as long as their SINR values satisfy the datarate requirements. To deal with such a scenario, we first need to state the notion of *defective coloring*, also known as (k, d) coloring, which was introduced by Harary and others [125].

Definition 4.3.1 (defective coloring). A (k, d) coloring of G is a vertex coloring with k colors where each vertex v in G can have at most d many neighbors having the same color (defect) as v .

Lemma 4.4. For a superslot, Algorithms 4.3 and 4.4 together have an approximation ratio of $\Delta(\beta + |\mathcal{F}|\Delta)$ when only direct communications are considered and interferences are allowed, subject to satisfying their required SINRs.

Proof. Algorithm 4.4 introduces some defective coloring into the frequency groups obtained using Algorithm 4.3. Suppose n_{APX}^0 and n_{OPT}^0 denote the number of links activated by Algorithm 4.3 and the maximum number of links that could have been activated without allowing any interference (that is, with zero defects, and hence the superscript 0). Let us denote n_{APX} as the total number of links activated by Algorithms 4.3 and 4.4 together. Now, from Lemma 4.3, we have

$$n_{\text{APX}} \geq n_{\text{APX}}^0 \geq \frac{n_{\text{OPT}}^0}{\beta + |\mathcal{F}|\Delta} \quad (4.23)$$

Suppose an optimal algorithm activates n_{OPT}^d links with d defects. This implies that the

activated links may suffer interference from at most d other links and still satisfy their required SINRs. Now we have $n_{\text{OPT}}^d \leq d \times n_{\text{OPT}}^0$. Using this in Equation (4.23), we get

$$n_{\text{APX}} \geq \frac{n_{\text{OPT}}^d}{d(\beta + |\mathcal{F}|\Delta)} \geq \frac{n_{\text{OPT}}^d}{\Delta(\beta + |\mathcal{F}|\Delta)} \quad (\text{since } d \leq \Delta) \quad \blacksquare$$

Lemma 4.5. *For a superslot, Algorithm 4.3 has an approximation ratio of $\frac{\Delta+1}{|\mathcal{F}|}(\beta + |\mathcal{F}|\Delta)^2$ when interference-free direct as well as relay-aided communications are considered.*

Proof. Suppose an optimal algorithm activates n_{OPT} links when interference-free direct as well as relay-aided communications are considered. Due to the unification of direct and relay-aided communications, for every D2D pair $i = (i_1, i_2)$ activated with some relay r by the optimal algorithm, the link (i_1, r) must have been activated during the first slot. Now suppose with Algorithm 4.3 we could only activate n'_{APX} links during the first slot. Therefore, by Lemma 4.3 we have

$$n'_{\text{APX}} \geq \frac{n_{\text{OPT}}}{\beta + |\mathcal{F}|\Delta} \quad (4.24)$$

Now for the second slot, Algorithm 4.3 constructs the graph G_2 with n'_{APX} number of vertices. Suppose n''_{APX} is the total number of vertices selected at the end of the second slot by Algorithm 4.3. Following the computation similar to Equation (4.22) in the proof of Lemma 4.3, we get

$$n''_{\text{APX}} \geq m_{G_2} \times \frac{|\mathcal{F}|}{\beta + |\mathcal{F}|\Delta} \quad (4.25)$$

where m_{G_2} is the size of the MIS of graph G_2 . Since the vertices of a graph can always be colored with $\Delta + 1$ colors, by the pigeonhole principle, we have $m_{G_2} \geq \frac{n'_{\text{APX}}}{\Delta + 1}$. Using this along with Equations (4.24) and (4.25) we get

$$n''_{\text{APX}} \geq \frac{n'_{\text{APX}}}{\Delta + 1} \times \frac{|\mathcal{F}|}{\beta + |\mathcal{F}|\Delta} \geq \frac{n_{\text{OPT}}}{\frac{\Delta+1}{|\mathcal{F}|}(\beta + |\mathcal{F}|\Delta)^2} \quad \blacksquare$$

Lemma 4.6. *For a superslot, Algorithms 4.3 and 4.4 together have an approximation ratio of $\frac{\Delta(\Delta+1)}{|\mathcal{F}|}(\beta + |\mathcal{F}|\Delta)^2$ when both direct and relay-aided communications are considered and interferences are allowed subject to satisfying their required SINRs.*

Proof. Following the proof of Lemma 4.4, we get an additional factor of Δ into the approximation ratio obtained in Lemma 4.5. \blacksquare

4.4 Simulation Results

The simulation environment is similar to [24, 26, 105]. More specifically, we have taken a service area of size $1000\text{m} \times 1000\text{m}$ with a grid size of $10\text{m} \times 10\text{m}$. The number of requesting D2D pairs, also referred to as system load, is varied from 50 to 200, whereas the number of idle D2D UEs willing to act as relays is taken to be 50. The maximum distance for a D2D pair is set to 20 m [99]. We assume that the UEs move according to a random waypoint mobility model where the velocity V is taken uniformly at random between 0 and V_{\max} with V_{\max} being 10 m/s and angle θ is also taken uniformly at random in the interval $[-\pi, \pi)$. The time slot duration Δt is assumed to be 200 ms. The beamwidth is taken as 45° . The mainlobe and sidelobe antenna gains are $G_m = 4$ and $G_s = 2$, respectively. The mmWave transmission is done in the 60 GHz frequency band with 10 frequency channel each of 200 MHz bandwidth. The maximum transmission power of the UEs are 24 dBm while the noise -174 dBm/Hz. The pathloss exponent for our mmWave LOS signal is 1.88 and the shadowing component follows a log-normal distribution with a zero mean and standard deviation of 3.5. The required bandwidth of each D2D link is set to 5 Mbps which is required for streaming full HD videos [183]. The various simulation parameters are summarized in Table 4.2.

Parameter	Value
D2D pairs	{50, 100, 150, 200}
idle D2D UEs	50
max D2D distance	20 m
velocity	$V \sim \mathcal{U}(0, V_{\max}), V_{\max} = 10$ m/s
angle	$\theta \sim \mathcal{U}(-\pi, \pi)$
beamwidth	45°
antenna gains	$G_m = 4, G_s = 2$
channel bandwidth	200 MHz
frequency channels	10
transmit power	24 dBm
noise	$\eta_0 = -174$ dBm/Hz
pathloss exponent	$L = 1.88$
shadowing component	$\phi \sim \mathcal{LN}(0, 3.5)$
data rate threshold	5 Mbps

Table 4.2: Simulation Parameters

As stated earlier, the expectation and standard deviation values shown in Equation (4.18) can be computed by solving the four-dimensional integrals involving the velocity and direction of the UEs, using numerical methods. But these computations take significant running times, which can be much larger than our stipulated time slot duration Δt . Instead, we opt for a fast Monte Carlo estimation of these values.

To the best of our knowledge, there is no other work that deals with the joint relay selection and channel allocation problem for mobile UEs in the presence of obstacles. The DRAPC algorithm [105] (described in Chapter 2) is one such work that closely resembles our considered resource allocation problem, but it does not consider device mobility or the presence of obstacles. Thus, for a fair comparison, we first demonstrate the benefit of jointly dealing with the resource allocation and relay selection problems in a static (with no user mobility) obstacle-free environment. Figure 4.5 depicts that our Proposed algorithm, activates a higher number of requesting D2D links than that of DRAPC algorithm and closely follows the Optimal solution. Here we should note that the Optimal solution is obtained through solving the MILP formulated in Section 4.2 using the Gurobi optimization solver [174]. Figure 4.6 shows that Proposed approach performs better than DRAPC algorithm in terms of average system throughput measured with Shannon’s capacity formula. Figure 4.6 depicts that the average throughput reduces as the system load increases. Here we also consider an environment with a relatively low number of available frequency channels (only 2). Our Proposed algorithm performs better in both cases. The suffix ‘s’ in the legends of Figure 4.6 denotes the case when a relatively small number of frequency channels have been used.

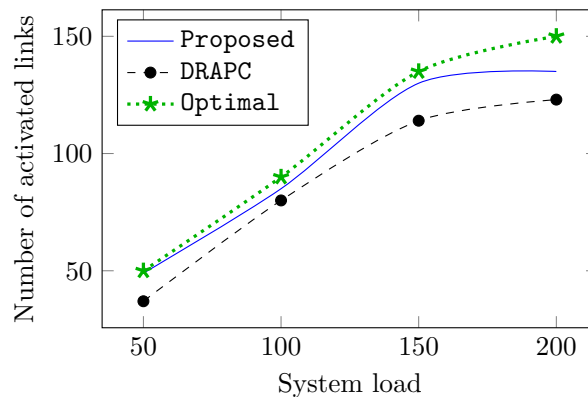


Figure 4.5: Plot of activated links count versus system load

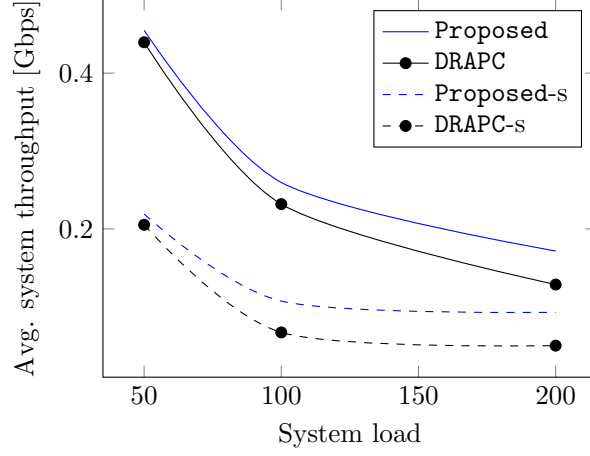


Figure 4.6: Plot of average throughput versus system load

In Figure 4.7, we have plotted the number of links activated for different datarate thresholds and two different noise levels. For the datarate, we consider the standard thresholds for standard definition (SD), high definition (HD), full HD (FHD), and 4K video streaming, which are 1 Mbps, 2 Mbps, 5 Mbps, and 20 Mbps, respectively [183]. As for the noise level, apart from the standard -174 dBm/Hz, we also consider a higher noise value -97 dBm/Hz, as given in [184]. Here, the system load is fixed at 200, and the number of

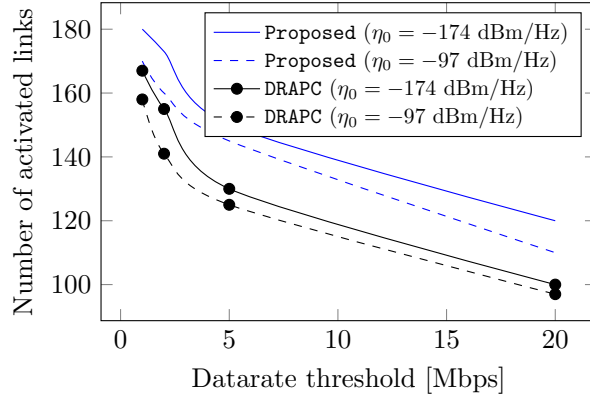


Figure 4.7: Plot of activated links count versus datarate threshold

frequency channels considered is 10. Figure 4.7 shows that our algorithm outperforms the DRAPC algorithm for these parameter values. As evident, for a fixed noise level and a fixed

load, the number of activated links increases with the decrease in datarate threshold. This is expected because it is easier to satisfy a D2D link with a lower datarate requirement for a fixed noise level. For a fixed datarate threshold and a fixed load, the number of activated links decreases with an increase in noise level. This is also quite expected, as it is comparatively harder to satisfy the required SINR when the noise level is higher for a fixed datarate requirement.

The true benefit of our proposed solution is exhibited when the presence of obstacles and device mobility are considered. Let us first consider the presence of only static obstacles while the UEs are kept stationary. Figure 4.8 shows the plot of the number of activated link failures as the system load increases with varying numbers of static obstacles. More specifically, we consider three cases where 100, 200, or 300 grid cells are blocked uniformly at random with static obstacles, respectively. In Figure 4.8, the plot legends are suffixed with corresponding static obstacle levels. As evident in this figure, our proposed solution has very few link failures in all three cases. Despite all the obstacles being static, our proposed solution suffers from a few link failures due to the approximation in LOS estimation.

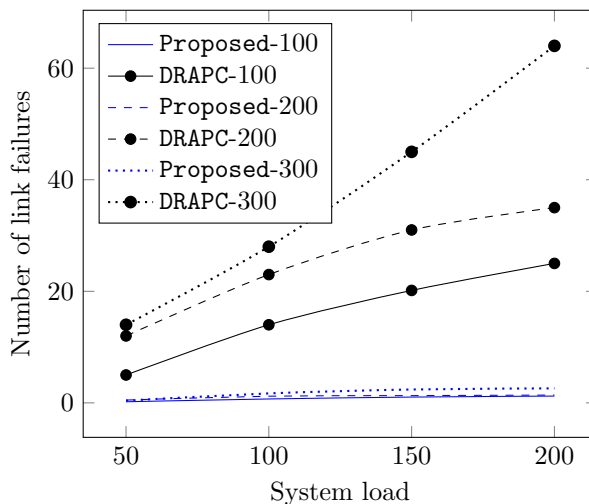


Figure 4.8: Plot of links failures versus system load (with only static obstacles)

Next, we consider the effect of dynamic obstacles along with a few static obstacles while the UEs are still kept stationary. Figure 4.9 shows the plot of the number of activated link failures as the system load increases with varying numbers of dynamic obstacles along with

a few static obstacles. Here we again consider three cases where 100, 200, or 300 number of the grid cells are blocked randomly with dynamic obstacles, respectively, while 300 grid cells are blocked with static obstacles. The dynamic obstacle levels are indicated by the appropriate suffixes in the plot legends. As evident in the figure, in the case of DRAPC, the number of link failures significantly increases as the load and number of obstacles increase, while our Proposed approach performs very well in all three cases.

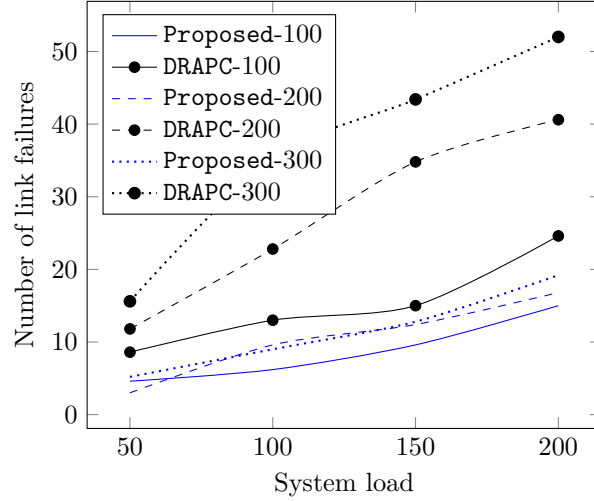


Figure 4.9: Plot of link failures versus the system load (with dynamic obstacles)

Figures 4.10 and 4.11 show how the presence of static as well as dynamic obstacles affects the average system throughput and fairness of link allocation, respectively. The average system throughput is computed as the mean of the data rates obtained by the requested links and computed using Shannon's capacity formula given in Equation (1.3). *Fairness* is measured by Jain's fairness index [105, 185] based on the data rates obtained by the requested links and given by the Equation (4.26).

$$\text{fairness} = \frac{\left(\sum_{l \in \mathcal{D}} \text{datarate}_l \right)^2}{|\mathcal{D}| \sum_{l \in \mathcal{D}} \text{datarate}_l^2} \quad (4.26)$$

Here \mathcal{D} denotes the set of requesting links, and datarate_l is the obtained datarate rate by a D2D link $l \in \mathcal{D}$. Here we have considered three scenarios: the absence of any obstacles, the presence of only static obstacles, and the presence of both static and dynamic obstacles.

Figure 4.10 shows that as the load increases, the average system throughput decreases. This is because the interference level increases with the increase in load, which in turn reduces the data rates of the requested links. The presence of static as well as dynamic obstacles further deteriorates the performance. Figure 4.11 shows that fairness is gradually decreasing as system load increases. As the system load increased, more and more link requests could not be satisfied. As a result, the disparity in data rates obtained by the links that are satisfied and the links that are not satisfied increases, which in turn decreases fairness. Here also, the presence of static and dynamic obstacles deteriorates the fairness.

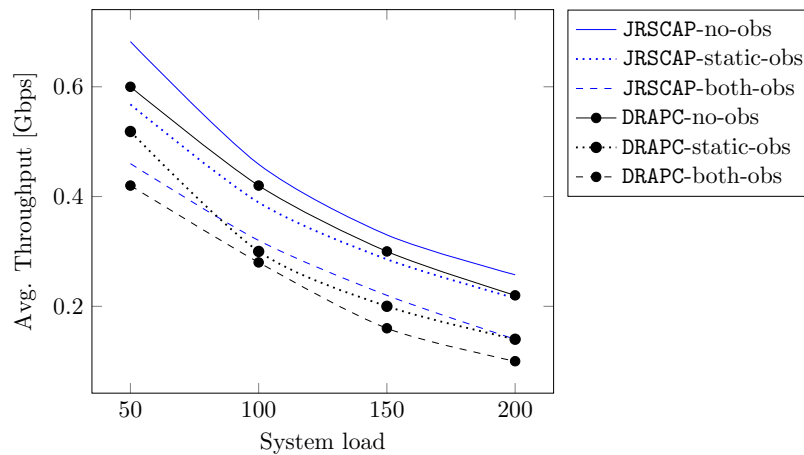


Figure 4.10: Plot of average system throughput versus system load (with obstacles)

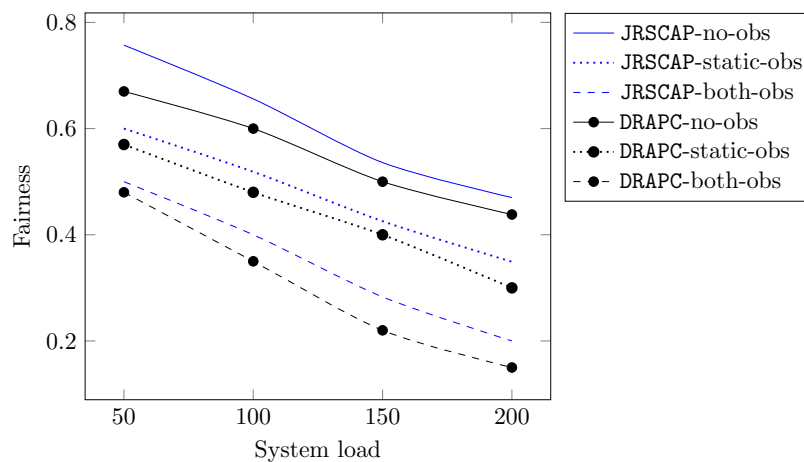


Figure 4.11: Plot of fairness versus system load (with obstacles)

Now, in Figure 4.12, we demonstrate the true benefit of our Proposed approach by considering device mobility. Here we again consider three cases: the first one, denoted as $(0, s)$, having no dynamic obstacles with stationary UEs; the second one, denoted as $(0, m)$, having no dynamic obstacles but UEs are now mobile; and the final one, denoted as $(200, m)$, having 200 dynamic obstacles along with mobile UEs. The number of static obstacles is kept at 300 in all three cases. As evident in the figure, our Proposed approach performs significantly well, specifically in cases of truly dynamic scenarios with device mobility and dynamic obstacles.

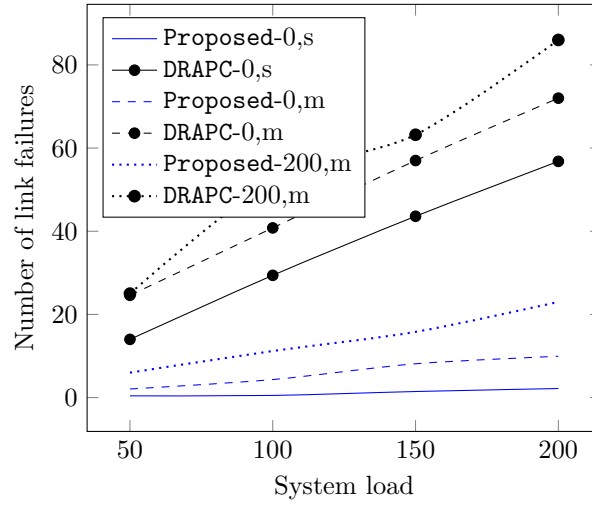


Figure 4.12: Plot of link failures versus system load (with user mobility and obstacles)

Finally, in Figure 4.13, we demonstrate the effect of the discretization of the service area and subsequently the assumption of a partially blocked grid cell as fully blocked. This assumption essentially overestimates the size of the obstacles. To capture the effect of this approximation, we introduce an *inaccuracy* metric, which is defined as the ratio of the *false-positive* link blockages to the total number of links blocked due to some obstacles. Here, the false-positive link blockage represents the difference between the number of links blocked due to the assumption that the partially blocked grid cells are fully blocked and the number of links blocked by some obstacles, considering their actual locations and sizes. This inaccuracy metric is computed through a Monte-Carlo simulation. In Figure 4.13, we plot the inaccuracy ratio for different grid sizes while varying the obstacle locations and sizes. We vary the grid sizes from $5\text{m} \times 5\text{m}$ to $20\text{m} \times 20\text{m}$. The obstacle sizes are

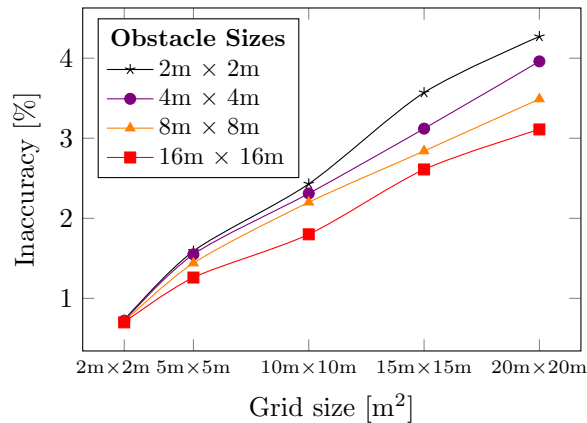


Figure 4.13: Plot of inaccuracy versus grid size with varying obstacle sizes

varied from $2\text{m} \times 2\text{m}$ to $16\text{m} \times 16\text{m}$, and their location is varied uniformly within the service area. The result shows that the inaccuracy increases as the grid size is increased, as expected. It also shows that larger obstacles cause less inaccuracy. It is evident that the overestimation of a partially blocked cell as a fully blocked one occurs only at the periphery of an obstacle. The proportion of partially blocked cells to the total number of blocked cells will decrease when the obstacle size is large. As a result, inaccuracy decreases with an increase in obstacle size.

4.5 Conclusion

In this work, we have developed a mobility-aware scheme that jointly deals with channel allocation and relay assignment for D2D communications using mmWave signals in the presence of obstacles. Our proposed framework is shown to significantly outperform an existing algorithm in terms of stable link activations when there are static as well as dynamic obstacles present in the system and the UEs are moving. As mentioned earlier, the resolution of the grid plays a crucial role in the accuracy and precision of obstacle modeling and has a trade-off with storage space. Determining an optimal grid resolution is a non-trivial task and an interesting problem in itself, which we would like to take up in the future. Another possible extension of this work is to eliminate the need for discretization of the service area.

Part II

Obstacle Aware Green Communications

CHAPTER 5

Joint Channel & Power Allocation using Reinforcement Learning*

The emergence of millimeter-wave (mmWave) technology has paved the way for high-speed data transmission in 5G and beyond wireless networks. In particular, device-to-device (D2D) communication using mmWave technology has gained significant attention due to its potential to enhance network performance and energy-efficiency, especially in internet of things (IoT) networks. Due to low latency and smaller antenna sizes, mmWave communication is very promising for IoT applications that involve smaller devices transmitting a large amount of data [15, 186]. However, mmWave signals are highly directional and susceptible to blockage from obstacles and therefore require obstacle-free line-of-sight (LOS) paths for communication [8, 24]. The presence of any obstacles significantly affects communications and may cause link failures, which result in significant delays. Thus, any resource allocation mechanism should address the presence of obstacles. Capturing the effect of static obstacles on resource allocation is comparatively easier, as information about them can be obtained from satellite imagery. Since dynamic obstacles move independently outside the purview of the base station (BS), capturing their effect on resource allocation is a challenging task.

Typically, the number of demanding D2D pairs is greater than the limited number of available frequency channels. Thus, to increase the spectral efficiency, we allow more than one D2D pair to reuse the same channel, provided their required signal-to-interference-plus-noise ratio (SINR) values are satisfied. Since the D2D pairs using the same frequency channel may interfere with each other, the channels need to be judiciously allocated among

*This chapter is based on the following publication:

- [C4] **Rathindra Nath Dutta** and Sasthi C. Ghosh. “Energy Efficient Resource Allocation for D2D Communications using Reinforcement Learning”. In: *2023 IEEE 48th Conference on Local Computer Networks (LCN)*. Oct. 2023, pp. 1–7. DOI: [10.1109/LCN58197.2023.10223387](https://doi.org/10.1109/LCN58197.2023.10223387)

the users. Furthermore, for battery-constrained IoT devices, we need to optimize the transmit-power level as well. It has been observed that wireless communications contributed significantly to global energy consumption and about 2% of carbon emissions worldwide. Thus, such energy consumption must be reduced for a sustainable smart environment and to promote green energy-efficient communications [10, 74]. Moreover, due to massive IoT device connectivity, energy-efficiency poses a critical concern [75, 186]. Thus, we must address the problem of resource allocation that deals with channel assignment along with transmit-power allocation to the demanding D2D devices in order to maximize the energy-efficiency of the system.

As pointed out in Chapter 2, most of the existing works, including our contribution in Chapter 3, consider an obstacle-free environment which is not very realistic. Although in Chapter 4, we have considered both static and dynamic obstacles, we assume a fixed power allocation for all devices, which is neither desirable for battery-constrained devices such as IoT nodes nor ascertains green communication. Thus, the joint power allocation and channel assignment problem in the presence of dynamic obstacles is yet to be investigated. To this end, in this chapter we propose a reinforcement learning (RL) framework for resource allocation in the presence of dynamic obstacles, which tries to maximize the overall energy-efficiency. We utilize the Q -learning algorithm to learn the optimal joint allocation of both channel and power in presence of dynamic obstacles. We also provide theoretical guarantees for this learning process. Our contributions in this chapter are listed below:

[Contribution 3.1] Since joint power and channel allocation problem (JPCAP) in presence of dynamic obstacles involves stochastic variables, we formulate a stochastic integer program (SIP) to maximize the overall energy-efficiency, which involves probabilistic constraints.

[Contribution 3.2] Blockages due to the dynamic obstacles can be learned by doing trials and taking feedback from the system, which brings us to the realm of RL. We thus pose our joint channel and power allocation problem as an RL framework and propose a solution based on Q -learning, which implicitly learns about the obstacle-prone zones and learns to allocate resources avoiding obstacles.

[Contribution 3.3] A formal proof has been crafted to show that our choice of reward function maximizes overall energy-efficiency.

[Contribution 3.4] We establish the convergence of our proposed algorithm both theoretically and experimentally. For the theoretical proof of convergence, we use the standard tool of stochastic approximation, namely the Robbins–Monro method [129].

[Contribution 3.5] Using extensive simulations, we show the effectiveness of our proposed algorithm over an existing baseline approach [107] in terms of energy-efficiency.

The rest of this chapter is organized as follows. In [Section 5.1](#), we state the various assumptions about the considered system. The mathematical formulation is given in [Section 5.2](#). In [Section 5.3](#), an RL framework has been devised. The simulation results are given in [Section 5.4](#). Finally, we conclude this paper with [Section 5.5](#).

5.1 System Model

As shown in [Figure 5.1](#), we consider a single cell controlled by a single BS. There are N D2D pairs which we collectively denote as a set \mathcal{D} . For each D2D pair $i = (i_1, i_2) \in \mathcal{D}$, user UE_{i_1} have some data demand d_i bits, which needs to be transmitted to user UE_{i_2} . Here, we assume that all user equipment (UEs) are stationary IoT nodes whose locations are known to the BS at the time of their deployment. We discretize the time as t_0, t_1, \dots time slots, each having a duration Δt unit. Notations used in this chapter are listed in [Table 5.1](#).

Communication channel

We consider that a limited number of orthogonal mmWave channels $\mathcal{F} = \{f_1, f_2, \dots, f_{|\mathcal{F}|}\}$ are available for D2D communications. Following [Equation \(1.1\)](#), for a D2D pair $i = (i_1, i_2)$, the received signal power at UE_{i_2} at time t can be expressed as:

$$P_i^{(t)} G_{i_1, i_2} h_{i_1, i_2} d_{i_1, i_2}^{-L}.$$

Here $P_i^{(t)}$ is the transmit-power at UE_{i_1} at time t , and L is the pathloss exponent. Here, G_{i_1, i_2} , h_{i_1, i_2} and d_{i_1, i_2} are the antenna gain, channel gain, and distance between UE_{i_1} and UE_{i_2} forming pair $i = (i_1, i_2)$, respectively. As before, we assume that the transmitter and receiver antennas are properly aligned for a communicating pair. Since we allow multiple D2D users to share a communication channel, the other devices communicating in the same channel may impose some interference to each other.

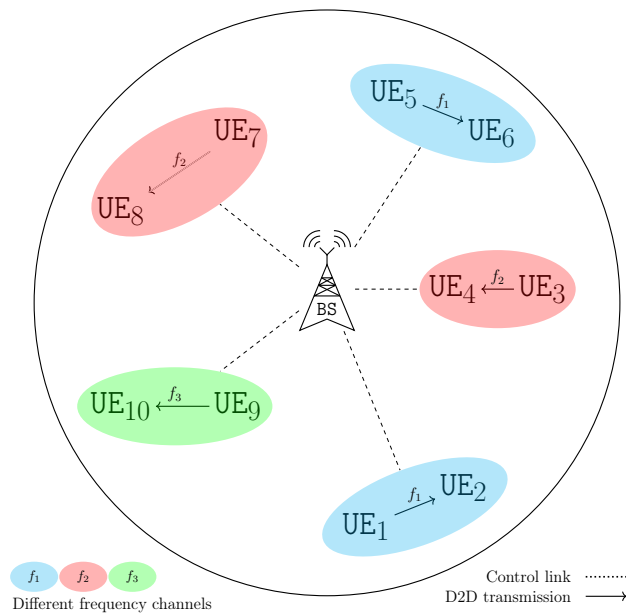


Figure 5.1: An example scenario

Therefore, the effective SINR is computed as:

$$\text{SINR}_i^{(t)} = \frac{P_i^{(t)} G_{i_1, i_2} h_{i_1, i_2} d_{i_1, i_2}^{-L}}{\eta_0 + \sum_{j \neq i} P_j^{(t)} G_{j_1, i_2} h_{j_1, i_2} d_{j_1, i_2}^{-L}}$$

Here η_0 is the thermal noise. Finally, the achievable data rate, measured in bits per second, is calculated by the Shannon's capacity formula:

$$\text{data}_i^{(t)} = \log_2(1 + \text{SINR}_i^{(t)})$$

Similar to [75], we define the overall energy-efficiency ξ of the system as the amount the data transmitted per unit time per unit power, i.e.

$$\xi = \frac{\frac{1}{\tau} \sum_{i=1}^N \text{demand}_i}{\sum_{i=1}^N \sum_{t=1}^{\tau} P_i^{(t)}}$$

Thus, the measuring unit of ξ is bits/sec/Joule. Here, τ is the total time taken to serve all demands.

Obstacle Modeling

Here we consider only dynamic obstacles are present in the service area and static obstacles can be avoided via relaying as suggested earlier. Note that unlike static obstacles, BS do not possess any information about the dynamic obstacles as they move independently. Here, we assume that the expected datarate for a D2D pair i at time slot t is given by

$$\mathbb{E}[\text{data}_i^{(t)}] = (1 - b_i) \times \text{data}_i^{(t)} + b_i \times 0 = (1 - b_i)\text{data}_i^{(t)}$$

where b_i is the probability of the link being blocked by a dynamic obstacle. Later we will show that $\mathbb{E}[\text{data}_i^{(t)}]$ can be directly learned without explicitly knowing b_i .

Notation	Meaning
\mathcal{D}	Set of D2D pairs
\mathcal{F}	Set of orthogonal frequency channels
t	Discrete time slots
Δt	Duration of a time slot
P_{\min}, P_{\max}	Minimum and maximum allowed transmit-powers
$P_i^{(t)}$	Transmit power of i -th user at time slot t
ξ	Energy-efficiency
$\xi^{(t)}$	Instantaneous energy-efficiency at time slot t
τ	Turn-around time
L_P	Number of discrete power levels
L_D	Number of discrete demand levels
\mathcal{S}	State space
\mathcal{A}	Action space
\mathcal{R}	Reward function
\mathcal{P}	Transition function
\mathcal{U}	Utility function
α_t	Learning rate at time t
ω	Constant for learning rate
X	Optimization variables

Table 5.1: Notations used throughout Chapter 5

5.2 Problem Formulation

Let us define a collection of indicator variables $X \in \{0, 1\}^{|\mathcal{D}| \times |\mathcal{F}| \times T}$ where for all $i \in \mathcal{D}$, $f \in \mathcal{F}$, $0 < t \leq T$ and T is an upper bound on τ .

$$X_{i,f,t} = \begin{cases} 1 & \text{if D2D pair } i \text{ uses frequency } f \text{ at time slot } t \\ 0 & \text{otherwise} \end{cases}$$

Here we want to maximize the energy-efficiency of the system, thus the objective function can be written as:

$$\text{maximize : } \quad \xi = \frac{\frac{1}{\tau} \sum_{i=1}^N \text{demand}_i}{\sum_{i=1}^N \sum_{t=1}^{\tau} P_i^{(t)}} \quad (5.1)$$

Suppose $\text{data}_i^{(t)}$ be the amount of data transmitted over a **D2D** link for pair i in (unit) time slot t , which is calculated as follows:

$$\text{data}_i^{(t)} = \log_2 \left(1 + \sum_{f=1}^{|\mathcal{F}|} \frac{X_{i,f,t} P_{i_1}^{(t)} G_{i_1,i_2} h_{i_1,i_2} d_{i_1,i_2}^{-L}}{\eta_0 + \sum_{j \neq i} X_{j,f,t} P_{j_1}^{(t)} G_{j_1,i_2} h_{j_1,i_2} d_{j_1,i_2}^{-L}} \right) \quad \forall i \in \mathcal{D}, 0 < t \leq T \quad (5.2)$$

Obviously we need:

$$\sum_{0 < t \leq T} \mathbb{E}[\text{data}_i^{(t)}] \geq \text{demand}_i \quad \forall i \in \mathcal{D} \quad (5.3)$$

The transmit-powers must be within the allowed range:

$$P_{\min} \leq P_i^{(t)} \leq P_{\max} \quad \forall i \in \mathcal{D}, 0 \leq t \leq T \quad (5.4)$$

Since after time τ , all demands of the users diminish, thus for all $t > \tau$, $X_{i,f,t}$ has to be zero, and we write:

$$X_{i,f,t} \leq \frac{\tau}{t} \quad \forall i \in \mathcal{D}, f \in \mathcal{F}, 0 < t \leq T \quad (5.5)$$

This will ensure that $X_{i,f,t} \leq 0$ as $\lfloor \frac{\tau}{t} \rfloor = 0$ for $t > \tau$; whereas $X_{i,f,t} \leq 1$ as $\lfloor \frac{\tau}{t} \rfloor \geq 1$ for $t \leq \tau$.

A D2D pair can use only one channel at a time. This can be encoded as:

$$\sum_{f=1}^{|\mathcal{F}|} X_{i,f,t} \leq 1 \quad \forall i \in \mathcal{D}, 0 < t \leq T \quad (5.6)$$

$$X_{i,f,t} \in \{0, 1\} \quad \forall i \in \mathcal{D}, f \in \mathcal{F}, 0 < t \leq T \quad (5.7)$$

The SIP defined by the objective function (5.1) along with the constraints (5.2) to (5.7), is not tractable for large input as the (5.2) is highly non-convex and (5.3) is a probabilistic constraint. Therefore, in the following section, we present an RL framework to solve the considered resource allocation problem.

5.3 Proposed Reinforcement Learning Framework

Before presenting our Q -learning based RL framework for joint power and channel allocation problem, we state a brief background on the RL with specific focus on Q -learning.

5.3.1 Basics of Q -learning

We consider a single agent interacting with the environment at some discrete time steps. The agent observes the current *state* of the system $s_t \in \mathcal{S}$ at time t , performs some *action* $a_t \in \mathcal{A}(s_t)$, receives some reward $R_t \in \mathbb{R}^1$ and finally changes the state to s_{t+1} . If the state transition obeys the *Markov property*, where the next state is determined only based on the current state and the current action without any dependence on historical events, we can model it as a *Markov decision process (MDP)*. Formally, a finite MDP is defined by a four-tuple $(\mathcal{S}, \mathcal{A}, \mathcal{R}, \mathcal{P})$, where \mathcal{S} is the discrete finite set of states, \mathcal{A} is the finite set of actions, the reward function is $\mathcal{R} : \mathcal{S} \times \mathcal{A} \rightarrow \mathbb{R}$ and $\mathcal{P} : \mathcal{S} \times \mathcal{A} \rightarrow \Delta$ is the transition function, where Δ is the probability distribution over state space \mathcal{S} .

Since in most cases we are interested in immediate reward and give less importance to future rewards, we consider a discount factor $0 < \gamma < 1$ and discount the reward R_t received at the time step t by a factor of γ^t . Thus, the aim is to find an optimal *policy* π which defines optimal action strategy of the agent, for maximizing the expected sum of the discounted rewards over an infinite horizon. The *value function* $v_\pi(s)$ of a state s under a

¹ \mathbb{R} is the set of all real numbers.

policy π is defined as the total expected reward gain starting at state s , that is:

$$v_\pi(s) = \mathbb{E} \left[\sum_{t=0}^{\infty} \gamma^t R_t \mid s_0 = s \right]$$

Thus, we need to find a policy π that maximizes $v_\pi(s_0)$. Here, s_0 denotes the initial state. Now, there always exists an optimal policy π^* such that the following Bellman equation holds for all state $s \in \mathcal{S}$ [187]:

$$v_{\pi^*}(s) = \max_{a \in \mathcal{A}(s)} \left\{ \mathcal{R}(s, a) + \gamma \sum_{s' \in \mathcal{S}} \mathcal{P}(s' \mid s, a) v_{\pi^*}(s') \right\}$$

Given complete knowledge of \mathcal{R} and \mathcal{P} functions, an agent can solve the Bellman equations and obtain π^* . The challenge arises when \mathcal{R} and \mathcal{P} are not known exactly. Fortunately, the optimal policy can still be learned by repeated interaction with the environment [188]. In RL, the agent starts with zero or a very limited knowledge about the environment, it observes the current state, performs some action, receives some reward, and the state changes. The agent updates its knowledge base and eventually learns the optimal strategy/policy. Q -learning is one of the popular RL methods in which the agent learns the optimal policy without explicitly knowing the reward function \mathcal{R} or the state transition function \mathcal{P} [187, 188].

In Q -learning, we use a Q -function where $Q^*(s, a)$ denotes the total discounted reward on taking action a in state s and then following the optimal policy π^* thereafter. Therefore,

$$Q^*(s, a) = \mathcal{R}(s, a) + \gamma \sum_{s' \in \mathcal{S}} \mathcal{P}(s' \mid s, a) v_{\pi^*}(s')$$

Thus we have, $v_{\pi^*}(s) = \max_{a \in \mathcal{A}(s)} \{Q^*(s, a)\}$.

In Q -learning, the agent starts with arbitrary initial Q -values and iteratively converges towards the optimal values Q^* . At each time step t , depending on the current state s , the agent chooses an action a , gets its reward R_t and observes the next state s' . The agent updates its Q -values by the following equation:

$$Q_{t+1}(s, a) = (1 - \alpha_t)Q_t(s, a) + \alpha_t[R_t + \gamma \max_{a' \in \mathcal{A}(s')} Q_t(s', a')] \quad (5.8)$$

Here $0 < \alpha_t < 1$, is the learning-rate at time step t . The agent follows an ϵ -greedy strategy,

where the agent chooses the action that has the highest Q -value for the current state with probability $1 - \epsilon$, and chooses a random action with probability ϵ . The ϵ -greedy strategy allows the agent to strike a balance between the exploration-exploitation dilemma. It allows the agent to explore new, possibly better actions and to escape from any local optima. The mechanism of Q -learning with ϵ -greedy strategy is formalized into [Algorithm 5.1](#). Here, a learning *episode* is a sequence of states, actions, and rewards, that starts from an initial state s_0 and ends with some terminal state.

Algorithm 5.1: The Q -learning algorithm [187, 188]

```

1 Initialize  $Q(s, a)$ , for all  $s \in \mathcal{S}$  and  $a \in \mathcal{A}$ 
2 foreach episode do
3   Initialize starting state  $s_0$  and set  $s \leftarrow s_0$ 
4   foreach step of current episode do           // until final state is reached
5     Set  $a \leftarrow \begin{cases} \arg \max_{a' \in \mathcal{A}} \{Q(s, a')\}, & \text{with probability } 1 - \epsilon \\ \text{pick a random action } a \in \mathcal{A}, & \text{with probability } \epsilon \end{cases}$ 
6     Apply action  $a$  on current state  $s \in \mathcal{S}$ 
7     Observe reward  $R_t$  and next state  $s' \in \mathcal{S}$ 
8     Update  $Q(s, a)$  by Equation \(5.8\)
9     Set  $s \leftarrow s'$ 

```

5.3.2 Frequency and Power Allocation Using Q -learning

Here we consider that the agent resides at a central location and is controlled by the BS. The environment comprises all D2D pairs along with their locations, demands, and channel conditions. Next, we present the proposed RL model for our joint power and channel allocation problem.

Action space

At each time step, we need to decide the frequency channel $f \in \mathcal{F}$ along with the transmit-power for each D2D pair. We discretize the transmit-power into L_P levels, as follows:

$$P = \left\{ P_{\min}, P_{\min} + \left\lfloor \frac{P_{\max} - P_{\min}}{L_P} \right\rfloor, P_{\min} + \left\lfloor 2 \frac{P_{\max} - P_{\min}}{L_P} \right\rfloor, \dots, P_{\max} \right\}.$$

Thus, the action space for N D2D pairs is $\mathcal{A} = (P \times \mathcal{F})^N$.

Reward function

We set the reward R_t at time t as the energy-efficiency $\xi^{(t)}$ at time t , that is,

$$R_t = \xi^{(t)} = \frac{\sum_{i=1}^N \text{data}_i^{(t)}}{\sum_{i=1}^N P_i^{(t)}}.$$

Note that this reward function implicitly considers the presence of a dynamic obstacle, as the blockage of the link due to a dynamic obstacle directly affects the value of obtained data rate $\text{data}_i^{(t)}$, and thus helps to learn the obstacle-prone zones. Note that our reward function essentially reflects a local version of the overall objective function. Later in [Section 5.3.3](#), we will formally show that choosing instantaneous energy-efficiency as a reward is actually aligned with the maximization of the overall system utility.

State space

For the environment state, we consider the remaining demands for each [D2D](#) pairs. We discretize the demands into L_D levels, as follows:

$$D = \left\{ 0, \left\lfloor \frac{\text{max_demand}}{L_D} \right\rfloor, \left\lfloor 2 \frac{\text{max_demand}}{L_D} \right\rfloor, \dots, \text{max_demand} \right\}.$$

Here `max_demand` is the maximum possible demand of a single [D2D](#) pair. Thus, the state space is given by $\mathcal{S} = D^N$.

For example, with only 3 devices, `max_demand` = 10 Gb and $L_D = 5$, a state may look like $s = \langle 4, 0, 3 \rangle$, which would imply that the [D2D](#) pairs 1, 2, and 3 have remaining 8 Gb, 0 Gb, and 6 Gb demands, respectively. Similarly, with $\mathcal{F} = 2$ and $L_P = 2$, an action $a = \langle 1, 0, 0, 1, 0, 1 \rangle$ would imply that the [D2D](#) pair 1 transmits at the maximum power using the frequency channel 0, and both [D2D](#) pairs 2 and 3 transmit with the minimum power in the frequency channel 1. The initial state s_0 is formed as per the input demands `demandi`, that is, $s_0 = \langle \text{demand}_1, \text{demand}_2, \dots, \text{demand}_N \rangle$ where each `demandi` value has been discretized according to D . With these, the Q -learning based joint channel and power allocation solution is presented as [Algorithm 5.2](#).

Note that the `rand()` function returns a value uniformly at random in the half-open interval $[0, 1)$. Here, we set the learning rate $\alpha_t = 1/t^\omega$, where $0.5 < \omega < 1$ is a constant. Next, we will show that not only [Algorithm 5.2](#) converges to optimal Q -values for our chosen learning-rate, but it also maximizes the objective function given in [Equation \(5.1\)](#).

Algorithm 5.2: Resource allocation using Q-learning

```

/* Initialization */
1 foreach  $s \in \mathcal{S}$  and  $a \in \mathcal{A}$  do
2    $Q(s, a) \leftarrow 0$ 

/* Learning */
3 for episode = 1 to max_episodes do
4   Initialize  $s_0$  as per input demands  $\forall i \in \mathcal{D}$ 
5   Set  $s \leftarrow s_0$  and  $t \leftarrow 0$ 
6   loop
7     if rand()  $\leq \epsilon$  then //  $\epsilon$ -greedy strategy
8       Pick a random action  $a \in \mathcal{A}$ 
9     else
10      Set  $a \leftarrow \arg \max_{a' \in \mathcal{A}} \{Q(s, a')\}$ 
11      Apply action  $a$  on current state  $s$ 
12      Observe the datarate  $\text{data}_i^{(t)}, \forall i \in \mathcal{D}$ 
13      Compute reward  $R_t$ 
14      Set  $\text{demand}_i \leftarrow \text{demand}_i - \text{data}_i^{(t)} \quad \forall i \in \mathcal{D}$ 
15      if all demands have been served then
16        break // terminate this episode
17      Get next state  $s' \in \mathcal{S}$  as per  $\text{demand}_i$  values discretized with respect to  $D$ 
18      Set  $\alpha_t \leftarrow 1/t^\omega$  // learning rate
19      Update  $Q(s, a)$  by Equation (5.8)
20      Set  $s \leftarrow s'$ 
21      Set  $t \leftarrow t + 1$ 

```

5.3.3 Convergence and Optimality Guarantees

To prove the convergence of our proposed Q -learning based approach, we first state the following known results as given in [Remarks 5.1](#) and [5.2](#).

Remark 5.1 (Convergence of Q -learning). Q -learning algorithm ([Algorithm 5.1](#)) converges to optimal Q -values only if the learning rate satisfies the following two conditions [[187](#), [188](#)]:

$$\sum_{t=1}^{\infty} \alpha_t = \infty \quad \text{and} \quad \sum_{t=1}^{\infty} \alpha_t^2 < \infty.$$

The two conditions mentioned above are referred to as the *Robbins–Monro conditions* of stochastic approximation [[129](#)]. These two conditions ensure that the learning rate approaches zero but not too quickly. Furthermore, they require that each state-action pair must be visited infinitely often.

Remark 5.2 (p -series test). A p -series, defined as $\sum 1/x^p$, converges if and only if the constant $p > 1$.

Theorem 5.1 (Convergence result). [Algorithm 5.2](#) converges to optimal Q -values.

Proof. Note that our reward values are positive and have a definite upper bound. Moreover, similar to the Q -learning algorithm ([Algorithm 5.1](#)), our proposed method updates each Q -value infinitely often. Following the convergence conditions of the original Q -learning algorithm [[187](#), [188](#)], all that remains to ensure the convergence of [Algorithm 5.2](#) is to show that the learning rate satisfies the two Robbins–Monro conditions stated above.

For $0.5 < \omega < 1$, with a p -series test, we can clearly observe that $\sum_{t=1}^{\infty} 1/t^\omega$ diverges, whereas $\sum_{t=1}^{\infty} 1/t^{2\omega}$ converges as $2\omega > 1$. Here, we have chosen $\alpha_t = 1/t^\omega$, where $0.5 < \omega < 1$ and $t > 0$. Therefore, we have

$$\begin{aligned} \sum_{t=1}^{\infty} \alpha_t &= \sum_{t=1}^{\infty} 1/t^\omega = \infty \\ \text{and} \quad \sum_{t=1}^{\infty} \alpha_t^2 &= \sum_{t=1}^{\infty} 1/t^{2\omega} < \infty \quad \blacksquare \end{aligned}$$

Thus, [Algorithm 5.2](#) converges to optimal Q -values and learns the optimal policy, which essentially maximizes the expected sum of discounted rewards over an infinite horizon. In

other words, [Algorithm 5.2](#) maximizes the utility function \mathcal{U} , defined as:

$$\mathcal{U} = \mathbb{E} \left[\sum_{t=1}^{\infty} \gamma^t R_t \right]$$

Here, the constant $0 < \gamma < 1$ is the discount factor. Next, in [Theorem 5.2](#), we will show that by maximizing the utility function \mathcal{U} , [Algorithm 5.2](#) indeed maximizes the overall energy-efficiency as required by the objective function given in [Equation \(5.1\)](#). For that, we first present the following two lemmas, which will be used in the proof of [Theorem 5.2](#).

Lemma 5.1. *For a fixed input instance, $\mathbb{E}[\xi^{(t)}] = \Theta\left(\frac{1}{\tau}\right)$.*

Proof. Here we have

$$\begin{aligned} \mathbb{E}[\xi^{(t)}] &= \mathbb{E} \left[\frac{\sum_{i=1}^N \text{data}_i^{(t)}}{\sum_{i=1}^N P_i^{(t)}} \right] && \text{(from definition)} \\ &\geq \mathbb{E} \left[\frac{\sum_{i=1}^N \text{data}_i^{(t)}}{\sum_{i=1}^N P_{\max}} \right] && \text{(since } P_i^{(t)} \leq P_{\max} \ \forall i) \\ &= \frac{1}{NP_{\max}} \sum_{i=1}^N \mathbb{E} \left[\sum_{i=1}^N \text{data}_i^{(t)} \right] && \text{(taking the constants outside)} \\ &= \frac{1}{NP_{\max}} \sum_{i=1}^N \mathbb{E} \left[\text{data}_i^{(t)} \right] && \text{(using linearity of expectation)} \\ &= \frac{1}{NP_{\max}} \sum_{i=1}^N \frac{\text{demand}_i}{\tau} = \frac{1}{\tau} \frac{\sum_{i=1}^N \text{demand}_i}{NP_{\max}} = \Omega\left(\frac{1}{\tau}\right) \end{aligned}$$

Similarly, we have

$$\mathbb{E}[\xi^{(t)}] \leq \mathbb{E} \left[\frac{\sum_{i=1}^N \text{data}_i^{(t)}}{\sum_{i=1}^N P_{\min}} \right] = \frac{1}{\tau} \frac{\sum_{i=1}^N \text{demand}_i}{NP_{\min}} = O\left(\frac{1}{\tau}\right).$$

Therefore, we have $\mathbb{E}[\xi^{(t)}] = \Theta\left(\frac{1}{\tau}\right)$. ■

Remark 5.3 (Taylor series expansion). *For any real number x , e^x can be expressed as an infinite sum as follows:*

$$e^x = 1 + x + \frac{x^2}{2!} + \frac{x^3}{3!} + \cdots$$

Lemma 5.2. *The function $f(x) = (1 - a^{x+1})/x$, is a decreasing function of x for all $x > 0$, where $0 < a < 1$ is a constant.*

Proof. To show, $f(x)$ is a decreasing function all we need to show is $f'(x) < 0$. Here,

$$f'(x) = \frac{d}{dx} \left(\frac{1 - a^{x+1}}{x} \right) = \frac{a^{x+1} - xa^{x+1} \ln a - 1}{x^2}$$

Since $x^2 > 0$, we need to show $a^{x+1} - xa^{x+1} \ln a < 1$. Substituting x with $c(1+x)$ in the above Taylor series expansion, we get

$$e^{c(1+x)} > 1 + c(1+x) > 1 + cx, \quad \forall c > 0, x > 0.$$

We can put $c = \ln(1/a)$, with $0 < a < 1$, as it satisfies the condition $c > 0$. Here, we have

$$\begin{aligned} 1 + cx &< e^c(1+x) = (e^c)^{1+x} \\ \implies 1 + x \ln(1/a) &< (1/a)^{1+x} && \text{(putting } c = \ln(1/a)\text{)} \\ \implies 1 - x \ln a &< 1/a^{x+1} \\ \implies a^{x+1} - xa^{x+1} \ln a &< 1 \quad \blacksquare \end{aligned}$$

With the above two lemmas, we now prove the following main theorem.

Theorem 5.2 (Optimality result). *Algorithm 5.2 maximizes overall energy-efficiency ξ .*

Proof. Recall that, using Q -learning, an agent learns the optimal policy that essentially maximizes the utility function \mathcal{U} [187]. Thus, all we need to show is that our utility function \mathcal{U} actually maximizes the energy-efficiency given in Equation (5.1). At any given time slot $t \geq \tau$, since the data demand of all devices has been exhausted, we receive zero rewards. Therefore, we have

$$\mathcal{U} = \mathbb{E} \left[\sum_{t=1}^{\infty} \gamma^t R_t \right] = \mathbb{E} \left[\sum_{t=1}^{\tau} \gamma^t R_t \right] \quad \text{(since } R_t = 0 \forall t > \tau \text{)}$$

$$\begin{aligned}
&= \mathbb{E} \left[\sum_{t=1}^{\tau} \gamma^t \xi^{(t)} \right] = \sum_{t=1}^{\tau} \gamma^t \mathbb{E} \left[\xi^{(t)} \right] && \text{(using linearity of expectation)} \\
&= \sum_{t=1}^{\tau} \gamma^t \Theta \left(\frac{1}{\tau} \right) && \text{(from Lemma 5.1)} \\
&= \Theta \left(\frac{1}{\tau} \right) \sum_{t=1}^{\tau} \gamma^t && \text{(since } \Theta(1/\tau) \text{ is independent of } t) \\
&= \Theta \left(\frac{1}{\tau} \right) \frac{1 - \gamma^{1+\tau}}{1 - \gamma} && \text{(sum of finite geometric series)} \\
\therefore \mathcal{U} &= \Theta \left(\frac{1 - \gamma^{1+\tau}}{\tau} \right) && \text{(since } 1 - \gamma \text{ is constant)}
\end{aligned}$$

Now, by [Lemma 5.2](#), we can observe that \mathcal{U} will be maximized as τ is minimized. Furthermore, from [Lemma 5.1](#), we know that $\mathbb{E}[\xi^{(t)}]$ attains its upper bound when all devices transmit at P_{\min} . Thus, \mathcal{U} also increases as the transmit-powers are lowered. Therefore, \mathcal{U} maximizes energy-efficiency ξ by lowering the transmit-power levels as well as minimizing the turn-around time τ . ■

5.4 Simulation Results

The simulation environment is similar to that of [24, 26, 107, 189]. We consider a small service area of 250 m radius having a single BS placed at its center. We consider the pairs to be randomly placed in the service area, where the transmitter and receiver of each D2D pair have a maximum 50 m distance. The 60 GHz mmWave band has been considered here, with each frequency channel having a 200 MHz bandwidth. We consider a beamwidth of 45°, the mainlobe and sidelobe antenna gains of 4 and 2 respectively. The UEs have minimum and maximum transmission power of 12dBm and 24dBm respectively, and the noise -174dBm/Hz . The LOS pathloss exponent is 1.88 and the shadowing component of channel gain obeys a log-normal distribution with zero mean and standard deviation 3.5. The demand of each D2D pair is between 1 Gb and 10 Gb for HD movies, CCTV footage or sensor data [190]. The simulation parameters are summarized in [Table 5.2](#).

As stated earlier, the joint channel and power allocation problem in the presence of dynamic obstacles has not been explored in the literature. We consider the randomized joint channel and power allocation (RJCPA) scheme given in [107] for our comparison, as it closely resembles our joint resource allocation problem. Although RJCPA does not consider

Parameter	Value
frequency band	60 GHz
bandwidth	200 MHz
radius of service area	250 m
maximum transmit distance	50 m
beamwidth	45°
mainlobe antenna gain	$G_m = 4$
sidelobe antenna gains	$G_s = 2$
noise	$\eta_0 = -174$ dBm/Hz
LOS pathloss exponent	$L = 1.88$
minimum transmit power	$P_{\min} = 12$ dBm
maximum transmit power	$P_{\max} = 24$ dBm
channel gain	$h \sim \mathcal{LN}(0, 3.5)$
demand	1–10 Gb

Table 5.2: Simulation Parameters

the presence of obstacles, it provides a fast polynomial algorithm that is shown to achieve an optimal solution with high probability. Recall that both the state space and the action space in our proposed framework grow exponentially with the number of D2D pairs N . Therefore, for demonstration purpose, we restrict ourselves to small instances only. For this we assume that the frequency channels are spatially separated, which actually partition the service area into fixed-sized zones [141]. In each such zone we consider that two frequency channels are available and there are up to 5 D2D pairs. We also assume only 3 power levels and 5 demand levels for our simulation, that is $L_P = 3$ and $L_D = 5$.

Figure 5.2 experimentally validates the convergence of our proposed Q-learning-based joint channel and power allocation algorithm. Here, we consider 5 D2D pairs, each having a demand of 10 Gb. We have varied the parameter $\omega \in \{0.5, 0.7, 0.9\}$ and plotted how fast our proposed algorithm converged to the optimum utility value \mathcal{U} . On an Intel i7-11700 CPU running Kubuntu 22.04 with 32 GB of main memory, a single run of the learning algorithm took less than a minute to converge. As evident, among the above three values, $\omega = 0.5$ converges the fastest, followed by $\omega = 0.7$ and $\omega = 0.9$. Note that with $\omega = 0.5$, it may be vulnerable to any initial bias, which is not the case with $\omega = 0.7$, as also mentioned in [191]. Thus, for the rest of the experiments, we take $\omega = 0.7$.

We assume that the dynamic obstacles are moving according to a random waypoint mobility model. We vary the number of dynamic obstacles from 0 to 80, and compare

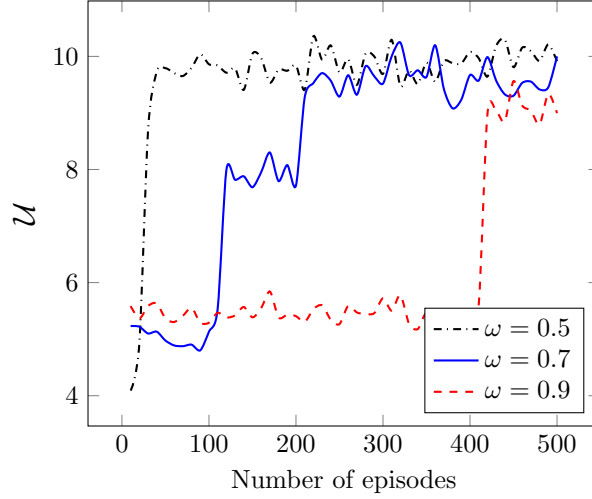


Figure 5.2: Plot of convergence of our proposed algorithm

our Proposed method against RJCPA. The corresponding plots are given in Figures 5.3 and 5.4. In Figure 5.3, we plot the turn-around time τ for varying levels of obstacles, while in Figure 5.4, we plot energy-efficiency ξ . As the number of obstacles increases, the chances of a link failure also increase, which causes τ to increase and ξ to decrease, as expected. Here, we consider that our agent's Q -values are pre-trained on 500 random input instances, and we test our agent against fresh random instances. As for RJCPA, we run it against the same random test instances and take the best solution among the 10 random initializations, as suggested by the authors [107]. It is also evident that when there are no obstacles, both methods perform almost identically, but as the number of obstacles increases, the performance of RJCPA gradually degrades.

We compare RJCPA against our proposed solution with varying demands while keeping the number of obstacles constant. As shown in Figure 5.5, the energy-efficiency ξ degrades with increasing demand level, as one would expect. Here also, our Proposed solution outperforms RJCPA method.

Lastly, we plot the running time of our experiments against the number of users. As evident in Figure 5.6, the running time grows exponentially with the number of users.

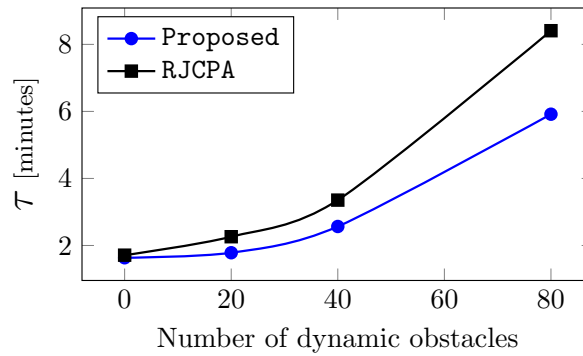


Figure 5.3: Plot of turn-around time versus obstacle count

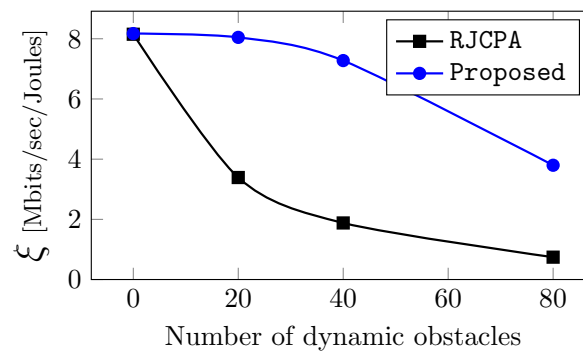


Figure 5.4: Plot of energy-efficiency versus obstacle count

5.5 Conclusion

In this work, we have considered the joint problem of channel and power allocation for **mmWave D2D** communications in the presence of dynamic obstacles. To solve this, we have proposed a Q -learning-based solution. We have established the convergence as well as the effectiveness of our proposed framework both theoretically and experimentally. As evident in this solution, we have discretized the power levels as well as the demands. Even with a reasonably small number of levels, the action/state space grows exponentially as the number of **D2D** pairs increases. This requires a large amount of memory, and the convergence becomes slow, making it intractable for any practical use. Thus, in the simulations, we considered only small zones having only a few **D2D** pairs and treated each zone independently. Although it is not very ideal, it serves as a proof-of-concept that an agent can indeed learn a (near) optimal channel and power allocation policy in the presence

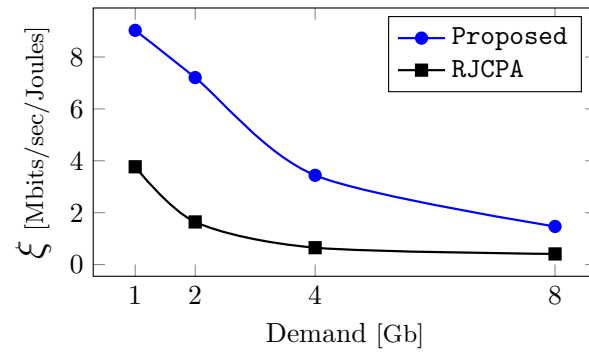


Figure 5.5: Plot of energy-efficiency versus demand levels

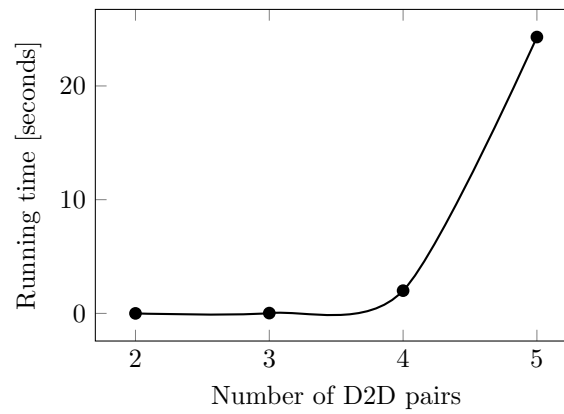


Figure 5.6: Plot of running time versus user count

of dynamic obstacles. To make it more practical, one can extend this framework to deep Q -learning models or even formulate a multi-agent [RL](#) framework, which we consider to be a possible future extension of this work.

CHAPTER 6

Non-Optimal is Good: Towards Long Term Stable Link Allocation*

The growing number of smart devices, together with modern applications with high bandwidth requirements, has already saturated the conventional communication spectrum. The use of **device-to-device (D2D)** communication using **millimeter-wave (mmWave)** signal promises a higher data rate, but it comes with its own set of challenges. They suffer from high penetration and propagation losses, thus requiring obstacle-free **line-of-sight (LOS)** communication [24]. Therefore, the presence of static as well as dynamic obstacles must be considered while allocating channel resources to the requesting **D2D** communication links. Since the number of available frequency channels is limited and is much smaller compared to that of requesting **D2D** links, the frequency channels must be shared among them. Two or more **D2D** links are allowed to communicate simultaneously using the same frequency channel as long as their required **signal-to-interference-plus-noise ratio (SINR)** is above some predefined threshold. Typically, the objective of resource allocation is to assign available frequency channels among the requesting links as well as to fix their transmit-powers so as to maximize resource utilization. As stated above, one must also consider the presence of obstacles while allocating these resources.

As mentioned in **Chapter 2**, most existing works consider an obstacle-free scenario for resource allocation, which is not very realistic. Although static obstacles can be captured through satellite imagery, dealing with dynamic obstacles is an all together challenging task. Since dynamic obstacles move outside the purview of the **base station (BS)**, they are much harder to deal with. They must be factored into a good resource allocation

*This chapter is based on the following manuscript:

- [C5] **Rathindra Nath Dutta** and Sasthi C. Ghosh. “Non-optimal is Good! Resource Allocation in Presence of Dynamic Obstacles in D2D Networks”. In: *2023 IEEE 48th Conference on Local Computer Networks (LCN)*. Oct. 2023, pp. 1–7. DOI: [10.1109/LCN58197.2023.10223393](https://doi.org/10.1109/LCN58197.2023.10223393)

scheme, as they severely affect the stability of the **mmWave** links. The authors in [114] assume that the probability distributions of link blockages due to dynamic obstacles are known apriori; however, they do not provide any mechanism to estimate these distributions. Typically, researchers have considered the use of expensive cameras [62] or radars [126] to detect the movement of dynamic obstacles. However, the way to accurately obtain these distributions without resorting to such expensive hardware is still an open problem. The authors in [61] attempt to learn these distributions from historical link activation data. One major limitation of such approach is that to obtain a good estimate, they assume there are sufficiently many requests coming from all over the service area, and all of them are served at some point of time. While the first requirement is almost always satisfied considering a dense urban scenario, the second one may not be ascertained.

One major drawback of the learning approach presented in [Chapter 5](#), is that it is not very scalable. Although there are methods such as function approximation, deep learning, and others for mitigating this scalability issue, they usually tend to slow down the convergence or do not provide any theoretical guarantees. Motivated by this, we went looking for other, possibly much simpler ways to address the joint power and channel allocation problem in the presence of dynamic obstacles. One obvious yet simple solution is to learn from mistakes, that is, to do an optimistic link allocation and then learn the blockages from link failures [61]. One major drawback of such link failure-based learning mechanisms is that they require links to be activated infinitely often over the entire service region. Most of the existing works, including our own works presented in [Chapters 3](#) and [4](#) of this thesis, try to optimize some metric such as active link count, system throughput, link stability, energy efficiency, and others. With limited resources, only a subset of the requesting links can be activated. This results in skewed knowledge about the environment as the bad links are never explored and only the good ones are repeatedly exploited. To explore these deprived bad links once in a while, we are to essentially perform some non-optimal resource allocation, which brings us to the infamous exploration-exploitation dilemma. Although such non-optimal allocations are undesirable, they ensure that all links are tried out for activation within some given period of time, giving us an accurate knowledge about their stability. This brings us to our fourth work, where we address this exploration-exploitation dilemma by systematically inducing a controlled amount of non-optimality. The contributions in this work are as follows.

[Contribution 4.1] To address the aforementioned exploration-exploitation dilemma, we

ensure that all requesting links are to be activated at least k number of times, where k is an input parameter. Subsequently, the joint power and channel allocation problem has been mathematically formulated.

[Contribution 4.2] We prove that the considered problem is \mathcal{NP} -Complete using a simple reduction and propose a greedy solution for the same. We construct a weighted interference graph where the weights are used to capture the notion of k time activation of a link as well as its stability. An approximation algorithm for weighted maximum independent set (MIS) construction and a linear program (LP) for power control have been used to solve the joint problem. The said LP, checks the admissibility of a new link by solving an energy-efficient power assignment problem for a group of D2D links.

[Contribution 4.3] The proposed greedy solution requires stability estimates for each of the requesting D2D links. We thus develop a *reservoir sampling* [130] based method to compute these stability values from the link failure information.

[Contribution 4.4] With extensive simulations, the effectiveness of our proposed framework is validated against the standard metrics, namely active links, link failures, fairness, and energy-efficiency. We show how the choice of the parameter k affects the performance of our algorithm in terms of these metrics and compare the performance of our proposed method against existing approaches [96, 105].

The remainder of this chapter is organized as follows. The system model and various assumptions are detailed in Section 6.1. In Section 6.2, we model the considered problem as a mathematical program and prove its hardness. The proposed solution is presented in Section 6.3, followed by the simulation results in Section 6.5, and finally we conclude this chapter with Section 6.6.

6.1 System Model

We consider a service area controlled centrally by a single BS. We discretize the service area into small grids having unit size. There are N D2D pairs that are collectively denoted as the set \mathcal{D} . For each D2D pair $i = (i_1, i_2) \in \mathcal{D}$, UE_{i_1} acts as a transmitter while UE_{i_2} receives. We discretize the time into slots, each having a small duration Δt unit. The devices are considered to be pseudo-stationary, that is, they do not change their positions

for the next T time slots, which is considered an *epoch*. The **user equipment (UEs)** know their current locations, which are reported to the **BS** at the beginning of every time epoch.

Communication channel

The limited number of orthogonal channels available for **D2D mmWave** communications are collectively denoted as \mathcal{F} . For each $i = (i_1, i_2) \in \mathcal{D}$, the received signal power $P_{i_2,t}$ at i_2 from i_1 at time t can be calculated as:

$$P_{i_2,t} = P_{i_1,t} G_{i_1,i_2} h_{i_1,i_2} d_{i_1,i_2}^{-L}$$

Here $P_{i_1,t}$ is the transmit-power of i_1 at time t , and L is the pathloss exponent. G_{i_1,i_2} , h_{i_1,i_2} and d_{i_1,i_2} are the antenna gain, channel gain, and distance between i_1 and i_2 , respectively. Since we allow multiple **D2D** users to share the same frequency channel, devices communicating using the same channel impose some interference on each other. Therefore, **SINR** is computed as:

$$\text{SINR}_{i,t} = \frac{P_{i_1,t} G_{i_1,i_2} h_{i_1,i_2} d_{i_1,i_2}^{-L}}{\eta_0 + \sum_{j \neq i} P_{j_1,t} G_{j_1,i_2} h_{j_1,i_2} d_{j_1,i_2}^{-L}}$$

Here η_0 is the thermal noise, and the summation in the denominator involves only those **D2D** pairs $j \in \mathcal{D}$ that share the same frequency channel with the **D2D** pair i . Each requesting **D2D** pair i has its own minimum **SINR** requirement ζ_i , depending upon its application.

Obstacle Modeling

We assume that the grid cells occupied by static obstacles are known to the **BS** and thus can be avoided with relays [61] or by using reflecting surfaces [42]. Therefore, we consider that the links in \mathcal{D} have **LOS** communication paths without any static obstacles in between. Since there might be dynamic obstacles as well, these **LOS** links may still break. For each grid cell (x, y) , we maintain a value $p_{x,y}$, which denotes the probability that the grid is blocked by a dynamic obstacle. For each link $i \in \mathcal{D}$, let us define S_i as a random variable that takes value 1 if link i is not blocked by any dynamic obstacles and 0 otherwise. Thus, $\mathbb{E}[S_i] = 1 \cdot s_i + 0 \cdot (1 - s_i) = s_i$, where s_i denotes the probability of link i not being blocked by any dynamic obstacle. The method of obtaining $p_{x,y}$, and subsequently $\mathbb{E}[S_i]$, is deferred to [Section 6.4](#).

6.2 Problem Formulation

Let us define a collection of indicator variables $X \in \{0, 1\}^{|\mathcal{D}| \times |\mathcal{F}| \times T}$ where for all $i \in \mathcal{D}, f \in \mathcal{F}, 1 \leq t \leq T$

$$X_{i,f,t} = \begin{cases} 1 & \text{if D2D pair } i \text{ uses frequency } f \text{ at time slot } t \\ 0 & \text{otherwise} \end{cases}$$

For each time slot t , the expected number of links successfully activated is given by

$$N_t = \mathbb{E} \left[\sum_{i \in \mathcal{D}} \sum_{f \in \mathcal{F}} S_i X_{i,f,t} \right] = \sum_{i \in \mathcal{D}} \left(\mathbb{E}[S_i] \sum_{f \in \mathcal{F}} X_{i,f,t} \right)$$

Here, we want to maximize the minimum N_t over an epoch T ; thus the objective function can be written as:

$$\text{maximize} : \min_{1 \leq t \leq T} \{N_t\} \quad (6.1)$$

In each time slot, the activated links must satisfy its minimum SINR requirements. Therefore, we write the following constraint $\forall i \in \mathcal{D}, f \in \mathcal{F}, 1 \leq t \leq T$:

$$\frac{P_{i_1,f,t} G_{i_1,i_2} h_{i_1,i_2} d_{i_1,i_2}^{-L}}{\eta_0 + \sum_{j \in \mathcal{D}, j \neq i} P_{j_1,f,t} G_{j_1,i_2} h_{j_1,i_2} d_{j_1,i_2}^{-L}} \geq X_{i,f,t} \zeta_i \quad (6.2)$$

Here, $P_{i_1,f,t} \in \mathbb{R}$ denotes the transmit-power of i -th D2D pair activated with frequency channel f at time t . Now the transmit-power must be within the allowable range $[P_{\min}, P_{\max}]$ whenever $X_{i,f,t} = 1$, otherwise we set $P_{i_1,f,t} = 0$. This can be encoded as a linear constraint as follows:

$$P_{\min} X_{i,f,t} \leq P_{i_1,f,t} \leq P_{\max} X_{i,f,t} \quad \forall i, f, t \quad (6.3)$$

Since each D2D pair must be activated at least k number of times, we write the following:

$$\sum_{f \in \mathcal{F}} \sum_{t=1}^T X_{i,f,t} \geq k \quad \forall i \quad (6.4)$$

At a particular time slot, a D2D pair can use at most one frequency channel, thus we have:

$$\sum_{f \in \mathcal{F}} X_{i,f,t} \leq 1 \quad \forall i, t \quad (6.5)$$

Finally we have the integrality constraint:

$$X_{i,f,t} \in \{0, 1\} \quad \forall i, f, t \quad (6.6)$$

Now notice that both the objective function (6.1) and the constraint (6.2) are nonlinear. We thus introduce another variable Z to linearize the objective function (6.1) as follows:

$$\text{maximize : } Z \quad (6.7)$$

$$Z \leq N_t, \quad \forall 1 \leq t \leq T \quad (6.8)$$

Now the constraint (6.2) essentially encodes that if $X_{i,f,t} = 1$, the SINR of D2D pair i using frequency channel f at time t must be larger than ζ_i . This can be rewritten as a linear inequality by introducing a suitably large positive constant M .

$$P_{i_1,f,t} G_{i_1,i_2} h_{i_1,i_2} d_{i_1,i_2}^{-L} + (1 - X_{i,f,t})M \geq \zeta_i \left(\eta_0 + \sum_{j \in \mathcal{D}, j \neq i} P_{j_1,f,t} G_{j_1,i_2} h_{j_1,i_2} d_{j_1,i_2}^{-L} \right) \quad (6.9)$$

Thus, the final integer linear program (ILP) is given by the objective function (6.7) and the constraints (6.3) through (6.6), (6.8), and (6.9). It is important to observe that the objective function will suffer due to constraint (6.8). Next, we prove the hardness of the considered problem via a simple reduction.

Proving Computational Hardness

Consider a special case of our problem where $T = 1$ and $k = 0$ and there are no dynamic obstacles present, that is, all $\mathbb{E}[S_i] = 1$. In this setting, the problem reduces to a classical resource allocation problem where we need to maximize the number of links activated with the available resources. This is a well-known \mathcal{NP} -Complete problem [107]. Given a solution (certificate) of our considered problem, we can easily verify its validity. Thus, the problem specified above is also \mathcal{NP} -Complete.

6.3 Proposed Solution

Here we first propose a greedy resource allocation scheme for our considered problem that tries to maximally allocate the links satisfying all the constraints specified above. Following this, we propose a technique for estimating the stability $\mathbb{E}[S_i]$ for each link. At the beginning of each time epoch T , we compute the $\mathbb{E}[S_i]$ values of the requesting links, and we pass that as input to our resource allocation algorithm. At the end of each epoch T , the link failure information is used to update the blockage probabilities, which are then used for computing $\mathbb{E}[S_i]$ values for the next time epoch.

6.3.1 Greedy Resource Allocation

We begin by computing an interference graph $G = (V, E)$, where a vertex $i \in V$ corresponds to each D2D link $i \in \mathcal{D}$ and for two vertices i and j we have an edge $(i, j) \in E$ if and only if the D2D link i and j interfere with each other. During a time slot t , where $t \leq T$, let k_i be the number of times the link i has been activated before current slot t . Now each link must be activated at least k times within the time epoch T . Let us define $\hat{k}_i = k - \min(k, k_i)$. Now, we attach a weight $w_i = \langle \hat{k}_i, \mathbb{E}[S_i] \rangle$ to each vertex $i \in V$. As is evident, the weights are two-tuple, where the first entry denotes how many times the link i is yet to be activated (out of k times), and the second entry denotes the link stability. Initially, at $t = 0$, the values of \hat{k}_i are set to k for all links, and they are decremented to 0 over time as k_i increases. Now, for two vertices $i, j \in V$, we say $w_i > w_j$ if either $(\hat{k}_i > \hat{k}_j)$ or $(\hat{k}_i = \hat{k}_j$ and $\mathbb{E}[S_i] > \mathbb{E}[S_j])$. For the rest of this section we would interchangeably use the terms ‘link’ and ‘vertex’ as convenient.

Now, for each time slot $t \leq T$, we need to obtain a power and frequency assignment of the requesting links. Observe that if no devices are allowed to interfere with each other, a valid frequency assignment would essentially partition the graph G into $|\mathcal{F}|$ independent sets. Each such independent set forms a frequency group \mathcal{G}_f where each links in that group can be activated with the same frequency channel $f \in \mathcal{F}$ without any interference. We can then obtain a maximum weighted independent set I of G to form one frequency group. To obtain the maximally weighted independent set, we call upon a subroutine `APX_WMIS()` as described in [Section 6.3.3](#). Now the second frequency group can be obtained by calling `APX_WMIS()` on the residual graph $G \setminus I$. Thus, all $|\mathcal{F}|$ frequency groups can be obtained in this fashion during a time slot $t \leq T$. Since the links in these initial frequency groups get zero interference from each other, they can be activated with the minimum possible power

satisfying their **SINR** requirement.

Since the number of frequency channels is limited, there still might be some links that have not been assigned to any of the frequency groups. Next, we try to accommodate these remaining links \mathcal{L} , into these initial frequency groups by allowing interference. We arrange the links in \mathcal{L} in decreasing order of their weights and select them one by one for insertion into the existing frequency groups. Here, the weight of the link i is the same w_i assigned to it in the interference graph G . For a link $i \in \mathcal{L}$, a frequency group \mathcal{G}_f is a possible candidate for insertion if there exists valid power assignment for all links in $\mathcal{G}_f \cup \{i\}$ satisfying their respective **SINR** requirements. Such a power assignment, if one exists, can be efficiently found by solving a **LP**, described in [Section 6.3.2](#). Now for a link i if two or more frequency groups become valid candidates, we prefer the one having minimum average power. We break the ties, if any, by the cardinality of the concerned groups. If for a link, no suitable frequency group is found, we discard it for the current time slot, and we try to accommodate it again in the next time slot t . We repeat this until the list \mathcal{L} exhausts, and we thus have a power and channel assignment for the current time slot t . We decrement the \hat{k}_i values for the links that have a valid channel and a power assignment in this round. The same process is repeated for each time slot $t \leq T$. This is formalized into [Algorithm 6.1](#).

6.3.2 Power Optimization using LP

For a particular time slot t and a frequency group \mathcal{G}_f we can pose the energy-efficient power assignment problem as an **LP**. Here the objective is to minimize the total power required as given by the following expression:

$$\text{minimize} : \sum_{i \in \mathcal{G}_f} P_i \quad (6.10)$$

Here the variable P_i denotes the transmit-power of link i . Since each link $i \in \mathcal{G}_f$ must satisfy its **SINR** requirement ζ_i , we write the following linear constraint:

$$P_i G_{i_1, i_2} h_{i_1, i_2} d_{i_1, i_2}^{-L} \geq \zeta_i \left(\eta_0 + \sum_{j \in \mathcal{G}_f, j \neq i} P_j G_{j_1, j_2} h_{j_1, j_2} d_{j_1, j_2}^{-L} \right) \quad \forall i \in \mathcal{G}_f \quad (6.11)$$

Algorithm 6.1: Greedy resource allocation

```

/* construct interference graph  $G = (V, E)$  */
1  $V \leftarrow \mathcal{D}$ 
2 forall  $i \in V$  do
3   | Set  $k_i = 0$  and  $\hat{k}_i \leftarrow k$  // remaining trials
4   | Set  $w_i \leftarrow \langle \hat{k}_i, \mathbb{E}[S_i] \rangle$  // vertex weights
5 forall  $i, j \in V$  do
6   | if  $i \neq j$  and  $UE_{i_1}$  interferes  $UE_{j_2}$  then
7   |   | add edge  $(i, j)$  into  $E$ 

/* schedule the requesting links */
8 for  $1 \leq t \leq T$  do
   | /* construct initial groups */
   | 9  $G' \leftarrow G$  // create a copy
   | 10 for  $1 \leq f \leq F$  do
   | 11   |  $\mathcal{G}_f \leftarrow \text{APX\_WMIS}(G')$ 
   | 12   |  $G' \leftarrow G' \setminus \mathcal{G}_f$  // remove vertices

   | /* add remaining links into the groups */
   | 13  $\mathcal{L} \leftarrow$  remaining vertices in  $G'$ 
   | 14 Sort  $\mathcal{L}$  in decreasing order of their weights
   | 15 foreach  $i \in \mathcal{L}$  do
   | 16   |  $\mathcal{C} \leftarrow \{f \mid \mathcal{G}_f \cup \{i\} \text{ has a feasible power allocation}\}$  // candidate groups
   | 17   | if  $\mathcal{C} = \emptyset$  then
   | 18   |   | continue // discard  $i$  for now
   | 19   |   | foreach  $f \in \mathcal{C}$  do
   | 20   |   |   |  $P_{\text{avg}} \leftarrow$  average power assigned to  $\mathcal{G}_f \cup \{i\}$ 
   | 21   |   |   |  $\text{Rank}_f \leftarrow \langle P_{\text{avg}}, |\mathcal{G}_f| \rangle$ 
   | 22   |   |   |  $f^* \leftarrow \arg \min_{f \in \mathcal{C}} \{\text{Rank}_f\}$  // best candidate
   | 23   |   |   |  $\mathcal{G}_{f^*} \leftarrow \mathcal{G}_{f^*} \cup \{i\}$  // permanently add

   | /* update weights in  $G$  */
   | 24 for  $1 \leq f \leq F$  do
   | 25   | foreach  $i \in \mathcal{G}_f$  do
   | 26   |   | if  $k_i > 0$  then
   | 27   |   |   | Update  $k_i \leftarrow k_i + 1$  and  $\hat{k}_i = k - \min(k, k_i)$ 
   | 28   |   |   | Update  $w_i \leftarrow \langle \hat{k}_i - 1, \mathbb{E}[S_i] \rangle$ 

```

Finally, the transmit-power P_i must obey the following constraint:

$$P_{\min} \leq P_i \leq P_{\max} \quad \forall i \in \mathcal{G}_f \quad (6.12)$$

Thus the LP for power optimization is given by the objective function (6.10) and the constraints (6.11) and (6.12).

6.3.3 Procedure APX_WMIS()

Recall that finding maximum weighted independent set of a graph is not only NP-hard but also APX-hard even when all the weights are uniform [192]. Although finding the optimal one is computationally intractable for large instances, one can find a maximal one quite easily by following a greedy selection scheme. The authors of [192] report that a simple greedy strategy that iteratively selects the vertex having maximum weight results in an approximation factor of $\bar{\delta}_w + 1$, where $\bar{\delta}_w$ is the average weighted degree of the graph. Thus, APX_WMIS(G) returns a maximal weighted independent set of G using the aforementioned greedy procedure reported in [192].

Complexity of Proposed Algorithm

Let $N = |\mathcal{D}|$ and $F = |\mathcal{F}|$. Then the time complexity of Algorithm 6.1 is $O(NFT)$ times the complexity of solving the LP for power optimization, which is at most $O(N^{3.5})$.

6.4 Estimating Link Stability $\mathbb{E}[S_i]$

At the end of each time slot, we know the status of each link, that is how many times they succeeded and how many times they were blocked. We can use this information to update the blockage probabilities of the grid cells, using which we can compute an estimate about the stability of the individual links. If, at a particular time, a link is successfully activated, we know that all the grid cells lying on its LOS communication path were free of dynamic obstacle at that time. Whereas, failure of a link indicates presence of a dynamic obstacle in some grid cell on its LOS path under our considered model. Note that, the LOS mmWave links are essentially straight lines. Therefore, the concerned grid cells can be efficiently obtained using the Bresenham line drawing algorithm [178] from computer graphics. We consider a procedure LINE(i), which returns the set of grid points along the link i .

Let 0 denote that a grid cell is free of obstacles and 1 denote the presence of an obstacle, which is obtained from link activation status. Thus, at the end of the time epoch T , we obtain a sequence of 0s and 1s for the grid cells lying on the LOS path of any requesting link. Therefore, over an infinite sequence of time, each grid cell (x, y) will have such a binary sequence, that is, a stream of 0s and 1s, which can be used to estimate the probability $p_{x,y}$ of containing a dynamic obstacle. Since this stream of 0s and 1s is infinitely long and new values come as time passes, one maintains a moving average as the estimated value of $p_{x,y}$. That is,

$$p_{x,y} = \frac{\text{number of 1s seen so far}}{\text{total number of 0s and 1s seen}}$$

Note although such point estimates works well in many situations, it lacks in capturing the fundamental information of how close this estimate is from the true mean. This is where the interval estimation comes into the picture.

Furthermore, in the above expression of $p_{x,y}$ both the numerator and denominator grow unboundedly as time passes, which creates a challenge for practical implementation. For this we can pick a finite-sized random sample from the stream, and then calculate the value of $p_{x,y}$ based on this sample. Now the confidence interval of a sample estimate is given by the expression: $\mu_{x,y} \pm z \frac{\sigma_{x,y}}{\sqrt{n}}$. Here n , $\mu_{x,y}$ and $\sigma_{x,y}$ are the size, mean, and standard deviation of the sample, respectively, and z is the confidence level typically taken to be 1. Note that a confidence interval involves both the mean and the standard deviation. Now let X be a random variable denoting the event of occurring a 0 or 1, then by the one-tailed Chebyshev's inequality, also known as Chebyshev–Cantelli inequality, we have

$$\Pr[X - \mu_{x,y} \geq c\sigma_{x,y}] \leq \frac{1}{1 + c^2} \quad \forall c > 0$$

Setting $\mu_{x,y} + c\sigma_{x,y} = 1$, we get

$$p_{x,y} = \Pr[X \geq 1] \leq 1 / (1 + (\frac{1 - \mu_{x,y}}{\sigma_{x,y}})^2)$$

Thus, we have an upper bound on the blockage probability $p_{x,y}$. Now stability of a link i is computed as:

$$\mathbb{E}[S_i] = s_i = \prod_{(x,y) \in \text{LINE}(i)} (1 - p_{x,y}) \geq \prod_{(x,y) \in \text{LINE}(i)} (1 - 1 / (1 + (\frac{1 - \mu_{x,y}}{\sigma_{x,y}})^2)) \quad (6.13)$$

Now all that remains is to get a uniform sample from a streaming sequence. Note that we cannot store all the values seen so far into some memory, as the size can grow unboundedly. To overcome this challenge, we employ the *reservoir sampling* method [130]. In reservoir sampling, we maintain a buffer \mathfrak{B} of size n that contains n past instances that are uniformly sampled from the stream. As we encounter a new item at time t from the stream, we update \mathfrak{B} as follows: we generate a random index j in the closed interval $[1, t]$; if $j \leq n$, we replace item $\mathfrak{B}[j]$ with the current item; otherwise we discard the current item. Initially \mathfrak{B} is filled with the first n items from the stream, and for $t > n$, we apply the above replacement scheme to update \mathfrak{B} . In this way, at any given iteration t , \mathfrak{B} always maintains a uniform sample of the items seen up to iteration t .

For each grid cell (x, y) , we maintain such a reservoir $\mathfrak{B}_{x,y}$ and update it as described above. From these uniform samples, we compute $\mathbb{E}[S_i]$ by equation (6.13) on the fly. This process is formalized into [Algorithm 6.2](#).

Algorithm 6.2: Updating blockage information

```

1 Initialize buffer  $\mathcal{B}_{x,y}$  of size  $n$  for each grid cell
2 foreach time slot  $t$  do
3   Let  $\mathcal{L}$  be set of links tried at time  $t$ 
4   foreach link  $l \in \mathcal{L}$  do
5     Set  $flag \leftarrow 1$  if  $l$  has failed, otherwise set  $flag \leftarrow 0$ ; // failure status
6     Let  $\mathcal{P}$  be the set of grid cells on  $l$ 
7     foreach  $(x, y) \in \mathcal{P}$  do
8       if  $\mathcal{B}_{x,y}$  has less than  $n$  samples then
9         Append  $flag$  to  $\mathcal{B}_{x,y}$ 
10      else
11        Let  $j \leftarrow \text{rand}(1, t)$ ; // generate random number between 1 and  $t$ 
12        if  $j \leq n$  then
13           $\mathcal{B}_{x,y}[j] \leftarrow flag$ 

```

6.5 Simulation Results

We consider the service area to be a circle centered around the BS and have a radius of 250 meters. The maximum allowed distance between a transmitter-receiver pair of a D2D link is set to 50 meters. We consider a maximum of 200 D2D links that are distributed

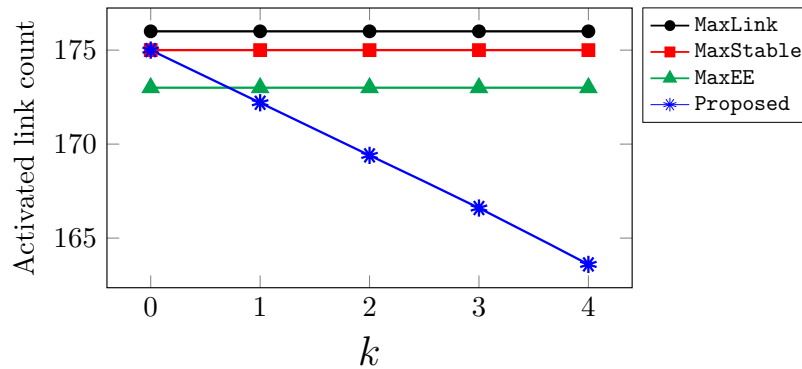
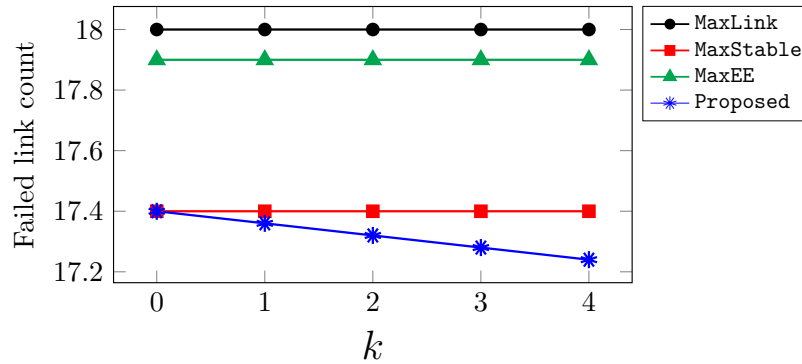
uniformly at random over the service area. The **mmWave** communication is being done in the 60 GHz band with 5 orthogonal frequency channels, each having a bandwidth of 200 MHz. We consider P_{\min} and P_{\max} to be 12 dBm and 24 dBm, respectively, and the noise value is -174 dBm/Hz. For **LOS** transmissions, the pathloss exponent is -1.88 , and we assume a log-normal shadowing component with zero mean with 3.5 standard deviation. The grid size is considered to be $5 \text{ m} \times 5 \text{ m}$. We consider a video streaming application scenario where each **D2D** link must be activated with a datarate of at least 20 Mbps. The simulation parameters are summarized in [Table 6.1](#).

Parameter	Value
frequency band	60 GHz
bandwidth	200 MHz
frequency channels	5
number of D2D pairs	200
maximum transmit distance	50 m
beamwidth	45°
antenna gain	$G_m = 4$ and $G_s = 2$
noise	-174 dBm/Hz
LOS pathloss exponent	$L = 1.88$
transmit power	$P_{\min} = 12$ dBm and $P_{\max} = 24$ dBm
channel gain	$h \sim \mathcal{LN}(0, 3.5)$
datarate threshold	20 Mbps

Table 6.1: Simulation Parameters

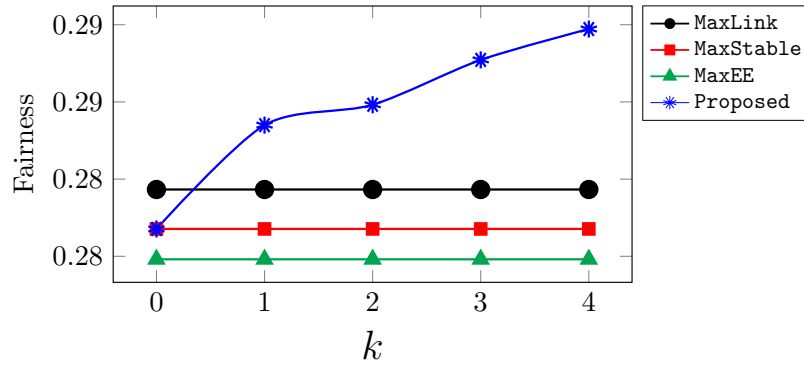
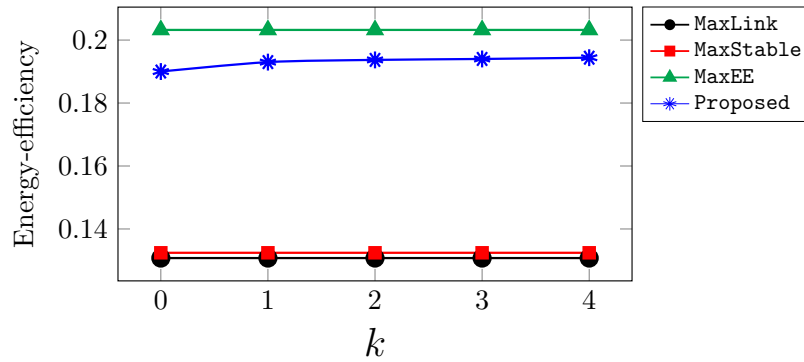
For comparison, we consider three different approaches, namely **MaxLink**, **MaxStable** and **MaxEE**. **MaxLink** uses the solution proposed in [105] to maximize the number of activated links, while for **MaxEE** we use the approach specified in [96] to maximize the energy-efficiency of the system. As for **MaxStable**, we consider a maximum stable link allocation, which is basically the case when we set $T = 1$ and $k = 0$ in our formulated **ILP**, and solve it using Gurobi optimizer [174]. In our **Proposed** approach, we set $T = 10$ and vary k from 0 to 4.

We consider four different metrics for our comparison, which are: number of activated links, number of link failures, fairness of link allocation, and energy efficiency. The first metric is, as the name suggests, the total number of links scheduled by the respective approach, whereas link failure is measured as the number of activated links that were blocked by some dynamic obstacles. Here the dynamic obstacle move according to the

Figure 6.1: Plot of activated links versus k Figure 6.2: Plot of link failures versus k

smooth random waypoint mobility model [193]. In this mobility model, an object moves with random (constant) velocity in a random direction for a time period; after that, it selects another random direction and moves in that direction with possibly some other velocity chosen randomly. The fairness is measured by Jain's fairness index [185], and we measure the energy-efficiency as the obtained datarate per unit power.

In Figures 6.1 to 6.4, we consider 200 number of requesting links and we plot all the four metrics for all four approaches considered. We repeat the experiment 100 times and report the average values. As evident in Figure 6.1, MaxLink of course activates the highest number of links followed by MaxStable and MaxEE. With $k = 0$, our Proposed method behaves exactly like MaxStable and the active link count decreases with increasing k . This is because, with larger values of k more non-optimal solutions are expected. In Figure 6.2, we observe the highest number of link failures with MaxLink followed by MaxEE.

Figure 6.3: Plot of fairness versus k Figure 6.4: Plot of energy-efficiency versus k

As expected **MaxStable** has a lower link failure count. In the case of our **Proposed** method, the decrease in link failure with larger k , is due to the fact the lesser number of links get activated with higher values of k . Among **MaxLink**, **MaxStable** and **MaxEE**, we observe that **MaxLink** achieves the highest level of fairness, as evident in [Figure 6.3](#). Increasing k actually ensures that all links get approximately the same chances of activation and thus resulting in an increased fairness level, as also evident in [Figure 6.3](#). In [Figure 6.4](#), we observe that **MaxEE**, achieves the highest energy-efficiency, as expected. Also, the energy-efficiency does not change much with k and our **Proposed** method remains much closer to **MaxEE** compared to the other two methods.

Now for the estimation approach presented in [Section 6.4](#), we measure its performance as the *mean squared error*, where we define the error as the deviation of the estimate from its true value. As depicted in [Figure 6.5](#), as we increase the size of the reservoir (n) from

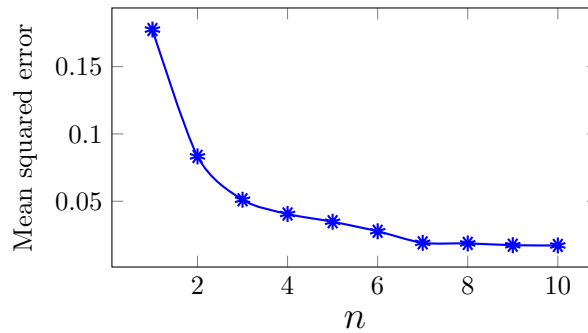


Figure 6.5: Plot of convergence of mean squared error

2 to 10, the error minimizes and saturates after 8.

6.6 Conclusion

In this work we have addressed the channel and power allocation problem for mmWave D2D networks in presence of dynamic obstacles. Such dynamic spectrum allocation is essential in modern networks and has applications in many internet of things (IoT) applications and smart cities. With limited resources available, we aim to maximize the number of stable links activated. We have argued that for some time slots, we have to perform non-optimal resource allocation in order to get an accurate picture about the blockage probabilities. To this end, we have presented a greedy approach which maximizes the number of stable links activated while ensuring that all requesting links are served at least k times. With extensive simulations, we have validated our approach. As evident, increasing k reduces the number of activated links and hence links failures, while fairness increases greatly. On the other hand, energy-efficiency does not change much with k . Note that the choice of k has a trade-off between the number of links served and the fairness of the allocation. We leave the optimal choice of k open-ended to the operator to decide, based on its quality-of-service requirement. Furthermore, the size of the reservoir along with grid size resolution also has a trade-off with the storage space and accuracy of the estimate. Figuring out these sizes is a non-trivial task and can be a possible future direction of this work. Moreover, in this work, all devices are assumed to be static. The link between two mobile users can also fail due to static obstacles also, which has not been considered in this work, and we would like to address this issue in our future work.

Part III

Multicast D2D Communications

CHAPTER 7

Obstacle Aware Multicasting for D2D Communications^{*}

The explosion in number of mobile devices together with the applications demanding high bandwidth have already saturated the conventional wireless communication systems. In next generation wireless communication, new strategies such as **millimeter-wave (mmWave)** **device-to-device (D2D)** communication has been proposed to satisfy the high bandwidth requirements [8]. One drawback of using high frequency **mmWave** signals is that they are more susceptible to propagation and penetration losses due to their smaller wavelengths. Therefore, it requires short distance obstacle free **line-of-sight (LOS)** communication path between the transmitter-receiver pair in order to achieve the promised high data rate [24]. Note that, here an obstacle can be anything from brick wall, signboard to moving objects like an automobile or can even be a person [61, 62].

Many modern applications such as video streaming, automotive, IoT, public safety systems requires same data packets to be delivered to multiple client devices [45, 46]. In many cases such messages are to be sent only to a selected small group of users in the network. In such cases, flooding the entire network in order to broadcast such data packets is not desirable and gave rise to the study of multicast techniques [48]. Moreover, in multicasting applications, a transmitter can simultaneously send data to more than one receiver [54], which further improves the spectral-efficiency. The ability of multicasting has already been considered in **LTE-advanced (LTE-A)** specs and also being considered for **D2D** communication in **5G** [49]. Given a source and set of destination devices, a multicast route

^{*}This chapter is based on the following publication:

- [C3] **Rathindra Nath Dutta** and Sasthi C. Ghosh. “Obstacle Aware Link Selection for Stable Multicast D2D Communications”. In: *Proceedings of the 3rd International Conference on Computer and Communication Engineering (CCCE 2023), Stockholm, Sweden, 10-12 March, 2023*. Vol. 1823. Communications in Computer and Information Science (CCIS). Springer, 2023, pp. 54–66. ISBN: 978-3-031-35299-7. DOI: [10.1007/978-3-031-35299-7_5](https://doi.org/10.1007/978-3-031-35299-7_5)

is first determined, following which the packets are transmitted. Typically, such multicast routes forms a *spanning tree* rooted at the source device [49]. Multicasting in mmWave D2D communications has its own challenges. Different wireless links in a multicast route are of different lengths and may suffer from different channel conditions. Apart from this heterogeneous links, presence of obstacles further varies the link quality [45, 53, 82]. Thus, all the links comprising a multicast route, must be judiciously chosen.

In a multicast network, the overall performance of the system relies on all the selected communication links forming the multicast route. Thus, presence of obstacles, specially dynamic obstacles, has a much greater impact on the overall system performance. In the previous chapters of this thesis, obstacle-aware link selection has been investigated for D2D unicast communications. These unicast solutions treat each of the links independently, which does not provide any guarantees on the overall performance for a multicast group. Thus multicast D2D communications in the presence of any obstacles is yet to be investigated. Very few recent studies proposes obstacle aware frameworks for D2D multicast communications. Since the dynamic obstacles move independently outside the purview of the base station (BS), they are much harder deal with. As mentioned earlier, researchers have typically used additional hardware, such as camera [66] or radar [126], to track the movements of such dynamic obstacles. Such solutions are expensive and sometimes restricted due to privacy concerns [127]. Some authors, as in [62, 114], assume a fixed known distribution of the dynamic obstacles, which cannot dynamically adapt the change in the environment. In this chapter, we present an inexpensive solution to dynamically learn the blockage patterns due to the dynamic obstacles. Armed with the capability of learning the link stability values in the presence of dynamic obstacles, we investigate the **multicast link selection problem (MLSP)** as our fifth and final work in this thesis. More specifically, we explore the MLSP for stability maximization. The contributions in this chapter are summarized below.

[Contribution 5.1] Given the link stability values, we present the MLSP as an optimization problem. We have formulated an **integer linear program (ILP)** where we utilize the spanning tree formulation given by Martin [131].

[Contribution 5.2] We provide an efficient algorithm to obtain the desired stable multicast route based on the standard **minimum spanning tree (MST)** finding algorithm.

[Contribution 5.3] Given the knowledge of link stability values, we prove the optimality of our proposed solution.

[Contribution 5.4] Our proposed solution requires the stability estimates of the candidate links. We use an *evidential theory* framework [132, 133] to estimate these stability values in presence of dynamic obstacles.

[Contribution 5.5] Through simulations, we demonstrate the effectiveness of our proposed method over baseline approaches namely a random allocation scheme and a fixed distribution scheme [62].

The rest of this chapter is organized as follows. In [Section 7.1](#), we present the system model along with various assumptions. Mathematical formulations of the considered problem is given in [Section 7.2](#). The proposed multicast link selection algorithm is described in [Section 7.3](#) along with the proof of its optimality. A mechanism for leaning the blockage probabilities is presented in [Section 7.4](#). [Section 7.5](#) demonstrates the benefit of proposed scheme through simulations. Finally, we conclude this chapter with [Section 7.6](#).

7.1 System Model

We consider a service area controlled by a central **BS**. We assume a **D2D** overlay communication scenario in the presence of static as well as dynamic obstacles. A multicast group \mathcal{M} consists of a single source **user equipment (UE)** and a N number of other **UEs** that receive the multicast data from the source **UE**. We also discretize the entire service area into a grid of small square cells, each of size $g \times g$. Furthermore, we consider the **UEs** to be pseudo-stationary, i.e., they do not change their positions during the execution of our proposed algorithm, and their locations are known to **BS**.

Static Obstacle Modelling

Similar to [Chapter 4](#), we assume that the approximate sizes and locations of the static obstacles are known apriori. Such information can be obtained through satellite imagery [61]. A grid cell that contains even a portion of an obstacle is considered to be fully *blocked*. [Figure 7.1](#) shows the blocked cells (shaded with gray color) due to the presence of an obstacle (black rectangle). As evident, here we essentially overestimate the sizes of

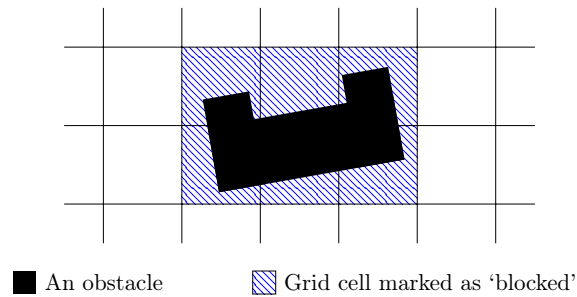


Figure 7.1: Discretization of the service area

the obstacles. The inaccuracy caused due to this grid approximation has been discussed in [Section 7.5](#).

Modelling Dynamic Obstacles

Suppose the grid cell (x, y) contains a dynamic obstacle with probability $b_{x,y}$. We assume that **BS** knows the blockage probability $b_{x,y}$ for every grid cell (x, y) . We set $b_{x,y} = 1$, whenever there is a static obstacle in the grid cell (x, y) . Furthermore, we maintain a matrix called **blockage**, where $\mathbf{blockage}[(x_s, y_s)][(x_e, y_e)]$ denotes the blockage probability of an **LOS** link between grid cells (x_s, y_s) and (x_e, y_e) . Note that this **blockage** matrix incorporates the presence of both static and dynamic obstacles. Thus, if there exists a static obstacle in between two grid cells, the corresponding entry in the **blockage** matrix will be 1. The computation of this probability matrix is described in [Section 7.4](#).

Multicast Communications

Similar to [46], we assume that a **transmitter (Tx)** can simultaneously transmit data to a bunch of **receiver (Rx)** residing in close proximity of each other and falls within the beamwidth of the transmitter. Here we consider sufficiently many orthogonal **mmWave** channels are available for the multicast **D2D** communications [61]. Although a multicast group member can reside relatively far from the source, it can still receive the packets via other group members, other relay devices [45] or even through the traditional communication via the **BS** [49]. For simplicity, we consider a multicast group \mathcal{M} , where the underlying communication graph of the members of \mathcal{M} is connected. Like the previous chapters, here we also assume that the **UEs** are capable of relaying. Therefore, any **UE** in \mathcal{M} can relay the multicast data to other members in \mathcal{M} following the constructed multicast tree.

7.2 Problem Formulation

Given a set \mathcal{M} of **D2D** users in a multicast group, let us construct another set \mathcal{L} of possible **D2D** links $l_{i,j}$ between UE_i to UE_j for all $i, j \in \mathcal{M}$. Now let us denote the selection of a link $l_{i,j}$ by a binary indicator variable $X_{i,j}$. That is,

$$X_{i,j} = \begin{cases} 1 & \text{when } l_{i,j} \text{ is selected in the multicast route} \\ 0 & \text{otherwise} \end{cases}$$

At any given time, a link $l_{i,j}$ being blocked due the presence of a (dynamic) obstacle is indicated by $b_{i,j}^t = 1$, and 0 otherwise. Let us define the *stability* of a link $l_{i,j}$ as the probability of the link not being blocked by any obstacles and denote it by $s_{i,j}$. Thus,

$$s_{i,j} = \Pr[b_{i,j} = 0]$$

Suppose $s_{\mathcal{T}}$ denotes the overall stability of a multicast tree \mathcal{T} . Then the objective is to maximize the expected stability $\mathbb{E}[s_{\mathcal{T}}]$. Since the stability of individual links is independent of each other, we have $s_{\mathcal{T}} = \prod_{l_{i,j} \in \mathcal{T}} s_{i,j}$. Thus, we can write

$$\mathbb{E}[s_{\mathcal{T}}] = \mathbb{E} \left[\prod_{l_{i,j} \in \mathcal{T}} s_{i,j} \right] = \prod_{l_{i,j} \in \mathcal{T}} \mathbb{E}[s_{i,j}] \quad (\text{using independence})$$

Here, we need to select links for \mathcal{T} such that $\mathbb{E}[s_{\mathcal{T}}]$ is maximum. This can be encoded as the linear expression (7.1).

$$\text{maximize : } \prod_{l_{i,j} \in \mathcal{L}} (X_{i,j} \mathbb{E}[s_{i,j}] + (1 - X_{i,j})) \quad (7.1)$$

Since the multicast route is essentially a spanning tree, the following constraints are adapted from Martin's formulation for **MST** [131]. Note that, a spanning tree of n nodes contains exactly $n - 1$ edges. This can be encoded as equation (7.2).

$$\sum_{l_{i,j} \in \mathcal{L}} X_{i,j} = |\mathcal{M}| - 1 \quad (7.2)$$

Next, we develop the constraints to ensure there is no cycle in the tree. Thus, it is evident that any user k can only be connected to only one side of a link $l_{i,j}$, whenever $l_{i,j}$ is selected. For this, let us first introduce another set of indicator variables $Y_{i,j}^k$ and define them as follows:

$$Y_{i,j}^k = \begin{cases} 1 & \text{when } l_{i,j} \text{ is selected in the multicast route and } k \text{ is connected at the side of } j \\ 0 & \text{otherwise} \end{cases}$$

Since a UE k can only be connected at only one side of link $l_{i,j}$, whenever $l_{i,j}$ is selected, we have the constraints (7.3) and (7.4). Constraint (7.3) ensures that any vertex k must be on one side of a selected edge (i, j) . On the other hand, constraint (7.4) ensures that if an edge (i, j) is selected, then vertex i is connected on the side of i , whereas if (i, j) is not selected in the tree, then there must be some selected edge such that j is on the side of k .

$$Y_{i,j}^k + Y_{j,i}^k = X_{i,j} \quad \forall l_{i,j} \in \mathcal{L}, \forall k \in \mathcal{M} \quad (7.3)$$

$$\sum_{k \in \mathcal{M} \setminus \{i,j\}} Y_{i,k}^j + X_{i,j} = 1 \quad \forall l_{i,j} \in \mathcal{L} \quad (7.4)$$

Finally, we have the integrality constraints as given by equations (7.5) and (7.6).

$$X_{i,j} \in \{0, 1\} \quad \forall l_{i,j} \in \mathcal{L} \quad (7.5)$$

$$Y_{i,j}^k, Y_{j,i}^k \in \{0, 1\} \quad \forall l_{i,j} \in \mathcal{L}, \forall k \in \mathcal{M} \quad (7.6)$$

Therefore, the maximum stable multicast route can be obtained by solving the integer program where the objective function is given by expression (7.1) and the constraints are given by Equations (7.2) to (7.6).

7.3 Obstacle-Aware Multicast Link Selection Algorithm

As stated earlier, a multicast route for a particular group \mathcal{M} is essentially a spanning tree of the UEs in \mathcal{M} [48]. Here, the objective is to build a multicast tree that has the maximum possible stability. Recall that the stability $s_{i,j}$ of a particular link $l_{i,j}$ is defined as the probability of not being blocked by any obstacle. Since the stability of two links is uncorrelated, the expected stability $\mathbb{E}[s_{\mathcal{T}}]$ of the entire multicast tree \mathcal{T} is essentially the

product of the expected stability of the individual links in \mathcal{T} , that is,

$$\mathbb{E}[s_{\mathcal{T}}] = \prod_{l_{i,j} \in \mathcal{T}} \mathbb{E}[s_{i,j}]$$

Let (x_i, y_i) and (x_j, y_j) be the grid cells containing the UEs i and j , respectively. Then, the stability of a link $l_{i,j}$ can be obtained from the **blockage** matrix:

$$s_{i,j} = 1 - \text{blockage}[x_i, y_i][x_j, y_j]$$

To obtain such a tree, we first construct a graph $G = (V, E)$, where V has a vertex corresponding to each UE in the multicast group \mathcal{M} , and we put an edge between two vertices i and j if their corresponding UE can establish a **LOS D2D** link between them, i.e. $l_{i,j} \in \mathcal{L}$. Each edge (i, j) in G is given a weight $w_{i,j}$, where

$$w_{i,j} = -\log(\mathbb{E}[s_{\mathcal{T}}])$$

Here the base of the logarithm can be any arbitrary positive constant larger than 1, and thus we omit it for notational simplicity. Note that, \mathcal{L} is the set of those links $l_{i,j}$ for which UE i and j are within a distance d_{\max} and do not have any static obstacle in between them i.e. $\text{blockage}[x_i, y_i][x_j, y_j] < 1$. Now we construct a **MST** \mathcal{T} of this graph G using Kruskal's algorithm [182]. We return \mathcal{T} as the required multicast tree. This process formalized as [Algorithm 7.1](#).

Algorithm 7.1: Stable multicast tree construction

```

/* Populate the set of candidate links  $\mathcal{L}$  */
1  $\mathcal{L} = \{l_{i,j} \mid \forall i, j \in \mathcal{M} \text{ s.t. } \text{dist}(i, j) \leq d_{\max} \text{ and } \text{blockage}[x_i, y_i][x_j, y_j] < 1\}$ 

/* Construct the graph  $G = (V, E)$  */
2  $V = \{i \mid \forall i \in \mathcal{M}\}$ 
3 foreach  $i \in V$  do
4   foreach  $i \in V$  do
5     if  $\exists l_{i,j} \in \mathcal{L}$  then                                     //  $i$  and  $j$  have an LOS D2D link
6     |   Put an edge  $(i, j)$  in  $E$  with weight  $w_{i,j} = -\log(\mathbb{E}[s_{i,j}])$ 
7  $\mathcal{T} \leftarrow \text{MST}(G = (V, E))$                                      // construct the minimum spanning tree
8 return  $\mathcal{T}$ 

```

Here the procedure $\text{MST}(G)$ returns a minimum spanning tree of the given graph G . In [Algorithm 7.1](#), the construction of the graph G takes $O(|\mathcal{M}|^2)$ time. We know that a minimum spanning tree of a graph G can be obtained by Kruskal's algorithm in $O(m \log n)$ time, where n and m are the number of vertices and edges in G respectively. Thus, [Line 7](#) takes $O(|\mathcal{L}| \log |\mathcal{M}|)$ time to execute. Therefore, the overall running time of [Algorithm 7.1](#) is $O(|\mathcal{M}|^2 + |\mathcal{L}| \log |\mathcal{M}|)$.

Lemma 7.1. *Algorithm 7.1 returns a spanning tree having maximum stability.*

Proof. Suppose [Algorithm 7.1](#) returns \mathcal{T}^* . Now consider any other spanning tree T of G for the given multicast group \mathcal{M} . Then by definition, we get

$$\begin{aligned}
& \sum_{l_{i,j} \in \mathcal{T}^*} w_{i,j} \leq \sum_{l_{i,j} \in T} w_{i,j} \\
\implies & \sum_{l_{i,j} \in \mathcal{T}^*} -\log(\mathbb{E}[s_{i,j}]) \leq \sum_{l_{i,j} \in T} -\log(\mathbb{E}[s_{i,j}]) && \text{(by construction)} \\
\implies & \sum_{l_{i,j} \in \mathcal{T}^*} \log(\mathbb{E}[s_{i,j}]) \geq \sum_{l_{i,j} \in T} \log(\mathbb{E}[s_{i,j}]) && \text{(negating both sides)} \\
\implies & \log \left(\prod_{l_{i,j} \in \mathcal{T}^*} \mathbb{E}[s_{i,j}] \right) \geq \log \left(\prod_{l_{i,j} \in T} \mathbb{E}[s_{i,j}] \right) && \text{(taking the log outside)} \\
\implies & \prod_{l_{i,j} \in \mathcal{T}^*} \mathbb{E}[s_{i,j}] \geq \prod_{l_{i,j} \in T} \mathbb{E}[s_{i,j}] && \text{(since log is an increasing function)} \\
\implies & \mathbb{E} \left[\prod_{l_{i,j} \in \mathcal{T}^*} s_{i,j} \right] \geq \mathbb{E} \left[\prod_{l_{i,j} \in T} s_{i,j} \right] && \text{(since the random variables are uncorrelated)} \\
\implies & \mathbb{E}[s_{\mathcal{T}^*}] \geq \mathbb{E}[s_{\mathcal{T}}] && \text{(by definition)}
\end{aligned}$$

Thus the expected stability of the multicast tree \mathcal{T}^* obtained through [Algorithm 7.1](#) is as good as that of any other spanning tree T for the given multicast group \mathcal{M} . \blacksquare

7.4 Learning Blockage Probabilities

A [D2D](#) communication link can be blocked by a static as well as by a dynamic obstacle. As stated in [Section 7.1](#), the knowledge of the static obstacles obtained from satellite imagery. As pointed out by the authors of [61], such information might not be very

accurate as the obstacle sizes can be small. On the other hand, the dynamic obstacles are much harder to deal with, since they move independently and are outside the purview of the BS. There are several methods proposed in the literature to track the movement of these dynamic obstacles, but those solutions requires extra hardware installation and are expensive. Instead, here we present a much cheaper solution to capture the notion of the dynamic as well as the static obstacle. As stated in Section 7.1, we have discretized the service area into small square grids. Now consider a D2D link between two grid cells (x_1, y_1) and (x_2, y_2) . If one can successfully establish a LOS link between (x_1, y_1) and (x_2, y_2) , then it is evident that there is no static obstacle on that path. Therefore, we may mark all the grid cells lying on that link to be free from static obstacles. Now if the link is blocked, there might be a static or dynamic obstacle present in some grid cell lying on that path. In this case, we mark each grid cell lying on this path between (x_1, y_1) and (x_2, y_2) as potentially containing an obstacle. As more and more links are tried to be established, we gather more such marking information for each grid cell. This information can be combined to obtain an estimate of the blockage probability at each grid cell. Now we need to consider the fact that the channel information itself is not very accurate, as there might be high interference and noise. This presents us with imperfect knowledge about the environment. Therefore, now a link blockage due to a significant drop in signal-to-interference-plus-noise ratio (SINR) value could be due to the presence of an obstacle, or it could be the case that there was high interference or noise.

To deal with such imperfect knowledge, we can take multiple such measurements and consider the evidences of blockage for a particular grid cell to update our knowledge about the blockage probabilities. We thus consider two type of events for a particular grid cell:

b: there is an obstacle present, the cell should be marked as blocked

f: there is no obstacle, the cell should be marked as free

Furthermore, we consider another case $\{\mathbf{b}, \mathbf{f}\}$ when we do not know which event has actually occurred. We consider an attempt of a link establishment as a trial. Thus, a trial can present us with one of these three evidences:

$$\{\mathbf{b}\}, \{\mathbf{f}\} \text{ and } \{\mathbf{b}, \mathbf{f}\}$$

We now utilize the Dempster-Shafer theory [132] to deal with such evidences. In our case,

the basic probability assignment m_{init} is taken as:

$$m_{\text{init}} = \left\langle \frac{1}{M}, \frac{M-2}{M}, \frac{1}{M} \right\rangle$$

where M is a suitably large value. We initialize evidence masses $m_{x,y}$ of all grid cells (x, y) to m_{init} . This essentially denotes the fact that all grid cells are initially assumed to be free of any obstacles. Whenever a link between (x_1, y_1) and (x_2, y_2) is blocked it provides evidence of blockage for to all grid cells on the line joining (x_1, y_1) and (x_2, y_2) . Those grid cells can be efficiently obtained with a subroutine `LINE()`. More specifically, `LINE(i, j)` runs the Bresenham line drawing algorithm [178], that uses only integral addition and subtractions, to compute the intermediate grid cells on the line joining the two grid cells containing `UE i` and `UE j`. Suppose there are n many grid cells on the line joining (x_1, y_1) and (x_2, y_2) , then we formulate the blocking evidence for each of these grid cells as follows:

$$e_{\mathbf{b}}(n) = \left\langle \frac{1}{n}, \frac{1}{M}, \frac{Mn - M - n}{Mn} \right\rangle$$

Now we use the Yager's rule [133] to combine this new evidence into the existing knowledge $m_{x,y}$ about any grid cell (x, y) lying on the line joining (x_1, y_1) and (x_2, y_2) . Let us denote this combination operation as:

$$m_{x,y} \leftarrow m_{x,y} \otimes e_{\mathbf{b}}(n)$$

Similarly, for an evidence of obstacle free `LOS` path we update the existing knowledge as:

$$m_{x,y} \leftarrow m_{x,y} \otimes m_{\text{init}}$$

Finally, we take the blockage probability $b_{x,y}$ of a grid cell (x, y) as the belief function $\text{bel}_{x,y}(\{\mathbf{b}\})$ defined as the probability mass value of $\{\mathbf{b}\}$ in $m_{x,y}$. This process is formalized as [Algorithm 7.2](#).

Note that this is an online learning process that is executed after each time slot and the blockage probabilities are updated accordingly.

Algorithm 7.2: Learning blockage probabilities

```

1 foreach grid cell  $(x, y)$  do
2    $m_{x,y} \leftarrow m_{\text{init}}$  // initial mass assignment
3 loop
4    $\mathcal{L} \leftarrow$  set of links selected by Algorithm 7.1
5    $\mathcal{B} \leftarrow$  links in  $\mathcal{L}$  that could not be activated // possibly blocked
6   foreach link  $l_{i,j} \in \mathcal{B}$  do
7      $\mathcal{P} \leftarrow \text{LINE}(i, j)$  // set of grid points between  $i$  and  $j$ 
8      $n \leftarrow |\mathcal{P}|$  // number of grid cells in  $\mathcal{P}$ 
9     foreach grid point  $(x, y) \in \mathcal{P}$  do
10     $m_{x,y} \leftarrow m_{x,y} \otimes e_b(n)$  // combine the new evidence
11  foreach link  $l_{i,j} \in \mathcal{L} \setminus \mathcal{B}$  do // obstacle free LOS links
12     $\mathcal{P} \leftarrow \text{LINE}(i, j)$ 
13    foreach grid point  $(x, y) \in \mathcal{P}$  do
14     $m_{x,y} \leftarrow m_{x,y} \otimes m_{\text{init}}$  // combine the initial mass
15  foreach grid cell  $(x, y)$  do
16     $b_{x,y} \leftarrow \text{bel}_{x,y}(\{\mathbf{b}\})$  // belief of blockage
17     $s_{x,y} \leftarrow 1 - b_{x,y}$  // stability

```

7.5 Simulation Results

We consider a simulation environment similar as before. The service area is considered to be of size 1000 m \times 1000 m. We take the grid sizes as 5 m \times 5 m. The number of UEs in the multicast group \mathcal{M} is varied from 50 to 200. The UEs are placed uniformly at random in the service area. The distance between two D2D pairs is at most 20 m. The static obstacle sizes are considered to be 10 m \times 10 m. We consider a fixed number (100) of static obstacles scattered over the service area uniformly at random. We vary their number of dynamic obstacles from 50 to 200. The mmWave D2D communications use the 60 GHz frequency band.

Figure 7.2 demonstrates the convergence of our proposed framework for learning the blockage probabilities obtained through Algorithm 7.2. We use a Monte-Carlo simulation where we move a few dynamic obstacles using Random Walk with a maximum velocity of 1.5 m/s and measure the link failures. The plot shows a span of a thousand time slots, that is, a thousand iterations of the outer loop of Figure 7.2. Here we consider the

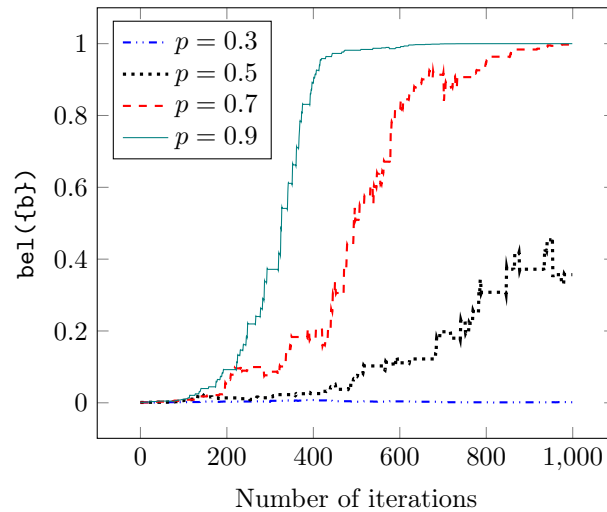


Figure 7.2: Plot of convergence of [Algorithm 7.2](#)

value of $\text{bel}(\{b\})$ for a single grid cell under four different cases where the probability of a grid being blocked is 0.3, 0.5, 0.7, and 0.9, respectively. As evident in the figure, the $\text{bel}(\{b\})$ approaches 1 when the blocking probability is greater than 0.5. Higher the blocking probability, quicker the value of $\text{bel}(\{b\})$ saturates to 1. In case of blocking probability being lesser than 0.5, the value of $\text{bel}(\{b\})$ stays almost always 0. Whereas if the blocking probability is near about 0.5, the $\text{bel}(\{b\})$ value keeps fluctuating, as one would expect.

Next we demonstrate the effectiveness of our proposed framework. For this we consider the [D2D](#) multicasting application with the objective of maximizing the stability of the route. To obtain a maximum stable multicast tree we use the [Algorithm 7.1](#) with the learned blockage probabilities. Let us denote this as **Proposed**. To compare the performance of our proposed scheme we consider the approach used in [62]. Here the blockage probabilities are fixed values distributed using a Poisson process. We run the same [Algorithm 7.1](#) using these probability values. We denote this as **Fixed**. Moreover, we also consider a random spanning tree generation algorithm irrespective of any knowledge of blockage probability. Let us call this algorithm **Random**. We perform a Monte-Carlo simulation where we similarly place few dynamic obstacles following random walks and test how many selected links are affected these obstacles. The stability of a constructed spanning tree is calculated as the

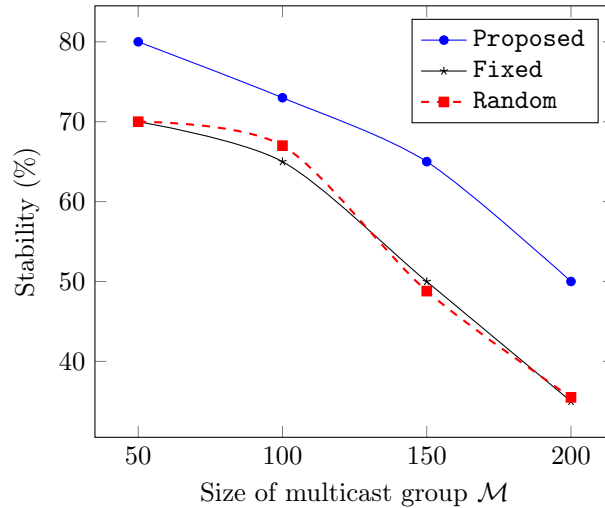


Figure 7.3: Plot of stability verses group size

percentage of links blocked by the dynamic obstacles. We repeat this process and take an average over that. Figure 7.3 plots the stability with varying size of multicast groups with number of dynamic obstacles fixed at 200. As evident in Figure 7.3, the Proposed scheme perform better than Fixed and Random scheme. As one would expect, the stability of the constructed multicast tree decreases as the spanning tree grows with the group size. Moreover, Figure 7.3 also suggests that using a static fixed distribution does not help much, compared to random selection of links for the spanning tree without considering the presence of any dynamic obstacles.

In Figure 7.4, we plot the stability with a fixed group size of 200 while we vary the number of dynamic obstacles from 50 to 200. Figure 7.4 shows that the stability of the constructed multicast tree decreases as the number of obstacles increase, as expected. A similar behavior is observed here also, that is, our Proposed scheme performs better than the Fixed and Random schemes.

As mentioned in Section 7.1, we have discretized the service area into grid of small squares. Furthermore, we have also assumed that a grid cell as fully blocked even if it contains only a portion of an obstacle. This approximation overestimates the actual blockage due to the presence of the obstacles. In Figure 7.5, we try to capture the effect of this discretization. For this we define a metric called *inaccuracy* which is defined as the

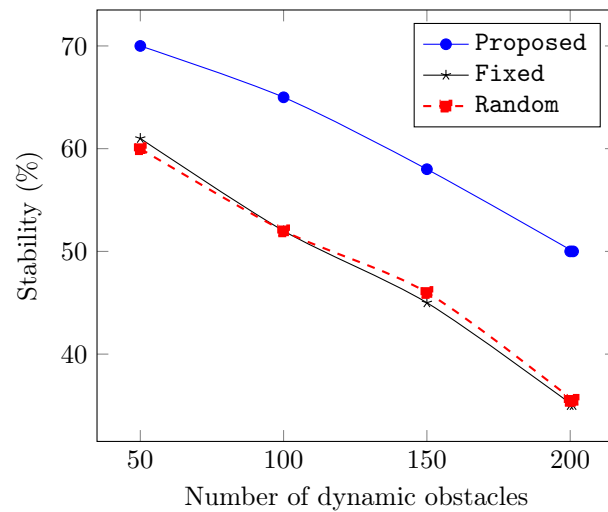


Figure 7.4: Plot of stability versus obstacle count

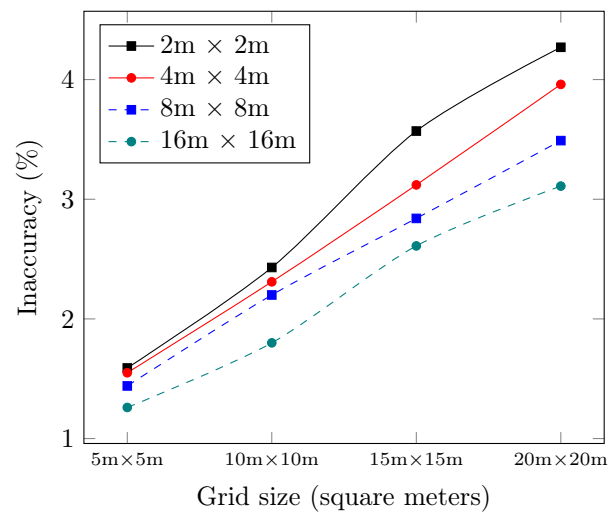


Figure 7.5: Plot of effect of grid approximation

ratio $\frac{n-n_a}{n}$ where n is the number of link blockages when we overestimate partial overlap between a grid cell and an obstacle as the grid cell being fully blocked, while n_a is the actual number of link blockages considering exact size and position of the obstacles. We vary the obstacle sizes from 2 m \times 2 m to 16 m \times 16 m and also vary the size of grid cells from 5 m \times 5 m to 20 m \times 20 m and do a Monte Carlo simulation to measure the inaccuracy. We plot the result in [Figure 7.5](#). As one would expect, the inaccuracy increases with the grid cell sizes as more and more overestimate is being done in case of larger grid cells. Moreover, the inaccuracy also increases as the obstacles size reduces as more overestimation is being done, which is also expected.

7.6 Conclusion

In this chapter we have addressed the stable link selection problem for multicast [D2D](#) communication in presence of static and dynamic obstacles. To this end, we have developed a greedy stable multicast tree construction algorithm. We have proven its optimality assuming the blockage probabilities are known to the [BS](#). We have shown the effectiveness of our proposed algorithm through simulations. Next we have presented a framework for learning these blockage probabilities based on the Dempster-Shafer evidential theory. We have shown the convergence of our proposed framework through simulations. The choice of size of the grid squares plays a crucial role in the accuracy of proposed framework which captures the blockage probabilities due to the dynamic obstacles. Furthermore, we also present the effect of the discretization of the service area and approximation of the obstacle to grid squares through simulation. Although finer grid sizes reduces the overestimation due to the grid approximation, it requires more storage space. Thus obtaining a balance between the two could be a possible extension of this work. Moreover, we have only considered stability maximization problem for multicast [D2D](#) communication, other metrics, such as delay minimization, capacity maximization, are yet to be explored.

CHAPTER 8

Conclusion and Future Directions

This thesis deals with link selection and channel resource allocation problems in the context of [device-to-device \(D2D\)](#) communications using [millimeter-wave \(mmWave\)](#) signals. We design efficient algorithms for resource allocation, dealing with dynamic obstacles, and multicast communications. More specifically, the following aspects have been addressed here:

- We consider the joint relay selection and channel allocation problem for [D2D](#) communications as our first work. Here, we first argue that the two problems, namely relay selection and channel allocation, have inherent interdependencies and thus must be jointly dealt with. To this end, in [Chapter 3](#), we propose a [linear program \(LP\)](#) relaxation-based solution for this [\$\mathcal{NP}\$ -Complete](#) problem. Through simulations, we show that our approach maximizes the number of activated links and improves the datarate.
- In the previous problem, we assumed that devices were stationary and that no obstacle was present in the service area. For [mmWave](#) communications having high penetration and propagation losses, both user mobility and the presence of static as well as dynamic obstacles can severely degrade the link quality. To this end, in [Chapter 4](#), we propose an obstacle aware joint resource allocation and relay selection framework for mobile users that involves probabilistic constraints. We then provide a mechanism for converting probabilistic constraints into deterministic ones using the Chebyshev–Cantelli inequality. We present a greedy algorithm for this and derive its approximation bound. Through simulations, we demonstrate that our proposed approach yields an improved active link count and fewer link failures.
- In the previous framework, we assumed that blockage probabilities due to dynamic obstacles were known. Obtaining such information without resorting to expensive

hardware, such as cameras and radar, is a challenging task. In this context, [Chapter 5](#) presents a [reinforcement learning \(RL\)](#) framework for energy-efficient green communication in the presence of dynamic obstacles. We show the convergence of our proposed framework both theoretically, and experimentally through simulations.

- The aforesaid [RL](#) framework is not very scalable. To this end, we present a new framework to address the exploration-exploitation dilemma in obstacle learning through link failures. In [Chapter 6](#), we devise a greedy strategy and validate it through extensive simulations. We further provide a framework for estimating the blockage probabilities using a *reservoir sampling* method.
- In all the aforesaid works, we have assumed a unicast communication scenario. Due to the variable conditions of wireless channels, especially in the presence of dynamic obstacles, link stability varies dramatically. We present a multicast stable link selection mechanism in [Chapter 7](#), and prove its optimality given the link stability values. We then propose a mechanism for calculating these stability values using the *Dempster-Shafer evidential theory framework*. Here also, we validate our proposed framework through simulations.

We believe that our methods and experimental results will open up a lot of scope for future research in [D2D mmWave](#) communications. Some possible future directions arising out of our work are outlined below.

- In [Part I](#) of this thesis, we have addressed the joint relay selection and channel allocation problem assuming fixed transmit powers, while in [Part II](#), we explore the joint channel and power allocations without any relay-aided communications. The combination of the three might result into better system utilization and is yet to be explored.
- All the works presented in this thesis are centralized in nature. A distributed local resource allocation mechanism may be desired in practical cases and is a promising future area for possible extensions of the presented works.
- We have assumed perfect [channel state information \(CSI\)](#) information is available at the [base station \(BS\)](#), which is rarely the case. Adapting the presented works for imperfect [CSI](#) cases is a challenging and interesting area to work on.

- For modeling the obstacles, we have discretized the service area into small square grids, which introduces some inaccuracies. Determining the ideal grid size or eliminating the need for this discretization is an all together interesting area to explore.
- Lastly, we have only explored the stable link selection problem in the context of multicast [D2D](#) communications. Other metrics, such as delay and capacity, may also be looked into to cater to different application requirements. Furthermore, the selected (stable) links must be allocated channel resources, which can be explored in the future.

List of References

- [1] *Cisco Annual Internet Report (2018–2023) White Paper*. URL: <https://www.cisco.com/c/en/us/solutions/collateral/executive-perspectives/annual-internet-report/white-paper-c11-741490.html>.
- [2] *Secretary Shri Apurva Chandra (Ministry of Information and Broadcasting, India) addresses first World Media Congress*. URL: <https://pib.gov.in/PressReleaseIframePage.aspx?PRID=1876553>.
- [3] *Benchmarking the Global 5G Experience*. URL: <https://www.opensignal.com/2022/06/22/benchmarking-the-global-5g-experience-june-2022>.
- [4] *NR; User Equipment (UE) radio transmission and reception; Part 1*. URL: <https://portal.3gpp.org/desktopmodules/Specifications/SpecificationDetails.aspx?specificationId=3283>.
- [5] *NR; User Equipment (UE) radio transmission and reception; Part 2*. URL: <https://portal.3gpp.org/desktopmodules/Specifications/SpecificationDetails.aspx?specificationId=3284>.
- [6] *mmWave Clocks Gigabit Speeds in the U.S. but Lacks Maturity Elsewhere*. URL: <https://www.ookla.com/articles/mmwave-spectrum-gigabit-speeds-us-q1-2023>.
- [7] Sasthi C. Ghosh, Bhabani P. Sinha, and Nabanita Das. “Coalesced CAP: An Improved Technique for Frequency Assignment in Cellular Networks”. In: *IEEE Transactions on Vehicular Technology* 55.2 (Mar. 2006), pp. 640–653. ISSN: 1939-9359. DOI: [10.1109/TVT.2005.863351](https://doi.org/10.1109/TVT.2005.863351).
- [8] Mohsen Nader Tehrani, Murat Uysal, and Halim Yanikomeroglu. “Device-to-device communication in 5G cellular networks: challenges, solutions, and future directions”. In: *IEEE Communications Magazine* 52.5 (May 2014), pp. 86–92. ISSN: 1558-1896. DOI: [10.1109/MCOM.2014.6815897](https://doi.org/10.1109/MCOM.2014.6815897).
- [9] Shuanshuan Wu, Rachad Atat, Nicholas Mastronarde, and Lingjia Liu. “Improving the Coverage and Spectral Efficiency of Millimeter-Wave Cellular Networks Using Device-to-Device Relays”. In: *IEEE Transactions on Communications* 66.5 (May 2018), pp. 2251–2265. ISSN: 1558-0857. DOI: [10.1109/TCOMM.2017.2787990](https://doi.org/10.1109/TCOMM.2017.2787990).

- [10] I Chih-Lin et al. “Toward green and soft: a 5G perspective”. In: *IEEE Communications Magazine* 52.2 (Feb. 2014), pp. 66–73. ISSN: 1558-1896. DOI: [10.1109/MCOM.2014.6736745](https://doi.org/10.1109/MCOM.2014.6736745).
- [11] Klaus Doppler et al. “Device-to-device communication as an underlay to LTE-advanced networks”. In: *IEEE Communications Magazine* 47.12 (Dec. 2009), pp. 42–49. ISSN: 1558-1896. DOI: [10.1109/MCOM.2009.5350367](https://doi.org/10.1109/MCOM.2009.5350367).
- [12] Theodore S Rappaport. *Wireless communications: Principles and practice, 2/E*. Pearson Education India, 2010. ISBN: 9788131731864.
- [13] H.T. Friis. “A Note on a Simple Transmission Formula”. In: *Proceedings of the IRE* 34.5 (May 1946), pp. 254–256. DOI: [10.1109/jrproc.1946.234568](https://doi.org/10.1109/jrproc.1946.234568).
- [14] Ibrahim A. Hemadeh, Katla Satyanarayana, Mohammed El-Hajjar, and Lajos Hanzo. “Millimeter-Wave Communications: Physical Channel Models, Design Considerations, Antenna Constructions, and Link-Budget”. In: *IEEE Communications Surveys & Tutorials* 20.2 (2018), pp. 870–913. ISSN: 1553-877X. DOI: [10.1109/COMST.2017.2783541](https://doi.org/10.1109/COMST.2017.2783541).
- [15] T.S. Rappaport, R.W. Heath, R.C. Daniels, and J.N. Murdock. *Millimeter Wave Wireless Communications*. Communications Engineering and Emerging Technology Series from Ted Rappaport Series. Prentice Hall, 2015. ISBN: 9780132172288. URL: https://books.google.co.in/books?id=%5C_Tt%5C_BAAAQBAJ.
- [16] Theodore S. Rappaport et al. “Millimeter Wave Mobile Communications for 5G Cellular: It Will Work!” In: *IEEE Access* 1 (2013), pp. 335–349. ISSN: 2169-3536. DOI: [10.1109/ACCESS.2013.2260813](https://doi.org/10.1109/ACCESS.2013.2260813).
- [17] Sundeep Rangan, Theodore S. Rappaport, and Elza Erkip. “Millimeter-Wave Cellular Wireless Networks: Potentials and Challenges”. In: *Proceedings of the IEEE* 102.3 (Mar. 2014), pp. 366–385. ISSN: 1558-2256. DOI: [10.1109/JPROC.2014.2299397](https://doi.org/10.1109/JPROC.2014.2299397).
- [18] Mikola Patlayenko, Olena Osharovska, and Valentyna Solodka. “Comparison of LTE Coverage Areas in Three Frequency Bands”. In: *2021 IEEE 4th International Conference on Advanced Information and Communication Technologies (AICT)*. IEEE, Sept. 2021, pp. 212–215.
- [19] *Small Cells: Microcell, Picocell and Femtocell Comparison*. URL: <https://dgtlinfra.com/small-cells-microcell-picocell-femtocell/>.
- [20] Zhenliang Zhang, Jung Ryu, Sundar Subramanian, and Ashwin Sampath. “Coverage and channel characteristics of millimeter wave band using ray tracing”. In: *2015 IEEE International Conference on Communications (ICC)*. IEEE, June 2015, pp. 1380–1385. DOI: [10.1109/ICC.2015.7248516](https://doi.org/10.1109/ICC.2015.7248516).
- [21] *Everything You Need to Know About 5G*. URL: <https://spectrum.ieee.org/everything-you-need-to-know-about-5g>.

- [22] Hossein Shokri-Ghadikolaie et al. “Millimeter Wave Cellular Networks: A MAC Layer Perspective”. In: *IEEE Transactions on Communications* 63.10 (Oct. 2015), pp. 3437–3458. ISSN: 1558-0857. DOI: [10.1109/TCOMM.2015.2456093](https://doi.org/10.1109/TCOMM.2015.2456093).
- [23] Lin Cai, Lin Cai, Xuemin Shen, and Jon Mark. “Rex: A randomized EXclusive region based scheduling scheme for mmWave WPANs with directional antenna”. In: *IEEE Transactions on Wireless Communications* 9.1 (Jan. 2010), pp. 113–121. ISSN: 1558-2248. DOI: [10.1109/TWC.2010.01.070503](https://doi.org/10.1109/TWC.2010.01.070503).
- [24] Jian Qiao et al. “Enabling device-to-device communications in millimeter-wave 5G cellular networks”. In: *IEEE Communications Magazine* 53.1 (Jan. 2015), pp. 209–215. ISSN: 1558-1896. DOI: [10.1109/MCOM.2015.7010536](https://doi.org/10.1109/MCOM.2015.7010536).
- [25] Sanjib Sur, Vignesh Venkateswaran, Xinyu Zhang, and Parmesh Ramanathan. “60 GHz Indoor Networking through Flexible Beams: A Link-Level Profiling”. In: *Proceedings of the 2015 ACM SIGMETRICS International Conference on Measurement and Modeling of Computer Systems*. SIGMETRICS ’15. Portland, Oregon, USA: ACM, June 2015, pp. 71–84. ISBN: 9781450334860. DOI: [10.1145/2745844.2745858](https://doi.org/10.1145/2745844.2745858).
- [26] Na Deng and Martin Haenggi. “A Fine-Grained Analysis of Millimeter-Wave Device-to-Device Networks”. In: *IEEE Transactions on Communications* 65.11 (Nov. 2017), pp. 4940–4954. ISSN: 1558-0857. DOI: [10.1109/TCOMM.2017.2725827](https://doi.org/10.1109/TCOMM.2017.2725827).
- [27] Roberto Congiu, Hossein Shokri-Ghadikolaie, Carlo Fischione, and Fortunato Santucci. “On the relay-fallback tradeoff in millimeter wave wireless system”. In: *2016 IEEE Conference on Computer Communications Workshops (INFOCOM WKSHPS)*. IEEE, Apr. 2016, pp. 622–627. DOI: [10.1109/INFOCOMW.2016.7562151](https://doi.org/10.1109/INFOCOMW.2016.7562151).
- [28] Chiranjib Saha, Mehrnaz Afshang, and Harpreet S. Dhillon. “Integrated mmWave Access and Backhaul in 5G: Bandwidth Partitioning and Downlink Analysis”. In: *2018 IEEE International Conference on Communications (ICC)*. IEEE, May 2018, pp. 1–6. DOI: [10.1109/ICC.2018.8422149](https://doi.org/10.1109/ICC.2018.8422149).
- [29] Stanley Chia, Max Gasparroni, and Patrick Brick. “The next challenge for cellular networks: backhaul”. In: *IEEE Microwave Magazine* 10.5 (Aug. 2009), pp. 54–66. ISSN: 1557-9581. DOI: [10.1109/MMM.2009.932832](https://doi.org/10.1109/MMM.2009.932832).
- [30] *Integrated access and backhaul: Why it is essential for mmWave deployments*. Nov. 2020. URL: <https://www.nokia.com/blog/integrated-access-and-backhaul-why-it-is-essential-for-mmwave-deployments/>.
- [31] *Integrated access and backhaul – a new type of wireless backhaul in 5G*. June 2020. URL: <https://www.ericsson.com/en/reports-and-papers/ericsson-technology-review/articles/introducing-integrated-access-and-backhaul>.

- [32] Raj Jain. *Introduction to Introduction to 60 GHz Millimeter Wave 60 GHz Millimeter Wave Multi-Gigabit Wireless Networks Gigabit Wireless Networks*. 2018. URL: https://www.cse.wustl.edu/~jain/cse574-18/ftp/j_07sgh.pdf.
- [33] Sai Shankar N., Debashis Dash, Hassan El Madi, and Guru Gopalakrishnan. *WiGig and IEEE 802.11ad - For multi-gigabyte-per-second WPAN and WLAN*. 2012. arXiv: [1211.7356](https://arxiv.org/abs/1211.7356) [cs.NI].
- [34] Nikolaos Giatsoglou et al. “D2D-Aware Device Caching in mmWave-Cellular Networks”. In: *IEEE Journal on Selected Areas in Communications* 35.9 (Sept. 2017), pp. 2025–2037. ISSN: 1558-0008. DOI: [10.1109/JSAC.2017.2720818](https://doi.org/10.1109/JSAC.2017.2720818).
- [35] Wen Wu et al. “Beef Up mmWave Dense Cellular Networks With D2D-Assisted Cooperative Edge Caching”. In: *IEEE Transactions on Vehicular Technology* 68.4 (Apr. 2019), pp. 3890–3904. ISSN: 1939-9359. DOI: [10.1109/TVT.2019.2896906](https://doi.org/10.1109/TVT.2019.2896906).
- [36] Xiaoya Li, Wei Zhou, Jinye Peng, and Hengsheng Shan. “Joint beamwidth and resource optimization in ultra-dense MmWave D2D communications”. In: *Wireless Networks* (Feb. 2023). DOI: [10.1007/s11276-023-03266-z](https://doi.org/10.1007/s11276-023-03266-z).
- [37] *GSMA 5G mmWave Factsheet*. URL: <https://www.gsma.com/futurenetworks/resources/gsma-5g-mmwave-factsheet/>.
- [38] Kiran Vanganuru, Steven Ferrante, and Gregory Sternberg. “System capacity and coverage of a cellular network with D2D mobile relays”. In: *MILCOM 2012 - 2012 IEEE Military Communications Conference*. Oct. 2012, pp. 1–6. DOI: [10.1109/MILCOM.2012.6415659](https://doi.org/10.1109/MILCOM.2012.6415659).
- [39] Yue Meng and Zhaowei Wang. “Contextual Multi-armed Bandit Based Pricing Scheme for Cooperative D2D Communications”. In: *2020 IEEE Wireless Communications and Networking Conference (WCNC)*. IEEE, May 2020, pp. 1–6. DOI: [10.1109/WCNC45663.2020.9120767](https://doi.org/10.1109/WCNC45663.2020.9120767).
- [40] Konstantinos Ntontin et al. “Autonomous Reconfigurable Intelligent Surfaces Through Wireless Energy Harvesting”. In: *2022 IEEE 95th Vehicular Technology Conference: (VTC2022-Spring)*. IEEE, June 2022, pp. 1–6. DOI: [10.1109/vtc2022-spring54318.2022.9860773](https://doi.org/10.1109/vtc2022-spring54318.2022.9860773).
- [41] Qingqing Wu et al. “Intelligent Reflecting Surface-Aided Wireless Communications: A Tutorial”. In: *IEEE Transactions on Communications* 69.5 (May 2021), pp. 3313–3351. ISSN: 1558-0857. DOI: [10.1109/TCOMM.2021.3051897](https://doi.org/10.1109/TCOMM.2021.3051897).
- [42] Özgecan Özdoğan, Emil Björnson, and Erik G. Larsson. “Intelligent Reflecting Surfaces: Physics, Propagation, and Pathloss Modeling”. In: *IEEE Wireless Communications Letters* 9.5 (May 2020), pp. 581–585. ISSN: 2162-2345. DOI: [10.1109/LWC.2019.2960779](https://doi.org/10.1109/LWC.2019.2960779).

- [43] Emil Björnson, Özgecan Özdogan, and Erik G. Larsson. “Reconfigurable Intelligent Surfaces: Three Myths and Two Critical Questions”. In: *IEEE Communications Magazine* 58.12 (Dec. 2020), pp. 90–96. ISSN: 1558-1896. DOI: [10.1109/MCOM.001.2000407](https://doi.org/10.1109/MCOM.001.2000407).
- [44] Cisco. *Cut-Through and Store-and-Forward Ethernet Switching for Low-Latency Environments*. URL: https://www.cisco.com/c/en/us/products/collateral/switches/nexus-5020-switch/white_paper_c11-465436.html (visited on 10/20/2018).
- [45] Francesco Chiti, Romano Fantacci, and Laura Pierucci. “Social-Aware Relay Selection for Cooperative Multicast Device-to-Device Communications”. In: *Future Internet* 9.4 (Dec. 2017), p. 92. ISSN: 1999-5903. DOI: [10.3390/fi9040092](https://doi.org/10.3390/fi9040092).
- [46] Devarani Devi Ningombam and Seokjoo Shin. “Resource-sharing optimization for multicast D2D communications underlying LTE-A uplink cellular networks”. In: *Proceedings of the 34th ACM/SIGAPP Symposium on Applied Computing*. SAC '19. Limassol, Cyprus: ACM, Apr. 2019, pp. 2001–2007. ISBN: 9781450359337. DOI: [10.1145/3297280.3297476](https://doi.org/10.1145/3297280.3297476).
- [47] Roy D. Yates. “The Age of Gossip in Networks”. In: *2021 IEEE International Symposium on Information Theory (ISIT)*. IEEE, July 2021, pp. 2984–2989. DOI: [10.1109/ISIT45174.2021.9517796](https://doi.org/10.1109/ISIT45174.2021.9517796).
- [48] Thomas A. Maufer and Chuck Semeria. *Introduction to IP Multicast Routing*. Internet-Draft draft-ietf-mboned-intro-multicast-03. Internet Engineering Task Force, Oct. 1997. 60 pp. URL: <https://datatracker.ietf.org/doc/draft-ietf-mboned-intro-multicast>.
- [49] Rolando Bettancourt. *LTE Broadcast Multicast*. <https://futurenetworks.ieee.org/images/files/pdf/applications/LTE-Broadcast-Multicast030518.pdf>.
- [50] Lin Li, Song Xu, Guoliang Nie, and Lingfeng Fang. “Overview of eMBMS Technique”. In: *Lecture Notes in Electrical Engineering*. Springer Singapore, 2020, pp. 882–888. DOI: [10.1007/978-981-15-4163-6_105](https://doi.org/10.1007/978-981-15-4163-6_105).
- [51] *The eMBMS Puzzle: Hype or Reality?* URL: <https://www.wipro.com/engineering/the-embms-puzzle--hype-or-reality/>.
- [52] *Google is Adding Support for eMBMS for Reduced Mobile Network Congestion*. URL: <https://www.xda-developers.com/embms-google-support-multicast/>.
- [53] Ajay Bhardwaj and Samar Agnihotri. “Multicast Protocols for D2D”. In: *Wiley 5G Ref*. Wiley, May 2020, pp. 1–18. ISBN: 9781119471509. DOI: [10.1002/9781119471509.w5GRef183](https://doi.org/10.1002/9781119471509.w5GRef183).

- [54] Shashank K. Gupta, Jamil Y. Khan, and Duy T. Ngo. “A D2D Multicast Network Architecture for Vehicular Communications”. In: *2019 IEEE 89th Vehicular Technology Conference (VTC2019-Spring)*. IEEE, Apr. 2019, pp. 1–6. DOI: [10.1109/VTCSpring.2019.8746673](https://doi.org/10.1109/VTCSpring.2019.8746673).
- [55] Hujun Yin and Siavash Alamouti. “OFDMA: A Broadband Wireless Access Technology”. In: *2006 IEEE Sarnoff Symposium*. IEEE, Mar. 2006, pp. 1–4. DOI: [10.1109/SARNOF.2006.4534773](https://doi.org/10.1109/SARNOF.2006.4534773).
- [56] D.B. West. *Introduction to Graph Theory*. Pearson Modern Classics for Advanced Mathematics Series. Pearson, 2018. ISBN: 9780131437371. URL: <https://books.google.co.in/books?id=61gtAAAACAAJ>.
- [57] L. Lovász and M.D. Plummer. *Matching Theory*. AMS Chelsea Publishing Series. AMS Chelsea Pub., 2009. ISBN: 9780821847596. URL: <https://books.google.co.in/books?id=0aoJBAAAQBAJ>.
- [58] Taejoon Kim and Miaomiao Dong. “An Iterative Hungarian Method to Joint Relay Selection and Resource Allocation for D2D Communications”. In: *IEEE Wireless Communications Letters* 3.6 (Dec. 2014), pp. 625–628. ISSN: 2162-2345. DOI: [10.1109/LWC.2014.2338318](https://doi.org/10.1109/LWC.2014.2338318).
- [59] James Cowling. “Dynamic Location Management in Heterogeneous Cellular Networks”. MA thesis. Advanced Networks Research Group, School of Information Technologies, University of Sydney, Australia, Oct. 2004. URL: <http://people.csail.mit.edu/cowling/hons/jcowling-dynamic-Nov04.pdf> (visited on 04/04/2018).
- [60] Travis Keshav. *Location Management in Wireless Cellular Networks*. 2006. URL: https://www.cse.wustl.edu/~jain/cse574-06/ftp/cellular_location.pdf.
- [61] Subhojit Sarkar and Sasthi C. Ghosh. “Relay selection in millimeter wave D2D communications through obstacle learning”. In: *Ad Hoc Networks* 114 (Apr. 2021), p. 102419. DOI: [10.1016/j.adhoc.2021.102419](https://doi.org/10.1016/j.adhoc.2021.102419).
- [62] S. Yuva Kumar and Tomoaki Ohtsuki. “Influence and Mitigation of Pedestrian Blockage at mmWave Cellular Networks”. In: *IEEE Transactions on Vehicular Technology* 69.12 (Dec. 2020), pp. 15442–15457. ISSN: 1939-9359. DOI: [10.1109/TVT.2020.3041660](https://doi.org/10.1109/TVT.2020.3041660).
- [63] B. Langen, G. Lober, and W. Herzig. “Reflection and transmission behaviour of building materials at 60 GHz”. In: *5th IEEE International Symposium on Personal, Indoor and Mobile Radio Communications, Wireless Networks - Catching the Mobile Future*. Vol. 2. IOS Press, Sept. 1994, 505–509 vol.2. DOI: [10.1109/WNCMF.1994.529141](https://doi.org/10.1109/WNCMF.1994.529141).

- [64] *Analysis of 28GHz and 60GHz Channel Measurements in an Indoor Environment (Telecom Infra Project)*. URL: https://telecominfraproject.com/wp-content/uploads/TIP_mmWave-Networks_Analysis-of-28GHz-and-60GHz-Channel-Measurements-in-an-Indoor-Environment_August-2019.pdf.
- [65] Theodore S. Rappaport, Eshar Ben-Dor, James N. Murdock, and Yijun Qiao. “38 GHz and 60 GHz angle-dependent propagation for cellular & peer-to-peer wireless communications”. In: *2012 IEEE International Conference on Communications (ICC)*. IEEE, June 2012, pp. 4568–4573. DOI: [10.1109/ICC.2012.6363891](https://doi.org/10.1109/ICC.2012.6363891).
- [66] Yusuke Koda, Koji Yamamoto, Takayuki Nishio, and Masahiro Morikura. “Reinforcement learning based predictive handover for pedestrian-aware mmWave networks”. In: *IEEE INFOCOM 2018 - IEEE Conference on Computer Communications Workshops (INFOCOM WKSHPS)*. IEEE, Apr. 2018, pp. 692–697. DOI: [10.1109/INFCOMW.2018.8406993](https://doi.org/10.1109/INFCOMW.2018.8406993).
- [67] George R. MacCartney, Sijia Deng, Shu Sun, and Theodore S. Rappaport. “Millimeter-Wave Human Blockage at 73 GHz with a Simple Double Knife-Edge Diffraction Model and Extension for Directional Antennas”. In: *2016 IEEE 84th Vehicular Technology Conference (VTC-Fall)*. IEEE, Sept. 2016, pp. 1–6. DOI: [10.1109/VTCFall.2016.7881087](https://doi.org/10.1109/VTCFall.2016.7881087).
- [68] Eshar Ben-Dor, Theodore S. Rappaport, Yijun Qiao, and Samuel J. Lauffenburger. “Millimeter-Wave 60 GHz Outdoor and Vehicle AOA Propagation Measurements Using a Broadband Channel Sounder”. In: *2011 IEEE Global Telecommunications Conference - GLOBECOM 2011*. IEEE, Dec. 2011, pp. 1–6. DOI: [10.1109/GLOCOM.2011.6133581](https://doi.org/10.1109/GLOCOM.2011.6133581).
- [69] Mate Boban et al. “Multi-Band Vehicle-to-Vehicle Channel Characterization in the Presence of Vehicle Blockage”. In: *IEEE Access* 7 (2019), pp. 9724–9735. ISSN: 2169-3536. DOI: [10.1109/ACCESS.2019.2892238](https://doi.org/10.1109/ACCESS.2019.2892238).
- [70] Qiang Hu and Douglas M. Blough. “Relay Selection and Scheduling for Millimeter Wave Backhaul in Urban Environments”. In: *2017 IEEE 14th International Conference on Mobile Ad Hoc and Sensor Systems (MASS)*. IEEE, Oct. 2017, pp. 206–214. DOI: [10.1109/MASS.2017.48](https://doi.org/10.1109/MASS.2017.48).
- [71] *OpenStreetMap 3D building data*. URL: <https://osmbuildings.org/>.
- [72] Durgesh Singh and Sasthi C. Ghosh. “Network-Assisted D2D Relay Selection Under the Presence of Dynamic Obstacles”. In: *2019 IEEE 44th Conference on Local Computer Networks (LCN)*. IEEE, Oct. 2019, pp. 129–132. DOI: [10.1109/LCN44214.2019.8990741](https://doi.org/10.1109/LCN44214.2019.8990741).
- [73] Caihong Kai et al. “Energy-Efficient Device-to-Device Communications for Green Smart Cities”. In: *IEEE Transactions on Industrial Informatics* 14.4 (Apr. 2018), pp. 1542–1551. ISSN: 1941-0050. DOI: [10.1109/TII.2017.2789304](https://doi.org/10.1109/TII.2017.2789304).

- [74] Daquan Feng et al. “A survey of energy-efficient wireless communications”. In: *IEEE Communications Surveys & Tutorials* 15.1 (2013), pp. 167–178. ISSN: 1553-877X. DOI: [10.1109/SURV.2012.020212.00049](https://doi.org/10.1109/SURV.2012.020212.00049).
- [75] James Adu Ansere et al. “Optimal Resource Allocation in Energy-Efficient Internet-of-Things Networks With Imperfect CSI”. In: *IEEE Internet of Things Journal* 7.6 (June 2020), pp. 5401–5411. ISSN: 2327-4662. DOI: [10.1109/JIOT.2020.2979169](https://doi.org/10.1109/JIOT.2020.2979169).
- [76] Dr. Steve E. Deering. *Host extensions for IP multicasting*. Tech. rep. 1112. Aug. 1989. 17 pp. DOI: [10.17487/RFC1112](https://doi.org/10.17487/RFC1112). URL: <https://www.rfc-editor.org/info/rfc1112>.
- [77] John Moy. *Multicast Extensions to OSPF*. Tech. rep. 1584. Mar. 1994. 102 pp. DOI: [10.17487/RFC1584](https://doi.org/10.17487/RFC1584). URL: <https://www.rfc-editor.org/info/rfc1584>.
- [78] D. Waitzman, C. Partridge, and S.E. Deering. *Distance Vector Multicast Routing Protocol*. Tech. rep. 1075. Nov. 1988. 24 pp. DOI: [10.17487/RFC1075](https://doi.org/10.17487/RFC1075). URL: <https://www.rfc-editor.org/info/rfc1075>.
- [79] C.E. Perkins. *Ad Hoc Networking*. Pearson Education, 2008. ISBN: 9788131720967. URL: <https://books.google.co.in/books?id=y6ry8TFqKvYC>.
- [80] S. Basagni, M. Conti, S. Giordano, and I. Stojmenovic. *Mobile Ad Hoc Networking: The Cutting Edge Directions*. IEEE Series on Digital & Mobile Communication. Wiley, 2013. ISBN: 9781118087282. URL: <https://books.google.co.in/books?id=XUMNywAACAAJ>.
- [81] Xiaohui Li et al. “Minimizing Multicast Routing Delay in Multiple Multicast Trees With Shared Links for Smart Grid”. In: *IEEE Transactions on Smart Grid* 10.5 (Sept. 2019), pp. 5427–5435. ISSN: 1949-3061. DOI: [10.1109/TSG.2018.2882182](https://doi.org/10.1109/TSG.2018.2882182).
- [82] Yunpeng Li, Zeeshan Kaleem, and KyungHi Chang. “Interference-Aware Resource-Sharing Scheme for Multiple D2D Group Communications Underlying Cellular Networks”. In: *Wireless Personal Comm.* 90.2 (Sept. 2016), pp. 749–768. ISSN: 1572-834X. DOI: [10.1007/s11277-016-3203-2](https://doi.org/10.1007/s11277-016-3203-2).
- [83] Pekka Jänis et al. “Device-to-Device Communication Underlying Cellular Communications Systems”. In: *International Journal of Communications, Network and System Sciences* 02.03 (2009), pp. 169–178. DOI: [10.4236/ijcns.2009.23019](https://doi.org/10.4236/ijcns.2009.23019).
- [84] Pekka Jänis et al. “Interference-Aware Resource Allocation for Device-to-Device Radio Underlying Cellular Networks”. In: *VTC Spring 2009 - IEEE 69th Vehicular Technology Conference*. IEEE, Apr. 2009, pp. 1–5. DOI: [10.1109/VETECS.2009.5073611](https://doi.org/10.1109/VETECS.2009.5073611).
- [85] Klaus Doppler, Chia-Hao Yu, Cassio B. Ribeiro, and Pekka Jänis. “Mode Selection for Device-To-Device Communication Underlying an LTE-Advanced Network”. In: *2010 IEEE Wireless Communication and Networking Conference*. IEEE, Apr. 2010, pp. 1–6. DOI: [10.1109/WCNC.2010.5506248](https://doi.org/10.1109/WCNC.2010.5506248).

- [86] Chia-Hao Yu, Klaus Doppler, Cassio B. Ribeiro, and Olav Tirkkonen. “Resource Sharing Optimization for Device-to-Device Communication Underlying Cellular Networks”. In: *IEEE Transactions on Wireless Communications* 10.8 (Aug. 2011), pp. 2752–2763. ISSN: 1558-2248. DOI: [10.1109/TWC.2011.060811.102120](https://doi.org/10.1109/TWC.2011.060811.102120).
- [87] Norbert Reider and Gabor Fodor. “A distributed power control and mode selection algorithm for D2D communications”. In: *EURASIP Journal on Wireless Communications and Networking* 2012.1 (Aug. 2012). DOI: [10.1186/1687-1499-2012-266](https://doi.org/10.1186/1687-1499-2012-266).
- [88] Chen Xu et al. “Efficiency Resource Allocation for Device-to-Device Underlay Communication Systems: A Reverse Iterative Combinatorial Auction Based Approach”. In: *IEEE Journal on Selected Areas in Communications* 31.9 (Sept. 2013), pp. 348–358. ISSN: 1558-0008. DOI: [10.1109/JSAC.2013.SUP.0513031](https://doi.org/10.1109/JSAC.2013.SUP.0513031).
- [89] Feiran Wang et al. “Joint scheduling and resource allocation for device-to-device underlay communication”. In: *2013 IEEE Wireless Communications and Networking Conference (WCNC)*. Apr. 2013, pp. 134–139. DOI: [10.1109/WCNC.2013.6554552](https://doi.org/10.1109/WCNC.2013.6554552).
- [90] Daquan Feng et al. “Device-to-Device Communications Underlying Cellular Networks”. In: *IEEE Transactions on Communications* 61.8 (Aug. 2013), pp. 3541–3551. ISSN: 1558-0857. DOI: [10.1109/TCOMM.2013.071013.120787](https://doi.org/10.1109/TCOMM.2013.071013.120787).
- [91] Rongqing Zhang, Xiang Cheng, Liuqing Yang, and Bingli Jiao. “Interference-aware graph based resource sharing for device-to-device communications underlying cellular networks”. In: *2013 IEEE Wireless Communications and Networking Conference (WCNC)*. IEEE, Apr. 2013, pp. 140–145. DOI: [10.1109/WCNC.2013.6554553](https://doi.org/10.1109/WCNC.2013.6554553).
- [92] Rongqing Zhang et al. “Interference Graph-Based Resource-Sharing Schemes for Vehicular Networks”. In: *IEEE Transactions on Vehicular Technology* 62.8 (Oct. 2013), pp. 4028–4039. ISSN: 1939-9359. DOI: [10.1109/TVT.2013.2245156](https://doi.org/10.1109/TVT.2013.2245156).
- [93] Guanding Yu et al. “Joint Mode Selection and Resource Allocation for Device-to-Device Communications”. In: *IEEE Transactions on Communications* 62.11 (Nov. 2014), pp. 3814–3824. ISSN: 1558-0857. DOI: [10.1109/TCOMM.2014.2363092](https://doi.org/10.1109/TCOMM.2014.2363092).
- [94] Tuong Duc Hoang, Long Bao Le, and Tho Le-Ngoc. “Radio resource management for optimizing energy efficiency of D2D communications in cellular networks”. In: *2015 IEEE 26th Annual International Symposium on Personal, Indoor, and Mobile Radio Communications (PIMRC)*. IEEE, Aug. 2015, pp. 1190–1194. DOI: [10.1109/PIMRC.2015.7343479](https://doi.org/10.1109/PIMRC.2015.7343479).
- [95] Wentao Zhao and Shaowei Wang. “Resource Sharing Scheme for Device-to-Device Communication Underlying Cellular Networks”. In: *IEEE Transactions on Communications* 63.12 (Dec. 2015), pp. 4838–4848. ISSN: 1558-0857. DOI: [10.1109/TCOMM.2015.2495217](https://doi.org/10.1109/TCOMM.2015.2495217).

-
- [96] Yanxiang Jiang et al. “Energy-Efficient Joint Resource Allocation and Power Control for D2D Communications”. In: *IEEE Transactions on Vehicular Technology* 65.8 (Aug. 2016), pp. 6119–6127. ISSN: 1939-9359. DOI: [10.1109/TVT.2015.2472995](https://doi.org/10.1109/TVT.2015.2472995).
- [97] Kuo-Yi Chen, Jung-Chun Kao, Si-An Ciou, and Shih-Han Lin. “Joint Resource Block Reuse and Power Control for Multi-Sharing Device-to-Device Communication”. In: *2016 IEEE 84th Vehicular Technology Conference (VTC-Fall)*. IEEE, Sept. 2016. DOI: [10.1109/vtcfall.2016.7881060](https://doi.org/10.1109/vtcfall.2016.7881060).
- [98] Wenson Chang, You-Ting Jau, Szu-Lin Su, and Yinman Lee. “Gale-Shapley-algorithm based resource allocation scheme for device-to-device communications underlaying downlink cellular networks”. In: *2016 IEEE Wireless Communications and Networking Conference*. IEEE, Apr. 2016, pp. 1–6. DOI: [10.1109/WCNC.2016.7564742](https://doi.org/10.1109/WCNC.2016.7564742).
- [99] Lili Wei, Rose Qingyang Hu, Yi Qian, and Geng Wu. “Energy Efficiency and Spectrum Efficiency of Multihop Device-to-Device Communications Underlying Cellular Networks”. In: *IEEE Transactions on Vehicular Technology* 65.1 (Jan. 2016), pp. 367–380. ISSN: 1939-9359. DOI: [10.1109/TVT.2015.2389823](https://doi.org/10.1109/TVT.2015.2389823).
- [100] Tuong Duc Hoang, Long Bao Le, and Tho Le-Ngoc. “Joint Mode Selection and Resource Allocation for Relay-Based D2D Communications”. In: *IEEE Communications Letters* 21.2 (Feb. 2017), pp. 398–401. ISSN: 1558-2558. DOI: [10.1109/LCOMM.2016.2617863](https://doi.org/10.1109/LCOMM.2016.2617863).
- [101] Zhenyu Zhou, Kaoru Ota, Mianxiong Dong, and Chen Xu. “Energy-Efficient Matching for Resource Allocation in D2D Enabled Cellular Networks”. In: *IEEE Transactions on Vehicular Technology* 66.6 (June 2017), pp. 5256–5268. ISSN: 1939-9359. DOI: [10.1109/TVT.2016.2615718](https://doi.org/10.1109/TVT.2016.2615718).
- [102] Demia Della Penda, Liqun Fu, and Mikael Johansson. “Energy Efficient D2D Communications in Dynamic TDD Systems”. In: *IEEE Transactions on Communications* 65.3 (Mar. 2017), pp. 1260–1273. ISSN: 1558-0857. DOI: [10.1109/TCOMM.2016.2616138](https://doi.org/10.1109/TCOMM.2016.2616138).
- [103] Indranil Mondal, Anushree Neogi, Prasanna Chaporkar, and Abhay Karandikar. “Bipartite Graph Based Proportional Fair Resource Allocation for D2D Communication”. In: *2017 IEEE Wireless Communications and Networking Conference (WCNC)*. IEEE, Mar. 2017, pp. 1–6. DOI: [10.1109/WCNC.2017.7925780](https://doi.org/10.1109/WCNC.2017.7925780).
- [104] Tinghan Yang, Rongqing Zhang, Xiang Cheng, and Liuqing Yang. “Graph Coloring Based Resource Sharing (GCRS) Scheme for D2D Communications Underlying Full-Duplex Cellular Networks”. In: *IEEE Transactions on Vehicular Technology* 66.8 (Aug. 2017), pp. 7506–7517. ISSN: 1939-9359. DOI: [10.1109/TVT.2017.2657791](https://doi.org/10.1109/TVT.2017.2657791).

- [105] Wei-Kuang Lai, You-Chiun Wang, He-Cian Lin, and Jian-Wen Li. “Efficient Resource Allocation and Power Control for LTE-A D2D Communication With Pure D2D Model”. In: *IEEE Transactions on Vehicular Technology* 69.3 (Mar. 2020), pp. 3202–3216. ISSN: 1939-9359. DOI: [10.1109/TVT.2020.2964286](https://doi.org/10.1109/TVT.2020.2964286).
- [106] Subhankar Ghosal and Sasthi C. Ghosh. “A Randomized Algorithm for Joint Power and Channel Allocation in 5G D2D Communication”. In: *2019 IEEE 18th International Symposium on Network Computing and Applications (NCA)*. Sept. 2019, pp. 1–5. DOI: [10.1109/NCA.2019.8935005](https://doi.org/10.1109/NCA.2019.8935005).
- [107] Subhankar Ghosal and Sasthi C. Ghosh. “A randomized algorithm for joint power and channel allocation in 5G D2D communication”. In: *Computer Communications* 179 (Nov. 2021), pp. 22–34. ISSN: 0140-3664. DOI: [10.1016/j.comcom.2021.07.018](https://doi.org/10.1016/j.comcom.2021.07.018).
- [108] Junjie Tan, Ying-Chang Liang, Lin Zhang, and Gang Feng. “Deep Reinforcement Learning for Joint Channel Selection and Power Control in D2D Networks”. In: *IEEE Transactions on Wireless Communications* 20.2 (Feb. 2021), pp. 1363–1378. ISSN: 1558-2248. DOI: [10.1109/TWC.2020.3032991](https://doi.org/10.1109/TWC.2020.3032991).
- [109] Helin Yang et al. “Distributed Deep Reinforcement Learning-Based Spectrum and Power Allocation for Heterogeneous Networks”. In: *IEEE Transactions on Wireless Communications* 21.9 (Sept. 2022), pp. 6935–6948. ISSN: 1558-2248. DOI: [10.1109/TWC.2022.3153175](https://doi.org/10.1109/TWC.2022.3153175).
- [110] Sudip Biswas, Satyanarayana Vuppala, Jiang Xue, and Tharmalingam Ratnarajah. “On the Performance of Relay Aided Millimeter Wave Networks”. In: *IEEE Journal of Selected Topics in Signal Processing* 10.3 (Apr. 2016), pp. 576–588. ISSN: 1941-0484. DOI: [10.1109/JSTSP.2015.2509951](https://doi.org/10.1109/JSTSP.2015.2509951).
- [111] Durgesh Singh and Sasthi C. Ghosh. “Mobility-Aware Relay Selection in 5G D2D Communication Using Stochastic Model”. In: *IEEE Transactions on Vehicular Technology* 68.3 (Mar. 2019), pp. 2837–2849. ISSN: 1939-9359. DOI: [10.1109/TVT.2019.2893995](https://doi.org/10.1109/TVT.2019.2893995).
- [112] Durgesh Singh, Arpan Chattopadhyay, and Sasthi C. Ghosh. “Distributed Relay Selection in Presence of Dynamic Obstacles in Millimeter Wave D2D Communication”. In: *ICC 2020 - 2020 IEEE International Conference on Communications (ICC)*. IEEE, June 2020, pp. 1–6. DOI: [10.1109/ICC40277.2020.9148816](https://doi.org/10.1109/ICC40277.2020.9148816).
- [113] Subhojit Sarkar and Sasthi C. Ghosh. “Relay Selection in Millimeter Wave D2D Communications Through Obstacle Learning”. In: *2020 International Conference on COMMunication Systems & NETWORKS (COMSNETS)*. IEEE, Jan. 2020, pp. 468–475. DOI: [10.1109/COMSNETS48256.2020.9027458](https://doi.org/10.1109/COMSNETS48256.2020.9027458).

- [114] Ravi Shukla and Sasthi C. Ghosh. “Distributed relay switching in the presence of dynamic obstacles in millimeter wave D2D communication”. In: *Computer Communications* 194 (Oct. 2022), pp. 124–134. ISSN: 0140-3664. DOI: [10.1016/j.comcom.2022.07.024](https://doi.org/10.1016/j.comcom.2022.07.024).
- [115] Harish Ganesan and Sasthi C. Ghosh. “Evidential Obstacle Learning in Millimeter wave D2D communication using Spatial correlation”. In: *2022 14th International Conference on COMMunication Systems & NETWORKS (COMSNETS)*. IEEE, Jan. 2022, pp. 344–352. DOI: [10.1109/COMSNETS53615.2022.9668369](https://doi.org/10.1109/COMSNETS53615.2022.9668369).
- [116] Durgesh Singh, Arpan Chattopadhyay, and Sasthi C. Ghosh. “To Continue Transmission or to Explore Relays: Millimeter Wave D2D Communication in Presence of Dynamic Obstacles”. In: *IEEE Transactions on Mobile Computing* (2022), (Early Access). ISSN: 1558-0660. DOI: [10.1109/TMC.2022.3160764](https://doi.org/10.1109/TMC.2022.3160764).
- [117] Subhojit Sarkar, Subhankar Ghosal, Subhadip Bandyopadhyay, and Sasthi C. Ghosh. “A Stable Link Allocation Algorithm for 5G Millimeterwave Networks”. In: *2023 15th International Conference on COMMunication Systems & NETWORKS (COMSNETS)*. IEEE, Jan. 2023, pp. 674–681. DOI: [10.1109/COMSNETS56262.2023.10041333](https://doi.org/10.1109/COMSNETS56262.2023.10041333).
- [118] Subhojit Sarkar and Sasthi C. Ghosh. “Mobility Aware Path Selection for Millimeterwave 5G Networks in the Presence of Obstacles”. In: *Communications in Computer and Information Science*. Springer Nature Switzerland, 2023, pp. 67–80. DOI: [10.1007/978-3-031-35299-7_6](https://doi.org/10.1007/978-3-031-35299-7_6).
- [119] Chen Zhengwen, Zhao Su, and Shao Shixiang. “Research on relay selection in device-to-device communications based on maximum capacity”. In: *2014 International Conference on Information Science, Electronics and Electrical Engineering*. Vol. 3. IEEE, Apr. 2014, pp. 1429–1434. DOI: [10.1109/InfoSEEE.2014.6946156](https://doi.org/10.1109/InfoSEEE.2014.6946156).
- [120] Yulei Zhao, Yong Li, Xiang Chen, and Ning Ge. “Joint Optimization of Resource Allocation and Relay Selection for Network Coding Aided Device-to-Device Communications”. In: *IEEE Communications Letters* 19.5 (May 2015), pp. 807–810. ISSN: 2373-7891. DOI: [10.1109/LCOMM.2015.2401557](https://doi.org/10.1109/LCOMM.2015.2401557).
- [121] Junquan Deng et al. “Resource Allocation and Interference Management for Opportunistic Relaying in Integrated mmWave/sub-6 GHz 5G Networks”. In: *IEEE Communications Magazine* 55.6 (June 2017), pp. 94–101. ISSN: 1558-1896. DOI: [10.1109/MCOM.2017.1601120](https://doi.org/10.1109/MCOM.2017.1601120).
- [122] Xinyu Gu et al. “A Two-Stages Relay Selection and Resource Allocation with Throughput Balance Scheme in Relay-Assisted D2D System”. In: *Mobile Networks and Applications* 22.6 (Feb. 2017), pp. 1020–1032. DOI: [10.1007/s11036-017-0824-y](https://doi.org/10.1007/s11036-017-0824-y).

- [123] Miaomiao Liu and Li Zhang. “Joint Power and Channel Allocation for Relay-Assisted Device- to- Device Communications”. In: *2018 15th International Symposium on Wireless Communication Systems (ISWCS)*. IEEE, Aug. 2018, pp. 1–5. DOI: [10.1109/ISWCS.2018.8491059](https://doi.org/10.1109/ISWCS.2018.8491059).
- [124] Jian Sun, Zhongshan Zhang, Chengwen Xing, and Hailin Xiao. “Uplink Resource Allocation for Relay-Aided Device-to-Device Communication”. In: *IEEE Transactions on Intelligent Transportation Systems* 19.12 (Dec. 2018), pp. 3883–3892. ISSN: 1558-0016. DOI: [10.1109/TITS.2017.2788562](https://doi.org/10.1109/TITS.2017.2788562).
- [125] L. J. Cowen, R. H. Cowen, and D. R. Woodall. “Defective colorings of graphs in surfaces: Partitions into subgraphs of bounded valency”. In: *Journal of Graph Theory* 10.2 (1986), pp. 187–195. DOI: <https://doi.org/10.1002/jgt.3190100207>.
- [126] Jeonghun Park and Robert W. Heath. “Analysis of Blockage Sensing by Radars in Random Cellular Networks”. In: *IEEE Signal Processing Letters* 25.11 (Nov. 2018), pp. 1620–1624. ISSN: 1558-2361. DOI: [10.1109/LSP.2018.2869279](https://doi.org/10.1109/LSP.2018.2869279).
- [127] Andrew Tzer-Yeu Chen, Morteza Biglari-Abhari, and Kevin I-Kai Wang. “Context is King: Privacy Perceptions of Camera-based Surveillance”. In: *2018 15th IEEE International Conference on Advanced Video and Signal Based Surveillance (AVSS)*. IEEE, 2018, pp. 1–6. DOI: [10.1109/AVSS.2018.8639448](https://doi.org/10.1109/AVSS.2018.8639448).
- [128] Durgesh Singh, Arpan Chattopadhyay, and Sasthi C. Ghosh. “Local Relay Selection in Presence of Dynamic Obstacles in Millimeter Wave D2D Communication”. In: *ICC 2021 - IEEE International Conference on Communications*. IEEE, June 2021, pp. 1–6. DOI: [10.1109/ICC42927.2021.9500570](https://doi.org/10.1109/ICC42927.2021.9500570).
- [129] Herbert Robbins and Sutton Monro. “A Stochastic Approximation Method”. In: *The Annals of Mathematical Statistics* 22.3 (Sept. 1951), pp. 400–407. DOI: [10.1214/aoms/1177729586](https://doi.org/10.1214/aoms/1177729586).
- [130] Jeffrey S. Vitter. “Random Sampling with a Reservoir”. In: *ACM Transactions on Mathematical Software* 11.1 (Mar. 1985), pp. 37–57. ISSN: 0098-3500. DOI: [10.1145/3147.3165](https://doi.org/10.1145/3147.3165). URL: <https://doi.org/10.1145/3147.3165>.
- [131] R.Kipp Martin. “Using separation algorithms to generate mixed integer model reformulations”. In: *Operations Research Letters* 10.3 (Apr. 1991), pp. 119–128. ISSN: 0167-6377. DOI: [10.1016/0167-6377\(91\)90028-n](https://doi.org/10.1016/0167-6377(91)90028-n).
- [132] Glenn Shafer. *A Mathematical Theory of Evidence*. Princeton: Princeton University Press, 1976. ISBN: 9780691214696. DOI: [10.1515/9780691214696](https://doi.org/10.1515/9780691214696).
- [133] Ronald R. Yager. “On the Dempster-Shafer Framework and New Combination Rules”. In: *Information Sciences* 41.2 (Mar. 1987), pp. 93–137. ISSN: 0020-0255. DOI: [10.1016/0020-0255\(87\)90007-7](https://doi.org/10.1016/0020-0255(87)90007-7).

- [134] Pavel Mach, Zdenek Becvar, and Tomas Vanek. “In-Band Device-to-Device Communication in OFDMA Cellular Networks: A Survey and Challenges”. In: *IEEE Communications Surveys & Tutorials* 17.4 (Fourthquarter 2015). large pdf, 6.5MB, pp. 1885–1922. ISSN: 1553-877X. DOI: [10.1109/COMST.2015.2447036](https://doi.org/10.1109/COMST.2015.2447036).
- [135] M. Simaan and J. B. Cruz. “On the Stackelberg strategy in nonzero-sum games”. In: *Journal of Optimization Theory and Applications* 11.5 (May 1973), pp. 533–555. DOI: [10.1007/bf00935665](https://doi.org/10.1007/bf00935665).
- [136] Stephen Boyd and Jacob Mattingley. *Branch and bound methods*. Notes for EE364b, Stanford University, Winter 2006-07. 2007. URL: https://see.stanford.edu/materials/lsoctee364b/17-bb_notes.pdf (visited on 06/16/2023).
- [137] Harold W. Kuhn and Albert W. Tucker. “Nonlinear Programming”. In: *Traces and Emergence of Nonlinear Programming*. Springer Basel, July 2013, pp. 247–258. DOI: [10.1007/978-3-0348-0439-4_11](https://doi.org/10.1007/978-3-0348-0439-4_11).
- [138] Stephen Boyd and Lieven Vandenbergh. *Convex Optimization*. Cambridge University Press, 2004, p. 730. ISBN: 9780521833783. eprint: https://web.stanford.edu/~boyd/cvxbook/bv_cvxbook.pdf.
- [139] Hoang-Hiep Nguyen, Mikio Hasegawa, and Won-Joo Hwang. “Distributed Resource Allocation for D2D Communications Underlay Cellular Networks”. In: *IEEE Communications Letters* 20.5 (May 2016), pp. 942–945. ISSN: 1558-2558. DOI: [10.1109/LCOMM.2015.2498925](https://doi.org/10.1109/LCOMM.2015.2498925).
- [140] Stefano Basagni. “Finding a Maximal Weighted Independent Set in Wireless Networks”. In: *Telecommunication Systems* 18.1/3 (2001), pp. 155–168. DOI: [10.1023/a:1016747704458](https://doi.org/10.1023/a:1016747704458).
- [141] Jeehyeong Kim, Nzabanita Karim, and Sunghyun Cho. “An Interference Mitigation Scheme of Device-to-Device Communications for Sensor Networks Underlying LTE-A”. In: *Sensors* 17.5 (May 2017), p. 1088. ISSN: 1424-8220. DOI: [10.3390/s17051088](https://doi.org/10.3390/s17051088).
- [142] Sreetama Mukherjee and Sasthi C. Ghosh. “Scalable and Fair Resource Sharing Among 5G D2D Users and Legacy 4G Users: A Game Theoretic Approach”. In: *2020 International Conference on COMMunication Systems & NETWORKS (COMSNETS)*. IEEE, Jan. 2020, pp. 229–236. DOI: [10.1109/COMSNETS48256.2020.9027395](https://doi.org/10.1109/COMSNETS48256.2020.9027395).
- [143] Sreetama Mukherjee and Sasthi C. Ghosh. “Scalable and fair resource sharing among 5G D2D users and legacy 4G users: A game theoretic approach”. In: *Ad Hoc Networks* 115 (2021), pp. 1024–36. ISSN: 1570-8705. DOI: <https://doi.org/10.1016/j.adhoc.2021.102436>.

- [144] Viveck R. Cadambe and Syed Ali Jafar. “Interference Alignment and Degrees of Freedom of the K -User Interference Channel”. In: *IEEE Transactions on Information Theory* 54.8 (Aug. 2008), pp. 3425–3441. ISSN: 1557-9654. DOI: [10.1109/TIT.2008.926344](https://doi.org/10.1109/TIT.2008.926344).
- [145] D. Gale and L. S. Shapley. “College Admissions and the Stability of Marriage”. In: *The American Mathematical Monthly* 69.1 (Jan. 1962), p. 9. DOI: [10.2307/2312726](https://doi.org/10.2307/2312726).
- [146] Werner Dinkelbach. “On Nonlinear Fractional Programming”. In: *Management Science* 13.7 (Mar. 1967), pp. 492–498. DOI: [10.1287/mnsc.13.7.492](https://doi.org/10.1287/mnsc.13.7.492).
- [147] Zhouyue Pi and Farooq Khan. “An introduction to millimeter-wave mobile broadband systems”. In: *IEEE Communications Magazine* 49.6 (June 2011), pp. 101–107. ISSN: 1558-1896. DOI: [10.1109/MCOM.2011.5783993](https://doi.org/10.1109/MCOM.2011.5783993).
- [148] Christian Hoymann et al. “Relaying operation in 3GPP LTE: challenges and solutions”. In: *IEEE Communications Magazine* 50.2 (Feb. 2012), pp. 156–162. ISSN: 1558-1896. DOI: [10.1109/MCOM.2012.6146495](https://doi.org/10.1109/MCOM.2012.6146495).
- [149] Maurice Pollack. “Letter to the Editor—The Maximum Capacity Through a Network”. In: *Operations Research* 8.5 (Oct. 1960), pp. 733–736. DOI: [10.1287/opre.8.5.733](https://doi.org/10.1287/opre.8.5.733).
- [150] Xiran Ma, Rui Yin, Guanding Yu, and Zhaoyang Zhang. “A distributed relay selection method for relay assisted Device-to-Device communication system”. In: *2012 IEEE 23rd International Symposium on Personal, Indoor and Mobile Radio Communications - (PIMRC)*. Sept. 2012, pp. 1020–1024. DOI: [10.1109/PIMRC.2012.6362495](https://doi.org/10.1109/PIMRC.2012.6362495).
- [151] Roberto Verdone and Alberto Zanella. “On the Effect of User Mobility in Mobile Radio Systems With Distributed DCA”. In: *IEEE Transactions on Vehicular Technology* 56.2 (Mar. 2007), pp. 874–887. ISSN: 1939-9359. DOI: [10.1109/TVT.2006.889568](https://doi.org/10.1109/TVT.2006.889568).
- [152] Yanyan Han, Hongyi Wu, Zhipeng Yang, and Deshi Li. “A New Data Transmission Strategy in Mobile D2D Networks — Deterministic, Greedy, or Planned Opportunistic Routing?” In: *IEEE Transactions on Vehicular Technology* 66.1 (Jan. 2017), pp. 594–609. ISSN: 1939-9359. DOI: [10.1109/TVT.2016.2540641](https://doi.org/10.1109/TVT.2016.2540641).
- [153] Aymen Omri and Mazen O. Hasna. “A Distance-Based Mode Selection Scheme for D2D-Enabled Networks With Mobility”. In: *IEEE Transactions on Wireless Communications* 17.7 (July 2018), pp. 4326–4340. ISSN: 1558-2248. DOI: [10.1109/TWC.2018.2822814](https://doi.org/10.1109/TWC.2018.2822814).
- [154] Tisha Brown et al. “Obstacle-Aware Wireless Video Sensor Network Deployment for 3D Indoor Monitoring”. In: *GLOBECOM 2017 - 2017 IEEE Global Communications Conference*. 2017, pp. 1–6. DOI: [10.1109/GLOCOM.2017.8254513](https://doi.org/10.1109/GLOCOM.2017.8254513).

- [155] Jiying Huang, Zhangdui Zhong, and Jianwen Ding. “An Adaptive Power Control Scheme for Multicast Service in Green Cellular Railway Communication Network”. In: *Mobile Networks and Applications* 21.6 (May 2016), pp. 920–929. ISSN: 1572-8153. DOI: [10.1007/s11036-016-0712-x](https://doi.org/10.1007/s11036-016-0712-x).
- [156] Jason Xie, Rajesh R. Talpade, Anthony McAuley, and Mingyan Liu. “AMRoute: Ad Hoc Multicast Routing Protocol”. In: *Mobile Networks and Applications* 7.6 (2002), pp. 429–439. DOI: [10.1023/a:1020748431138](https://doi.org/10.1023/a:1020748431138).
- [157] Zhijun Wang, Yong Liang, and Lu Wang. “Multicast in Mobile ad hoc Networks”. In: *Computer And Computing Technologies In Agriculture, Volume I*. Ed. by Daoliang Li. Boston, MA: Springer US, 2008, pp. 151–164. ISBN: 978-0-387-77251-6. DOI: [10.1007/978-0-387-77251-6_17](https://doi.org/10.1007/978-0-387-77251-6_17).
- [158] Zheng Wang and J. Crowcroft. “Quality-of-service routing for supporting multimedia applications”. In: *IEEE Journal on Selected Areas in Communications* 14.7 (Sept. 1996), pp. 1228–1234. ISSN: 1558-0008. DOI: [10.1109/49.536364](https://doi.org/10.1109/49.536364).
- [159] Nachum Shacham. “Multicast routing of hierarchical data”. In: *[Conference Record] SUPERCOMM/ICC '92 Discovering a New World of Communications*. IEEE, June 1992, 1217–1221 vol.3. DOI: [10.1109/ICC.1992.268047](https://doi.org/10.1109/ICC.1992.268047).
- [160] Jaakko Seppälä, Timo Koskela, Tao Chen, and Sami Hakola. “Network controlled Device-to-Device (D2D) and cluster multicast concept for LTE and LTE-A networks”. In: *2011 IEEE Wireless Communications and Networking Conference*. IEEE, Mar. 2011, pp. 986–991. DOI: [10.1109/WCNC.2011.5779270](https://doi.org/10.1109/WCNC.2011.5779270).
- [161] Izhak Rubin, Choo-Chin Tan, and Reuven Cohen. “Joint scheduling and power control for multicasting in cellular wireless networks”. In: *EURASIP Journal on Wireless Communications and Networking* 2012.1 (Aug. 2012), p. 250. ISSN: 1687-1499. DOI: [10.1186/1687-1499-2012-250](https://doi.org/10.1186/1687-1499-2012-250).
- [162] Ting-Chao Hou. “Minimizing delay in D2D-assisted resource-efficient two-stage multicast in LTE access networks”. In: *2017 10th IFIP Wireless and Mobile Networking Conference (WMNC)*. Sept. 2017, pp. 1–8. DOI: [10.1109/WMNC.2017.8248847](https://doi.org/10.1109/WMNC.2017.8248847).
- [163] Ajay Bhardwaj and Samar Agnihotri. “Energy- and Spectral-Efficiency Trade-Off for D2D-Multicasts in Underlay Cellular Networks”. In: *IEEE Wireless Communications Letters* 7.4 (Aug. 2018), pp. 546–549. ISSN: 2162-2345. DOI: [10.1109/LWC.2018.2794353](https://doi.org/10.1109/LWC.2018.2794353).
- [164] Fred Glover, Eric Taillard, and Eric Taillard. “A user’s guide to tabu search”. In: *Annals of Operations Research* 41.1 (Mar. 1993), pp. 1–28. DOI: [10.1007/bf02078647](https://doi.org/10.1007/bf02078647).
- [165] Pengshuo Ji et al. “Joint optimization for RIS-assisted multicast D2D communications”. In: *Computer Networks* 211 (July 2022), p. 108977. DOI: [10.1016/j.comnet.2022.108977](https://doi.org/10.1016/j.comnet.2022.108977).

- [166] Samuel K. Moore. *Superaccurate GPS Chips Coming to Smartphones in 2018*. 2017. URL: <https://spectrum.ieee.org/superaccurate-gps-chips-coming-to-smartphones-in-2018>.
- [167] Jun Huang, Hamid Gharavi, Huifang Yan, and Cong-Cong Xing. “Network Coding in Relay-Based Device-to-Device Communications”. In: *IEEE Network* 31.4 (July 2017), pp. 102–107. DOI: [10.1109/MNET.2017.1700063](https://doi.org/10.1109/MNET.2017.1700063).
- [168] Lu Lu et al. “Real-Time Implementation of Physical-Layer Network Coding”. In: *Proceedings of the Second Workshop on Software Radio Implementation Forum. SIGCOMM’13*. Hong Kong, China: Association for Computing Machinery, Aug. 2013, pp. 71–76. ISBN: 9781450321815. DOI: [10.1145/2491246.2491256](https://doi.org/10.1145/2491246.2491256). URL: <https://doi.org/10.1145/2491246.2491256>.
- [169] Soung Chang Liew, Shengli Zhang, and Lu Lu. “Physical-layer network coding: Tutorial, survey, and beyond”. In: *Physical Communication* 6 (Mar. 2013), pp. 4–42. ISSN: 1874-4907. DOI: [10.1016/j.phycom.2012.05.002](https://doi.org/10.1016/j.phycom.2012.05.002).
- [170] Yidong Lang and Dirk Wubben. “Generalized Joint Channel Coding and Physical Network Coding for Two-Way Relay Systems”. In: *2010 IEEE 71st Vehicular Technology Conference. IEEE*, May 2010, pp. 1–5. DOI: [10.1109/VETECS.2010.5493997](https://doi.org/10.1109/VETECS.2010.5493997).
- [171] Shengli Zhang, Soung Chang Liew, and Patrick P. Lam. “Hot Topic: Physical-Layer Network Coding”. In: *Proceedings of the 12th Annual International Conference on Mobile Computing and Networking. MobiCom ’06*. Los Angeles, CA, USA: Association for Computing Machinery, Sept. 2006, pp. 358–365. ISBN: 1595932860. DOI: [10.1145/1161089.1161129](https://doi.org/10.1145/1161089.1161129). URL: <https://doi.org/10.1145/1161089.1161129>.
- [172] Jian Xiong et al. “Physical-Layer Network Coding Enhanced Visible Light Communications Using RGB LEDs”. In: *IEEE Photonics Journal* 15.1 (Feb. 2023), pp. 1–10. ISSN: 1943-0655. DOI: [10.1109/JPHOT.2023.3240438](https://doi.org/10.1109/JPHOT.2023.3240438).
- [173] Haoyuan Pan, Tse-Tin Chan, Victor C. M. Leung, and Jianqiang Li. “Age of Information in Physical-Layer Network Coding Enabled Two-Way Relay Networks”. In: *IEEE Transactions on Mobile Computing* 22.8 (Aug. 2023), pp. 4485–4499. ISSN: 1558-0660. DOI: [10.1109/TMC.2022.3166155](https://doi.org/10.1109/TMC.2022.3166155).
- [174] Gurobi Optimization, LLC. *Gurobi Optimizer Reference Manual*. 2023. URL: <https://www.gurobi.com>.
- [175] Pei Zhou et al. “IEEE 802.11ay-Based mmWave WLANs: Design Challenges and Solutions”. In: *IEEE Communications Surveys & Tutorials* 20.3 (thirdquarter 2018), pp. 1654–1681. ISSN: 1553-877X. DOI: [10.1109/COMST.2018.2816920](https://doi.org/10.1109/COMST.2018.2816920).
- [176] Yasaman Ghasempour, Claudio R. C. M. da Silva, Carlos Cordeiro, and Edward W. Knightly. “IEEE 802.11ay: Next-Generation 60 GHz Communication for 100 Gb/s Wi-Fi”. In: *IEEE Communications Magazine* 55.12 (Dec. 2017), pp. 186–192. ISSN: 1558-1896. DOI: [10.1109/MCOM.2017.1700393](https://doi.org/10.1109/MCOM.2017.1700393).

- [177] Magnús M. Halldórsson and Jaikumar Radhakrishnan. “Greed is good: Approximating independent sets in sparse and bounded-degree graphs”. In: *Algorithmica* 18 (May 1997), pp. 145–163. DOI: <https://doi.org/10.1007/BF02523693>.
- [178] J. E. Bresenham. “Algorithm for computer control of a digital plotter”. In: *IBM Systems Journal* 4.1 (1965), pp. 25–30. DOI: [10.1147/sj.41.0025](https://doi.org/10.1147/sj.41.0025).
- [179] Dan E. Willard. “New Data Structures for Orthogonal Range Queries”. In: *SIAM Journal on Computing* 14.1 (Feb. 1985), pp. 232–253. DOI: [10.1137/0214019](https://doi.org/10.1137/0214019).
- [180] Mark de Berg, Otfried Cheong, Marc van Kreveld, and Mark Overmars. *Computational Geometry: Algorithms and Applications*. Springer Berlin Heidelberg, 2014. ISBN: 9783662042465. DOI: [10.1007/978-3-540-77974-2](https://doi.org/10.1007/978-3-540-77974-2).
- [181] *Efficiently find points inside a circle sector*. URL: <https://stackoverflow.com/questions/13652518/efficiently-find-points-inside-a-circle-sector>.
- [182] Tim Roughgarden. *Algorithms Illuminated Omnibus Edition. Omnibus Edition*. Soundlikeyourself Publishing, LLC, 2022, p. 690. ISBN: 9780999282984.
- [183] *Requirements for watching YouTube videos*. Google Support. 2023. URL: <https://support.google.com/youtube/answer/78358?hl=en>.
- [184] Umur Karabulut et al. “Average downlink SINR model for 5G mmWave networks with analog beamforming”. In: *2018 IEEE Wireless Communications and Networking Conference (WCNC)*. Apr. 2018, pp. 1–6. DOI: [10.1109/WCNC.2018.8376957](https://doi.org/10.1109/WCNC.2018.8376957).
- [185] Raj Jain, Dah-Ming Chiu, and W. Hawe. “A Quantitative Measure Of Fairness And Discrimination For Resource Allocation In Shared Computer Systems”. In: *CoRR* cs.NI/9809099 (1998). URL: <https://arxiv.org/abs/cs/9809099>.
- [186] Mohammad H. Mazaheri, Soroush Ameli, Ali Abedi, and Omid Abari. “A Millimeter Wave Network for Billions of Things”. In: *Proceedings of the ACM Special Interest Group on Data Communication. SIGCOMM '19*. Beijing, China: Association for Computing Machinery, 2019, pp. 174–186. ISBN: 9781450359566. DOI: [10.1145/3341302.3342068](https://doi.org/10.1145/3341302.3342068). URL: <https://doi.org/10.1145/3341302.3342068>.
- [187] Christopher J C H Watkins and Peter Dayan. “Q-learning”. In: *Machine Learning* 8.3 (May 1992), pp. 279–292.
- [188] Richard S. Sutton and Andrew G. Barto. *Reinforcement Learning: An Introduction*. Cambridge, MA, USA: MIT Press, 2018. ISBN: 0262039249.
- [189] *Evolved Universal Terrestrial Radio Access (E-UTRA); Radio Frequency (RF) system scenarios (3GPP TR 36.942 version 13.0.0 Release 13)*. URL: https://www.etsi.org/deliver/etsi_tr/136900_136999/136942/13.00.00_60/tr_136942v130000p.pdf.

-
- [190] Chedia Jarray and Anastasios Giovanidis. “The effects of mobility on the hit performance of cached D2D networks”. In: *2016 14th International Symposium on Modeling and Optimization in Mobile, Ad Hoc, and Wireless Networks (WiOpt)*. IEEE, May 2016, pp. 1–8. DOI: [10.1109/WIOPT.2016.7492958](https://doi.org/10.1109/WIOPT.2016.7492958).
- [191] Eyal Even-Dar and Yishay Mansour. “Learning Rates for Q-Learning”. In: *Journal of Machine Learning Research* 5 (Dec. 2004), pp. 1–25. ISSN: 1532-4435.
- [192] Akihisa Kako, Takao Ono, Tomio Hirata, and Magnús M. Halldórsson. “Approximation algorithms for the weighted independent set problem in sparse graphs”. In: *Discrete Applied Mathematics* 157.4 (Feb. 2009), pp. 617–626. ISSN: 0166-218X. DOI: <https://doi.org/10.1016/j.dam.2008.08.027>.
- [193] Aarti Munjal, Tracy Camp, and William C. Navidi. “SMOOTH: A Simple Way to Model Human Mobility”. In: *Proceedings of the 14th ACM International Conference on Modeling, Analysis and Simulation of Wireless and Mobile Systems*. MSWiM ’11. Miami, Florida, USA: Association for Computing Machinery, 2011, pp. 351–360. ISBN: 9781450308984. DOI: [10.1145/2068897.2068957](https://doi.org/10.1145/2068897.2068957). URL: <https://doi.org/10.1145/2068897.2068957>.